Sputtering niobium films into a RFQ model & Sputtering of superconducting V3Si films

Zhang Yan

China Institute of Atomic Energy

Dissertation for the degree of Ph.D

Tutor: Prof. Guan Xialing
China Institute of Atomic Energy

Prof. Zhao Kui
Peking University

Advisor: Dr. V. Palmieri
Legnaro National Laboratories of the
Istituto Nazionale di Fisica Nucleare

To my dear wife Zhang Xue
and to my beloved daughter Yiyi

Acknowledgement

First I wish to thank the Instituto Nazionale di Fisica Nucleare (INFN) and in particular the Laboratori Nazionali di Legnaro (LNL) for the support that made possible this thesis.

I'm grateful to Prof. Suehiro Takeuchi of Japan Atomic Energy Research Institute (JAERI). He taught me measurement and design of SRF cavities, and leaded me to the RF superconductivity field. Here, I'll express my gratitude and appreciation to Dr. Walter Venturini of LNL for all his kind help, cooperation and fruitful discussions, under his supervision I performed the first sputtering of this thesis.

I'm deeply indebted to Dr. I. Kulik, Dr. S. Stark, Dr. V. Tchitchkov, Mr. L. Badan and F. Stivanello and all members of the superconductivity group at LNL. Their kind help and suggestions had a great contribution to the thesis. Mr. R. Preciso of the mechanical workshop at LNL is gratefully acknowledged for all the mechanical jobs involved. Many thanks to Dr. S. Zandolin and Dr. D. Boscarino for EDS, RBS analysis, Dr. A. Cassinese of Napoli University for RF measurements and the young German student Mr. K. Schirmer for sample measurements. There are still many people at LNL, CIAE and Peking University that gave various contributions to the thesis, I cannot list all of their names, I just express my acknowledgement at here.

Special thanks to my tutors Prof. Guan Xialing, Prof. Zhao Kui and my advisor Dr. Enzo Palmieri. I could not conduct or complete any of the studies without their always-patient guidance and kind encouragement. The thesis is an accomplishment of all the hard works.

Curriculum Vitae of Dr. Zhang Yan

July, 1967	Born in Henan, China
1985-1990	Peking University B.S. degree on Nuclear physics Beijing, China
Since 1990	HI-13 tandem accelerator laboratory – CIAE Beijing, China M.S. degree on Accelerator physics
Since March to September, 1995	Tandem accelerator Laboratory – JAERI Tokai, Japan
1997-1999	Legnaro National Laboratory - INFN Legnaro (Padova), Italy

Publications:

1. Zhang Yan, Guan Xialing, Non standard bunching mode of single drift buncher, Atomic Energy Science and Technology (Chinese), Vol.27, 1993
2. Guan Xialing, Zhang Yan, Concept design of a superconducting linac booster and a RIB On-Line Isotope Separator for the BRNBF project, CIAE report (Chinese), 1995
3. Zhang Yan, Suehiro Takeuchi, Study of beam optics of the booster, JAERI-memo. 119, 1995
4. S. Takeuchi, T. Ishii, M. Matsuda, Y. Zhang, T. Yoshida, Acceleration of heavy ions by the JAERI tandem superconducting booster, Nucl. Instr. Meth. in Phys. Res., Vol.A382, 1996
5. Zhang Yan, Jiang Weisheng, Guan Xialing, Concept design of an RIB thick target, CNIC-01194, IAE-0175, 1997
6. Y. Zhang, V. Palmieri, W. Venturini, R. Preciso, Reactive sputtered V3Si films, LNL-INFN Rep.144/99, 1999
7. I. Kulik, Y. Zhang, V. Palmieri, W. Venturini, F. Stivanelo, R. Preciso, Preliminary result of sputtered niobium films on a model RFQ, LNL-INFN Rep.149/99, 1999
8. Y. Zhang, V. Palmieri, R. Preciso, W.Venturini, “Preliminary results on cosputtering of V3Si films by the facing target magnetron technique"” LNL-INFN (REP) 143/99.
9. Y. Zhang, V. Palmieri, W. Venturini, F. Stivanello, R. Preciso, “Thermal diffusion of V3Si films”, LNL-INFN (REP) 157/2000

Dissertation for the degree of Ph.D

Contents

Abstract --- 1

Chapter 1 An introduction to SC cavities -------------------------------- 6
1.1 RF acceleration --- 7
1.2 SC material for RF resonators -- 11
1.3 Design consideration of SC cavities --------------------------------- 15
1.4 Measurement of SC cavities -- 19
1.5 Cavity fabrication and high gradient --------------------------------- 21

Chapter 2 Sputtering coated niobium film cavities -------------------- 23
  2.1 Introduction to sputter technique --------------------------------- 24
  2.2 Sputter of niobium film --- 29
  2.3 Sputtering coated niobium QWRs -------------------------------- 32
  2.4 Sputtered 1.5GHz monocell spherical cavities ------------------ 36
  2.5Discussion of sputtered niobium cavities ------------------------- 40

Chapter 3 Sputter niobium films on a model RFQ -------------------- 41
  3.1 Design of SC RFQs -- 42
  3.2 The magnetron sputtering system for SRFQ -------------------- 48
  3.3 Experiments with Stainless steel and copper ------------------- 52
  3.4 Sputtering of niobium films -------------------------------------- 55
  3.5 Discussion --- 60

Chapter 4 Cosputtering of V3Si films ---------------------------------- 61
  4.1 Introduction -- 62
  4.2 Facing-target magnetron -- 64
  4.3 Vacuum system -- 66
  4.4 Sputter with niobium --- 69
  4.5 Co-sputter of V3Si -- 71
  4.6 Film analysis --- 73
  4.7 Discussion -- 78

Chapter 5 Reactive sputtered V3Si films ------------------------------- 81
  5.1 Introduction -- 82
  5.2 Reactive sputtering -- 84
  5.3 Sample measurement -------------
  5.4 Discussion and conclusion ----------

Chapter 6 Thermal diffusion of V3Si films ---------------
    6.1 Introduction -------------------------
    6.2 Magnetron sputtered V3Si films --------------
    6.3 Thermal diffusion V3Si films on sapphire substrates ---
    6.4 Niobium and copper substrates --------------------------
    6.5 Bulk vanadium substrates -------------------------------
    6.5 Remained problems -------------------------------------

References --

Abstract

Super-conducting technique has been widely applied to linac particle accelerators for more than two decades. Cryogenic RF performance of SC cavities has been improved a lot due to improvement on purification of SC material, as well as SC cavity design, fabrication and surface treatment techniques. The Sputtering technique of SC cavities provided another chance to particle accelerators: the cost of cavity fabrication greatly decreased, while the performances of sputtering coated niobium cavities are competitive with those of bulk material SC cavities.

In this thesis some important features of RF cavities are briefly introduced; the difference in design of a SC cavity and that of a normal conducting cavity are indicated. The design parameters of a 144 MHz SC QWR and an 1.5GHz monocell spherical cavity are presented. The SC material for cavity fabrication, and measurement method of SC cavity are introduced, then the fabrication and surface treatment technique of SC cavities are discussed.

The application of sputtering technique in SC cavities is a recent development of SRF technique. After nearly two decades study, the sputtering coated niobium film SC cavities achieved a cryogenic RF performance close to that of bulk niobium cavities. The thesis introduced various sputtering techniques on this purpose from preliminary glow discharge, discusses the LNL, Peking University and Australia National University's QWR sputtering configurations, and introduces LNL's surface treatment technique for copper substrate cavity.

In the study of niobium sputtering for 1.5GHz monocell spherical cavity, different magnetron configurations were tried and measured a large amount of sputtered niobium samples. By improving the magnetron configuration and surface treatment technique of the substrate cavity, sputtered niobium cavities with better RF performance were obtained. It was found out that substrate surface treatment takes a very important role in the sputtering of a SC cavity, as sample measurement cannot give out helpful information of the RF performance, the study with substrate cavity is the most important procedure in sputter-coated SC cavities.

Design and fabrication of super-conducting RFQ is one of the most difficult tasks in SRF technique. The thesis introduced some important

parameters and consideration in RFQ design, listed the design parameters of LNL's SRFQs. Because OFHC copper sputtering coated with niobium film could provide a better thermal stability and reduce the cost of a SRFQ structure, study of sputtering niobium films on RFQ became another important field in the sputtering technique.

The thesis introduced magnetron configuration and dummy SS RFQ model in the SRFQ sputtering study. In order to get an uniformly distributed sputter-coated niobium film on the entire surface of the complicated RFQ electrode, a lot of film thickness simulations and experimental sputtering studies with stainless steel and copper were carried out. They showed that with a simple four-target configuration, the film uniformity could be adjusted by argon pressure so that the entire RFQ surface would be uniformly coated.

Although in the niobium film sputtering experiment, by adjusting argon pressure at approximately 3Pa, the entire RFQ surface was uniformly sputtering coated, the quality of sputtered niobium film got worse for an increasing argon pressure. In order to get high quality niobium film, the argon pressure should be kept low in the sputtering and, the film uniformity need to be solved by other methods.

A rotating target system was designed and fabricated, during the sputtering, rotate the target to enhance film deposition on the RFQ electrode external areas. At lower argon pressure, uniformity of the film thickness was greatly improved. After a few experiments, quality of deposited niobium films on the entire RFQ electrode surface was close to the requirement of sputter-coated niobium film SRFQ.

Besides niobium films, traditional superconductors with Tc higher than that of niobium have been investigated as surface coating material for SC cavities. Among the materials, Nb_3Sn has shown a promising result for SC cavity upgrade. V_3Si is expected to be a potential material for SRF applications, since it has a Tc close to that of Niobium, but is a much less resistive material.

In the study of V_3Si films, co-sputtering was studied first. By a home-made facing–target magnetron, vanadium and silicon target was sputtered simultaneously, V_3Si films were deposited on substrate. The characteristic property of a facing-target magnetron sputtering was observed and analyzed. From EDS and RBS measurements, it was found out that composition of the co-sputtered V_3Si films could be controlled by adjusting voltages of the two targets.

In the co-sputtering, V_3Si films sputtered at lower temperature are highly disordered or even amorphous, film quality measured by RRR and Tc is quite poor. Only those samples sputtered and annealed at higher temperature showed better crystalline structure and got higher RRR or Tc, the optimum process temperature of V_3Si film sputtering is above 800C. In the sputtering of V_3Si film, composition is not so important as that of bulk material compared with the process temperature. After annealed at 800C for a few hours, V_3Si films with silicon content 20% to 30% got Tc higher than 15.5K, while the best sample is 15.9K, less than that of bulk V_3Si.

But in surface coating of a SC V_3Si cavity, co-sputtering method would be very difficult, at the same time, quality of the deposited films were not good enough, and other film coating technique should be investigated. Reactive sputtering technique would be a better solution. Vanadium target could be easily shaped to suit the sputtering of a SC cavity while introducing silane (SiH_4) atmosphere in the discharge to form V_3Si films. Silane is however a dangerous gas, ans safety precautions must be carefully studied and adopted in the experimental research.

In the reactive sputtering of V_3Si films, many V-Si phases could be formed. Film composition is related to the deposition rate, silane partial pressure and substrate temperature. By controlling the deposition rate, stoichiometric V_3Si films could be sputtered at various silane partial pressures. From the observation of the experiment, it is known that reactions take place on the deposited film surface as well as on the target surface in the reactive sputtering of V_3Si films.

Sample temperature is the most important factor determining the quality of deposited V_3Si films in the reactive sputtering too. While sputtered at 500C, V_3Si films with silicon 10% to 30% showed SC transition lower than 12K, after annealing at 800C, all these samples got Tc higher than 15K, and the best one got Tc 16.2K with RRR near 17. Although by means of this procedure are achieved better results than by co-sputtering, this is not enough for good SC cavities, because of the non-uniformity of the film composition along the cavity profile.

In DC measurement of SC property of the sputtered films, it was found out that its SC transition width is 0.4K to 0.5K, and this is too large for low losses. In AC measurements, Tc was at least 1K lower than that of DC measurements, Δ Tc as high as 1 to 2K. They indicated that the sputtered V_3Si films suffered from many weak SC phases that should be eliminated in SRF applications of SC film. In RF measurement of the sputtered V_3Si samples by a 14GHz dielectric resonator, the measured result showed a high residual surface resistance.

Because sputtered A15 SC films generally get very high residual surface resistance, for coating a V_3Si SC cavity, other coating technique instead of magnetron sputtering is needed. As the successful going of thermal diffused Nb_3Sn film cavities, thermal diffusion of V_3Si films could reduce the residual surface resistance and get a better SRF performance. The study so shifted into thermal diffusion of V_3Si films. Bulk vanadium was annealed in silane atmosphere, and magnetron sputtered vanadium films on various substrates were studied too, the diffusion experiment got very good V_3Si samples.

Sputtered vanadium films on sapphire substrates annealed in silane atmosphere at 850C for about 10 hours got V_3Si samples with Tc higher than 16.8K, very close to the bulk material, and transition width less than 0.1K, superior to magnetron sputtered V_3Si films although the diffused V_3Si sample got a RRR less than that of the sputtered V_3Si film. In AC measurement, Tc of thermal diffused V_3Si films is 16K and Δ Tc about 0.4K.

Bulk vanadium annealed in silane got good V_3Si films too. The process temperature is approximately 900C and total annealing time about 100 hours. Thermal diffused V_3Si samples showed a similar performance like those on sapphire substrates in AC measurement. In the experiment, it was found out that there is room to improve the quality of V_3Si film on bulk vanadium by increasing diffusion time or annealing temperature. Unlike annealing of magnetron sputtered vanadium films that longer diffusion time or higher temperature will cause silicon content increased too much that the sample became non-superconductor.

Thermal diffusion experiment was studied in sputtered vanadium films on niobium and copper substrate. But the experiment on niobium substrate failed to get SC V_3Si samples as the thermal diffusion rate of vanadium in niobium is quite large that no stable V_3Si film formed on the sample surface. Therefor, niobium cannot serve as the substrate in thermal diffusion of V_3Si films unless a stable thermal diffusion buffer layer was coated on niobium surface prior to sputtering and annealing of vanadium films.

In thermal diffusion study on copper substrate, the process temperature is about 800C, by sputtering coated vanadium films on both side of the copper sheet and increasing the sputtering temperature of the sample, the problem of copper sample damage was solved. The experiments performed were not exhaustive, but the results prove that the topic is very interesting and deserves further investigation..

The device for thermal diffusion of V_3Si films on SC cavities was designed, fabricated and installed. Although there is still a lot of technical difficulty to be solved for a V_3Si film coated SC cavity, the study is on the right track: it could be expected that higher SRF performance V_3Si film coated SC cavity would be in a not so long future.

Chapter 1

An introduction to Superconducting RF cavities

1.1 RF acceleration

RF acceleration is the major technique applied in present particle accelerators. It includes travelling wave acceleration and standing wave acceleration. Although the travelling wave acceleration by periodic wave-guide structures takes another important role in RF acceleration, it will not be discussed in this limited thesis. Here, only give a very brief introduction to RF cavities, while detail aspects of RF acceleration had been introduced by many authors[1-8].

In the RF field, RF currents flow only on the surface of conductors without passing through the internal conductor bodies, unlike that of DC currents. The penetration depth of RF current in conductor is

$$\delta = \frac{1}{\sqrt{\pi f \mu \sigma}}$$

Where, f is the frequency, μ is the permeability and σ is conductivity of the conductor.

In fact, after only a few penetration depths, in conductor internal body the RF current becomes negligible. The surface resistance of a conductor is

$$Rs = \frac{1}{\delta\sigma} = \sqrt{\frac{\pi f \mu}{\sigma}}$$

It is obvious that the penetration depth will increase and the surface resistance will decrease when frequency increases. At GHz range, only a few microns of the copper surface gives a contribution to the RF current, while the rest major part served as substrate.

RF currents flowing through the metal dissipate energy through ohmic heating. The RF power loss in a conductor is

$$P = \frac{Rs \cdot \iint Ht^2 \cdot ds}{2}$$

Where, Ht is the parallel component of the magnetic field. The power loss is integrated over all the conductor boundaries.

Fig.1-1 shows the sketch of an Alvarez type acceleration cavity. Excited by an RF generator, the cavity could be driven to one of its resonant mode – π mode, in which mode, the phase difference between adjacent drift tubes is π (or 2π, in 2π mode). Charged particles injected in with synchronous phases will be accelerated in every gap, while in another half of RF period, they are shielded by the drift tubes and immune from deceleration force. In order to get the synchronous phase, distance between two adjacent gaps should be

$$l = \frac{1}{2}\beta\lambda$$

Where, β is the normalised velocity, and λ is the free-space wavelength.

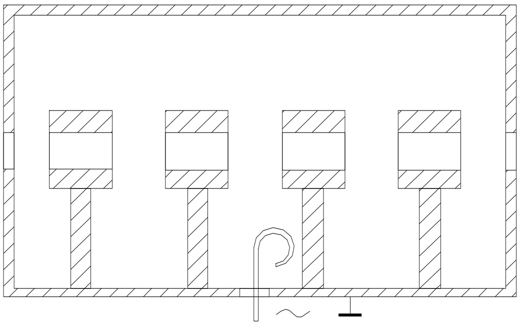

Fig.1-1 Sketch of an Alvarez acceleration structure

Actually, the acceleration voltage is always sinusoidal as it mostly simplifying the RF engineering. Because the charged particles passing through a gap experience a field that changes with the time and position, there is a transit-time effect on the energy gain. Transit-time factor can be solved numerically[9]. Assume field is uniformly distributed in the acceleration gap, and the average velocity of the particle keeps constant in the gap, then the particle will "see" an acceleration field,

$$E(t,z) = E_0 \cdot \cos(\omega \cdot t + \phi) = E_0 \cdot \cos(\frac{\omega \cdot t}{c\beta} + \phi)$$

Where, E_0 is amplitude of the rf field, ω is the angular frequency and ϕ is the reference phase.

Energy gain of the single charged particle is

$$\begin{aligned}\Delta U &= \int E_0 \cdot \cos(\omega \cdot t + \phi) \cdot dz \\ &= \int_{-\frac{g}{2}}^{\frac{g}{2}} \mathrm{E}_0 \cdot \cos(\frac{\omega \cdot z}{c\beta} + \phi) \cdot dz \\ &= E_0 \cdot g \cdot \cos\phi \cdot \frac{\sin(\theta/2)}{\theta/2}\end{aligned}$$

Where, $\theta = \frac{\omega g}{c\beta}$, transit angle, g – effective gap length.

Then, the transit-time factor becomes

$$T = \frac{\sin(\theta/2)}{\theta/2}$$

In RF cavities, there are many important parameters beside resonant frequency and transit-time factor, such as: quality factor Q, shunt impedance R_{sh}, stored energy U, peak surface electric field Ep and peak surface magnetic field Hp and so on.

$$Q = \frac{\omega \cdot U}{Ps} = \frac{f_0}{\Delta f} = \frac{\omega \cdot \tau}{2}$$

Where, Δf is bandwidth of the resonant mode, τ is decay time.

$$U = \frac{1}{2}\iiint \{\varepsilon_0 \, |E|^2 + \mu_0 \, |H|^2\} \cdot dv$$

$$Rsh = \frac{(\Delta V)^2}{2Ps}$$

There is an dependent parameter – geometry factor G, it is a constant to a selected cavity and a given mode.

$$G = Q \cdot Rs$$

In practice, R_{sh}/Q is generally used too. When R_{sh}/Q, ω and Q are given, the equivalent LCR circuit of the RF cavity is known:

$$R = Rsh$$

$$C = \frac{Q}{\omega \cdot Rsh}$$

$$L = \frac{Rsh}{\omega \cdot Q}$$

Electromagnetic energy is typically transported from an RF source to the cavity by means of either a wave guide or a transmission line. Three types of connections are often used to connect the input line to the resonant structure. A hole in the cavity wall can provide a coupling aperture to a wave guide. A coupling loop may be made on the end of a transmission line and passed through the wall of the cavity to make a transformer, or the centre conductor of a transmission line may be capacitively coupled to a site inside the cavity.

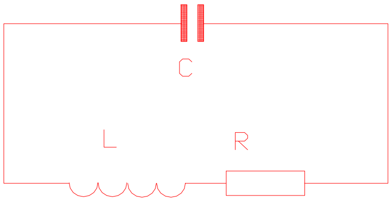

Fig.1-2 Equivalent LCR circuit of a cavity

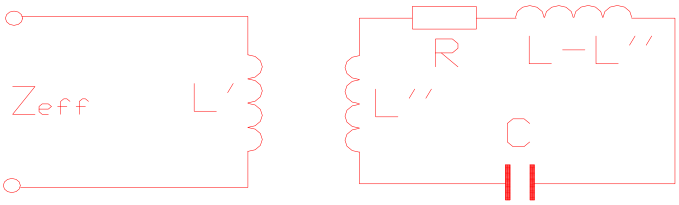

Fig.1-3 Equivalent circuit of a loop of inductance couple.

The reflection coefficient, defined as the ration of reflected to incident RF voltage for a signal from the end of a transmission line, can be written as

$$\Gamma = \frac{Ze - Z_0}{Ze + Z_0}$$

Where, Z_0 is the characteristic impedance of the line (usually 50 ohm), Ze is the effective impedance of the load attached to the end of the line.

The RF power is most efficiently transferred to the cavity when Z_0 =Ze, there is no reflection and the power dissipated in the cavity's wall equals the power being supplied by the RF source. In this case, the power converted to heat in the cavity wall will be an equal amount being dissipated in the transmission line. Then, to a correctly matched cavity, the loaded Q_L will be

$$Q_L = \frac{Q}{2}$$

When an accelerated beam passing through the cavity, the power losses will increase by the amount of power being supplied to the beam.

Normal conducting cavities are generally optimised to have a larger R_{sh}, since the surface resistance being high and the removable amount of heat generated by the dissipated rf power from the site set the performance limit. While the peak surface electric field or maximising acceleration gradient become of less importance. There is an experimental formula for sparking limit of surface field [10,11]

$$f(MHz) = 1.64 \cdot Ek^2 \cdot e^{-\frac{8.5}{Ek}}$$

The frequency-dependent field strengths are referred to as one "Kilpatrick", it is pessimistic for clean surfaces with short pulses, Ep=2Ek is usually tolerated in cavities with polished surface and short pulse operation mode.

1.2 Super-conducting material for cavities

Superconductivity was discovered by H. K. Omnes in 1911. Under the critical temperature, resistance of superconductor drops to an immeasurable small value. In 1933, Meissner effort of superconductor was discovered. When a superconductor cooled below Tc, weak magnetic field was completely expelled from its interior. While in strong fields, superconductivity broke down and the material went to normal state[12,13].

It is only in type I superconductors that a direct transition from the Meissner state to the normal state and an abrupt drop of the magnetisation to zero takes place at the critical field Hc. However, many alloys and elements belong to a second class – type II superconductor, the Meissner state is followed by a mixed state before the normal state is reached while increasing magnetic field. In this mixed state, single-quantum magnetic flux lines penetrate the superconductor forming a flux line lattice representing a mixture between the super-conducting and the normal phases. Further increase of magnetic field beyond Hc_2, the superconductor will be driven to the normal state.

The Bardeen-Cooper-Schrieffer (BCS) theory based on electron paring is one of the most successful theories in superconductivity. It came from experimental observation that electron gas in a metal is unstable at low temperature with even respect to very weak attractive forces between electrons. Attractive forces are provided by low-frequency distortions of the background ionic lattice and, form electron paired states, which accounts for superconductivity in most low Tc superconductors. The discovery of high temperature caprate superconductors in 1986 had posed the greatest challenge to the BCS theory.

The power dissipated on a superconductor surface in RF regime is related to its surface resistance and like normal conductors, but at here, the surface resistance of a superconductor is in a different form,

$$Rs = R_{BCS} + Rres$$

$$R_{BCS} = \frac{A}{T} \cdot \sigma_n \cdot \omega^3 \cdot \lambda^2 \cdot e^{-\frac{B \cdot Tc}{T}}$$

Where, R_{BCS} is the BCS resistance, Rres is residual surface resistance. A and B are two constants weakly depend on material, ω is the RF angular frequency, σ_n is the normal state conductivity of the material, λ is the effective penetration depth, and Tc - critical temperature.

$$\lambda = \lambda_L \cdot \sqrt{\frac{\xi}{\xi_0}}$$

Where, λ_L is the London penetration depth, ξ_0 and ξ are the coherence lengths in the pure and real material respectively.

$$\frac{1}{\xi} = \frac{1}{\xi_0} + \frac{1}{l}$$

Where, l is the electron mean free path.

For clean superconductors, $l \gg \xi_0$, thus, $\xi \approx \xi_0$, and give $R_{BCS} \propto l$. While for dirty superconductors, $l \ll \xi_0$, thus $\xi \approx l$, and hence $R_{BCS} \propto l^{-1/2}$. Between clean and dirty limits, R_{BCS} takes a minimum value when the electron mean free path becomes comparable to the coherence length[14].

Pure metals and pure intermetallic compounds with well defined stoichiometric composition, if they have not many crystalline defects, are usually belong to clean superconductors. On the other hand, alloys are dirty superconductors, due to their very small electron mean free path. Consequently, alloys display large BCS surface resistance, as the same reason - small electron mean free path, they have poor thermal conductivity, and hampering the thermal stability of a cavity. For these reasons, alloys are not suitable materials for super-conducting cavities.

Usually, the optimum operation condition of the super-conducting cavities is R_{BCS} ==Rres. Therefore it is important to minimise the residual surface resistance. Among the factors that define the Rres, there are extrinsic causes e.g. trapped magnetic flux, can be avoided. Other causes are intrinsic and due to the structural imperfections of the material. Like inhomogeneities, grain boundaries or surface serrations. Materials with a large coherent length will be insensitive to large defects without an appreciable increase of the Rres. This is quite desirable for applications of the SC cavity, since the super-conducting surfaces are exposed to RF field, and are difficult to prepare completely 'defect-free'.

The ideal superconductor in RF applications should has,

1. small penetration depth
2. large coherence length
3. high critical temperature and
4. high critical field.

The first two requirements come the type I superconductors, but it is known that type I superconductors usually have low critical temperature and low critical magnetic field. They are not suit to the second two demands and the BCS resistance is larger. From BCS theory, large coherence length indicates a low Tc, therefore the conflicting is indeed, and the ideal material for superconducting RF cavities does not exist. Today's superconducting materials in RF cavities' application chosen result from compromises.

In SRF cavities, most widely applicated superconductors are lead and niobium. Lead is one type I superconductor, has been used in many low frequency cavities. It has a very low residual surface resistance, cheap and easily available in a pure form. But its Tc and critical magnetic field is low, at frequency higher than a few hundred MHz, the BCS surface resistance becomes prohibitive, and it cannot be used in high gradient cavities too. Moreover, it has a poor mechanical characteristic and oxidises easily. While lead-tin alloy (around 3% Sn) is not so sensitive to oxidation, it is confined to low frequency applications and tends to be replaced by niobium.

High magnetic fields are present in accelerating cavities, thus a superconducting material with a high critical field is desirable for RF applications. Since the nucleation time of a vortex (10^{-6}s) is usually larger compared with the RF period (10^{-8} to 10^{-9}s), the relevant critical field of an RF superconductor is not the usual critical field Hc1 or Hc2, but is believed to be the superheating field Hsh[15,16]. Hsh is related to the thermodynamic critical field Hth. For type I superconductors, Hth is Hc. While for type II superconductors, Hth is Hc_2

$$\begin{aligned} Hsh &= \frac{0.9 \cdot Hth}{\sqrt{k}} && k << 1 \\ Hsh &= 1.2 Hth && k = 1 \\ Hsh &= 0.75 Hth && k >> 1 \end{aligned}$$

Where k is the Ginzburg-Landau parameter.

Table 1-1 Characteristics of various superconductors

	Tc (K)	λ (nm)	ξ_0 (nm)	Hth (A/m)	Hsh (A/m)
Pb	7.2	39	80-90	6.4. 10^{4}	8.4. 10^{4}
Nb	9.2	30-40	30-60	1.6. 10^{5}	1.9. 10^{5}
V_3Si	17	110-140	3-7	2.4. 10^{5}	3.0. 10^{5}
Nb_3Sn	18	110-170	3-6	2.5. 10^{5}	3.2. 10^{5}
YBCO	94	140	0.2-1.5	6. 10^{5}	6-8. 10^{5}

Niobium has the highest Tc and Hsh of all pure metals, being a soft type II superconductor, it occupies a position of compromise between the four requirements. Its homogeneity and purity are important issues for RF applications because they determine the thermal stability of the SC cavity.

Two parameters are relevant for the description of the thermal behaviour of the cavity, they are thermal conductivity and the Kapitza resistance at the

$$RRR = \frac{R_{300}}{R_{0K}}$$

niobium-helium interface. In the case of a hot spot, most of the thermal gradient is located in the niobium sheet, and the thermal properties of interface play a minor role. At cryogenic temperature, the major heat carriers in niobium are electrons, the mean free path can be given in terms of a quantity. The Residual Resistance Ratio is a key component.

Theoretical RRR value of niobium is 32000. Usually, measured RRR of niobium is the ratio of its resistance at room temperature and at 10K. ($\rho = 1.45\times10^{-7}\Omega\ m^{-1}$)

Electron mean free path of bulk niobium is given by

$$l(nm, T = 0K) = 2.7RRR$$

And the thermal conductivity is

$$\sigma(W \cdot m^{-1}K^{-1}, T = 4.2K) = \frac{RRR}{4}$$

In fact, bulk niobium cavities are generally made from RRR 200-300 sheets, their thermal conductivity is an order less that that of OFHC copper (approximately 400W m^{-1} K^{-1}). Post-purification of niobium can be operated by a heat treatment associated with titanium gettering. The technique is capable of improving the RRR by a factor of 10, but its drawbacks are significant, cost and severe degradation of the mechanical properties of niobium cavities. Post purification can considerably improve niobium thermal conductivity with a consequent improvement of the cavity thermal break down threshold[17].

Numerical value of the BCS surface resistance of niobium is approximately

$$R_{BCS}(n\Omega) = \frac{10^5 \cdot f(GHz)^2 \cdot e^{-\frac{18}{T}}}{T(K)}$$

To Nb_3Sn,

$$R_{BCS}(n\Omega) = \frac{10^5 \cdot f(GHz)^2 \cdot e^{-\frac{40}{T}}}{T(K)}$$

And V_3Si,

$$R_{BCS}(n\Omega) = \frac{10^5 \cdot f(GHz)^2 \cdot e^{-\frac{37}{T}}}{T(K)}$$

As a comparation, surface resistance of copper is

$$Rs(m\Omega) = 7.8 \cdot \sqrt{f(GHz)}$$

1.3 SRF cavities design considerations

It is known that normal conducting cavities are often optimised for high shunt impedance. The dissipated RF power by the cavity wall to be removed gives the performance limit, and issues of low surface electric and magnetic field are of minor importance. Consequently, the cavities are generally designed in re-entry shapes with small beam holes.[18]

Super-conducting cavities, on the other hand, are designed for low surface electric field and other features, e.g. to avoid electron multipacting, to efficiently extract the power which the ion beam transfers into high order modes, high mechanical stability, high thermal stability, easy to access the inner surface and so on. Hence, larger iris openings and rounded shapes are commonly used.

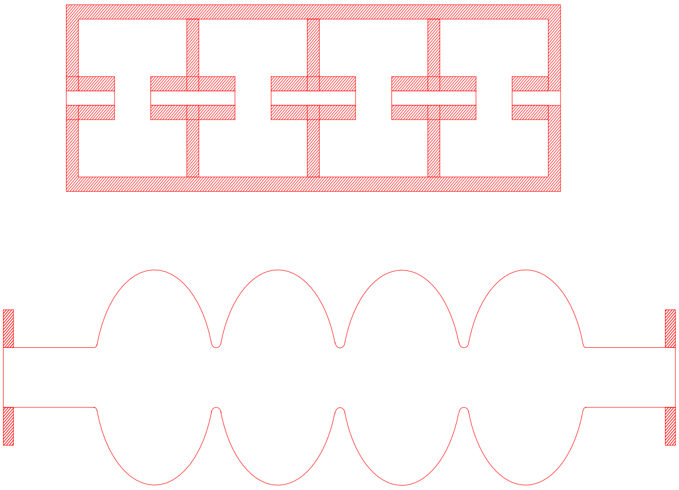

Fig.1-4 SRF cavity and normal conducting cavity.

A key component of any accelerator is the device that imports energy gain to the charged particle. Usually, SC niobium cavities are operated at frequencies between 100MHz and 3GHz. Lower frequency need to build a cavity with a larger size and a higher stored energy, while higher frequency will increase the BCS resistance. In the continuous wave (CW) operation mode, RF power dissipated on the wall of a copper structure is of the order of 0.1MW/m for accelerating field around 1MV/m. A SC cavity has a surface resistance 5-6 orders of magnitude less than that of a copper cavity, the wall RF loss is only a few watts in a single SC cavity at the same field level.

Niobium cavities often have Q values 10^9 to 10^{10}, consequently, its band width is as narrow as only a fraction of one Hz. The RF generator has to be stabilised by the cavity itself or close a self-excited loop of an amplifier with the cavity circuit. The former method is very convenient in a single cavity measurement, but in an accelerator with many SC cavities, the later is generally employed. Since frequencies and phases of all the individual cavities must be locked to a reference RF generator, in this case, frequency tuning and phase shifter system for each cavity is required.

Mechanical tuning system equipped with stepping motor and corresponding control circuit is referred to 'slow tuning' compared with 'fast tuning' - by changing phase conditions in the self-excited loop, resonant frequency changes on the phase curve. The fast tuning is widely adopted to lock the frequency and phase of the cavity to an standard external frequency. The range of this tuning is limited by the loaded bandwidth of the cavity and the most demanding parameters, concerning the operation in self-excited loops, is the RF energy stored[19,20]

$$P = 2\pi \cdot U \cdot \Delta f$$

Where, P is the required input RF power, Δf is the control bandwidth and U is the stored energy.

To optimise the operation of the RF circuit and SC cavity, the RF power provided by the generator should be doubled by the above value.

Based on quarter-wave resonant line, Quarter Wave Resonators have been a successful SRF structure for heavy ion linear boosters. The resonant frequency is usually between 80 and 200MHz, and the optimum beta from 0.05 to 0.20. Equipped with simple straight and rigid electrodes, QWR posses high mechanical stability comparing with the earlier helix or slept-ring resonators. It has a broad transit-time factor curve that benefit to accelerate various ion beam with different velocities, as it has only two acceleration gaps[21,22]. A RF structure with fewer acceleration gaps surely has lower acceleration efficiency, but in QWR, the drawback is compensated by the high acceleration gradient achieved.

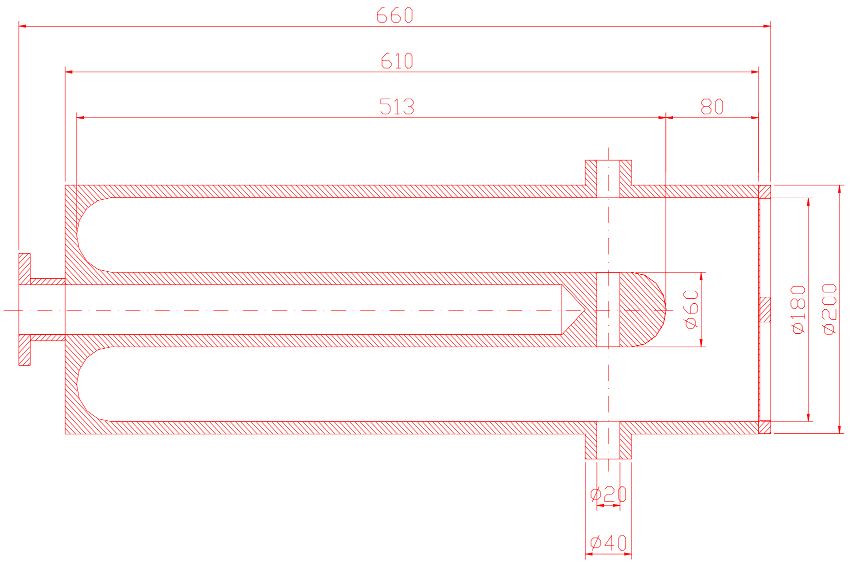

Fig.1-5 sketch of a 144MHz QWR

Fig.1-5 is a designed 144MHz QWR for the RIB facility project of CIAE, its parameters were calculated by the computer code MAFIA and listed in table 1-2. Inner electrode of the cavity is cooled by liquid helium, while that of the outer conductor wall by thermal conduction from the top end plate. The nearest High Order Modes are about 3, 5, 7, ... times as that of the frequency of the acceleration mode, and because very rare RIBs are accelerated, there is no need to damp the HOMs that usually done in high intensity beam acceleration structures.

Table 1-2 Design parameters of the 144MHz QWR

Β opt	0.125	
U	70	mJ/(MV/m)^2
G	27	Ω
Rsh/Q	500	Ω
Ep/Ea	5.0	
Hp/Ea	100	Gs• m/MV

Many computer codes are used in eigenmode computation of RF cavities, wave-guide and related problems. SUPERFISH is the most famous code of finite integral, and the first widely used code for monopole mode in cylindrical cavities. URME and MAFIA are codes with finite difference. While MAXWELL, HFSS and EMAS are commercial codes based on finite element approaches. Thanks to the rapid development of computer and software in recent years, eigenfrequency of circular symmetric structures can be obtained at extremely high precision[23], the traditional 'cut and try' method seems no use. But for more complex structures, e.g. RFQs, or to simulate some cavity performances other than resonant frequency, present codes are still not precise enough[24].

For high energy applications, the most widely used SRF cavity is spherical cavity or more correctly, elliptical cavity. It designed with optimum beta 1.0, and the shape is optimised to suppress multipacting. In operation, the cavity is immersed in liquid helium and gives a very good thermal stability. At resonant frequency around a few hundred MHz, the operation temperature is 4.2K like that of low beta structures. While frequency increased to GHz range, BCS resistance dominates the surface resistance, the cavity is needed to further cool down below 2K to achieve a good performance.

Table 1-3 Calculated parameters of the 1.5GHz cavity

G	290	Ω
Rsh/Q	94	Ω
Ep/Ea	1.9	

Hp/Ea	40	Gs.m/MV

Table 1-3 is calculated parameters of the 1.5GHz cavity by MAFIA. The dipole mode (accelerating mode) is TM010, HOMs with wavelength shorter than the cut wavelength of the beam tubes will propagate out from them, unfortunately, there are three HOMs have wavelength larger and will be trapped in the cavity.

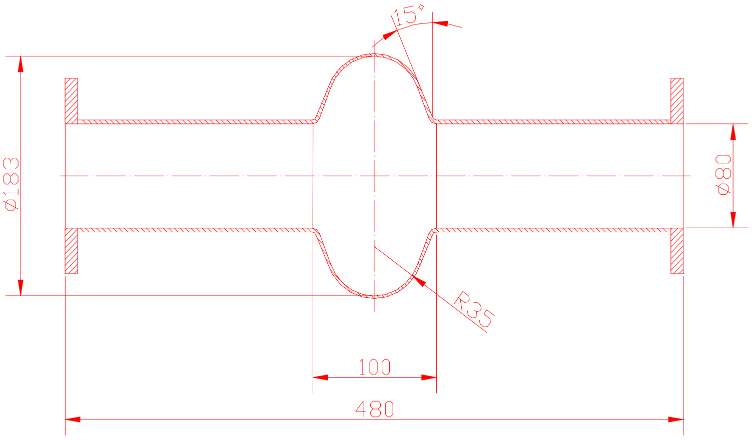

Fig.1-6 An 1.5GHz monocell spherical cavity.

When high intensive beam is accelerated, these HOMs could be excited by the beam current, and generate a field that degrade the beam quality or hamper the proper cavity operation. There are two methods used in suppressing the HOMs: enlarge the beam tubes and put RF lossy ferrite materials in some locations of the beam line so that HOMs propagated out and absorbed, or reshape the cavity with HOMs dampers[25-28].

Super-conducting cavities have been widely used in heavy ion accelerators (low beta cavity) and in electron accelerators (high beta) for more than twenty years. In recent years, high intensity proton beam linac accelerators are proposed for many applications, the energy range is between 100MeV and 1GeV with beta ranges from 0.2 to 0.8. In the medium beta applications, super-conducting structures with reduced beta cavities are at the beginning of design and fabrication[29-31].

1.4 Measurement of SRF cavities

Generally, SC cavities are very sensitive to trapped magnetic flux, in which case, the trapped flux will cause significant increasing of the residual surface resistance and greatly degrade the cavity features. And surrounding mechanical vibrations are another hinder of the routine cavity operation. Cryostat is used both in operation and measurement of SC cavities, it not only provides a stable controlled cryogenic temperature, but also a magnetic flux shielding and a vibration-proof environment.

SC cavities have a bandwidth only a fraction of one Hz. To measure its bandwidth, RF generator has to be more stable than that, on the other hand, the SC cavity will vibrate due to noise from cryogenic or the surrounding environment. Therefore the resonant curve itself will shift and a fixed highly stable oscillator will be unable to excite the resonator. The solution is that the generator generally has to be stabilised by the cavity itself, and locked to the central frequency of the cavity.

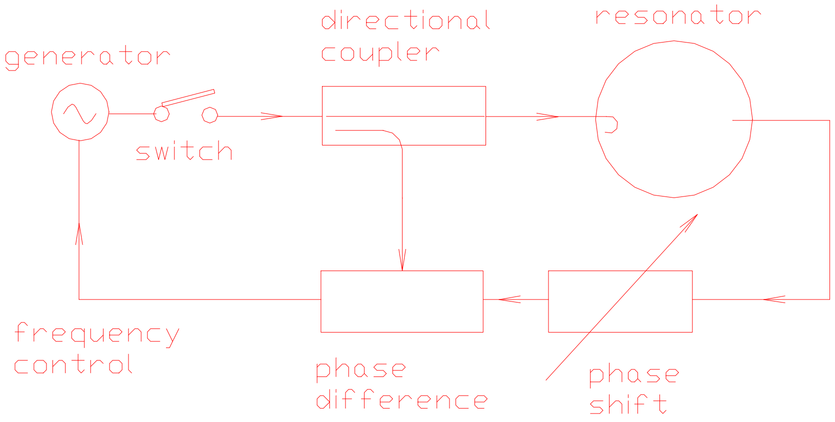

Fig.1-7 Principal circuit of a frequency stabilisation system

Since high Q factors of SC cavities, the decay time commonly reaches the order of a second, it is very convenient to measure and deduce the Q value. Because the Q factor is related to the stored energy in a cavity, this method only valid to small stored energy or Ea ≈ 0, where Q value is nearly a constant independent to the acceleration gradient[32]. After the Q being deduced, the stored energy U can be derived by $U=Ps*Q/\omega$, where Ps is the absorbed energy by the cavity. Using the result of computer code calculation or perturbation measurement carried out at room temperature[33,34], acceleration gradient Ea of the cavity is known then, since U/Ea^2 is a constant to a given cavity[35].

At high accelerating gradient, when the Q value is related to Ea, the Ea-Q curve is got by measuring the absorbed power and test of port voltage of the cavity at each field level. Fig.2-8 is a block diagram of a SC cavity measurement circuit, by measuring RF power of the port 1, 2 and 3, Ea-Q relation of the cavity can be given.

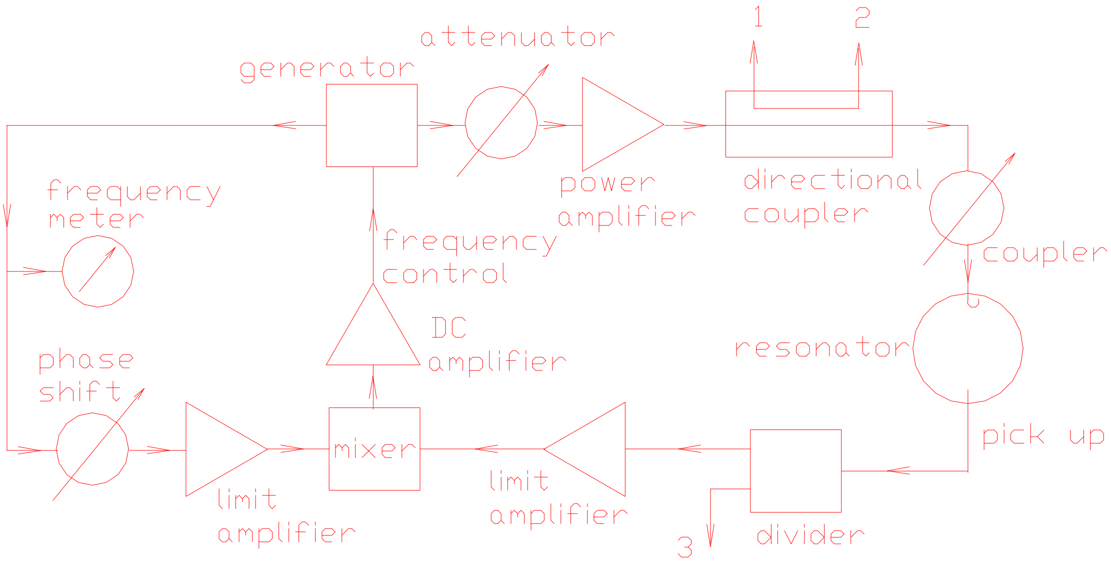

Fig.1-8 Block diagram of a SC cavity measurement circuit.

1.5 Fabrication of SC cavities and high gradient

In SRF technology, up to now, niobium cavities achieved the best performance both in low beta acceleration structures and in high beta resonators. Many laboratories around the world involved in the improvement of SC cavities including niobium purification, cavity fabrication, surface polishing, RF conditioning, and some industry companies have joined in the progress for many years[36,37].

The maximum accelerating gradient occupied in low beta SC structures, is JAERI's Cu-Nb clad 130MHz QWR cavities. The optimum beta value is 0.10, and the maximum accelerating gradient is approximately 13MV/m, corresponding to a peak surface electric field of about 60MV/m. Its outer conductor is explosively bonded 2mm thick bulk niobium (RRR from 80 to 100) sheet with 8mm thick OFHC copper. And the inner electrode is bulk niobium sheet about 2mm in thickness. After mechanical polishing, the inner electrode was welded to a bulk niobium top plate by electron beam welding, which then EBW welded with the niobium layer of the outer conductor. Finally, the cavity was electrical polishing, chemical polishing, pure water rinsing and RF conditioning as that of bulk niobium cavities[38].

Some of the Cu-Nb clad cavities get a problem of absorbing hydrogen and Q degradation, since large stress existed on the Cu-Nb clad, it is impossible to degas the absorbed hydrogen by heating up the cavities to high temperature which is frequently employed in bulk niobium cavities in such case. Consequently, the average accelerating gradient with beam load is 5 to 6MV/m, similar to that of general bulk niobium cavities.

The world record of accelerating gradient of SC cavities is 43MV/m, close to the theoretical limit of about 50MV/m, it is achieved by a 1.3GHz bulk niobium monocell spherical resonator fabricated by the co-operation works of CEBAF and KEK. Different parts of the cavities were made from niobium sheets (RRR no less than 200) by deep-drawing, and EBW welded together, then electrical polishing and chemical polishing more than 100um. After heat treatment, high pressure pure water rinsing (100kg/cm^2) and high pulsed power RF conditioning[39,40], the residual surface resistance reduced to 2.6nΩ , while measuring at 1.6K, the cavities get a peak electric field about 80MV/m.

The most important principle of SC cavity besides material is a very clean and finely polished surface. Since a rough surface will significantly increase the surface resistance and severely decrease the performance of cavities, while dusts generally served as electric field emitters and local hot-spots, which are the two major factors that prevent for high gradient. Therefore, high quality SC cavities are often assembled in class 100 clean room, chemical or/and electrical polishing of the surface 100 to 200um to remove all defects generated in mechanical process. High pressure pure water rinsing at 80-100kg/cm^2, and high pulsed power RF conditioning with an ambient helium gas 10^{-3}Pa also take important roles.

Seamless cavities developed rapidly in recent years, the important advantages of them are material saving and cost saving, as there is no need of EBW. But hydroform of niobium cavity generally need three intermedium annealing steps and the process is quite difficult, and became less adopted. Spinning of niobium seamless cavities have been successfully realised in monocell cavities, five cells, seven cells and seems there is no principle difficulties to spin a nine cell cavity or with even more cells. Today, the maximum accelerating gradients reached by spun single cell cavities and multicell ones[41] are around 30MV/m.

Chapter 2

Sputter niobium cavities.

2.1 Introduction to sputter

Sputtering technology has been widely used in semiconductor industry for about only three decades, and in other applications are even later, e.g. in super-conducting cavities is recent 10 years. It would come as a surprise to find that sputter process is a very 'old' discovery, W. R. Grove discovered glow discharge[42] in 1852. It was in the 1920's that pioneering works of I. Langmuir laid the foundation for modern plasma physics and let us to a much better understanding of the gas discharge environment in which sputtering operates[43].

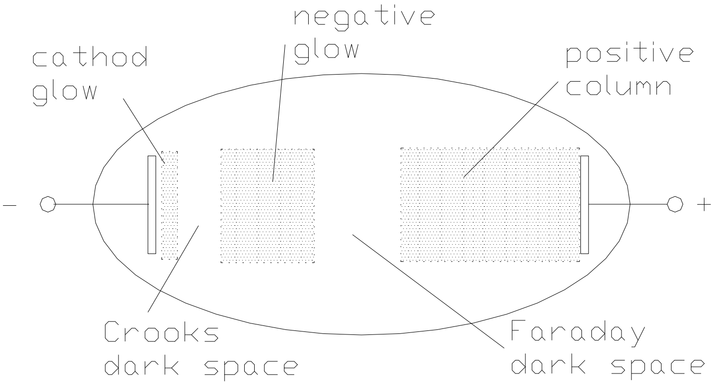

Fig.2-1 Glow discharge

The most simple device of glow discharge is a vacuum tube enclosed in two electrodes and inert gas. Applied DC voltage to the electrodes, while above the threshold, glow-discharge occurs. In the glow-discharge, there are several intervered glow and dark zones. While the most important zone is the crooks dark space, where electrons from the cathode accelerated and travel to the negative glow and ionize, at here, positive ions accelerated toward the cathode and cause sputter and generate secondary electrons that sustain the discharge. The distance of crooks dark space is the average distance an electron ionize, which is about five to ten time larger as the electron mean free path (since there are many collisions that do not generate ionization). In the region of negative glow, numbers of positive ions and electrons are approximately equal, the region is nearly neutral and called plasma.

The sputtering process removes atoms of the bombarding surface, so the target surface being eroded or sputter etched, while the sputtered atoms will deposit on the anode and on the wall of vacuum chamber. Therefore, sputtering technology is applicated in deposition of thin films or, in surface etching. In practice, sputter deposition of films often operate in 'abnormal' regime that the power to the discharge is past the point where the glow covers the entire available cathode area.

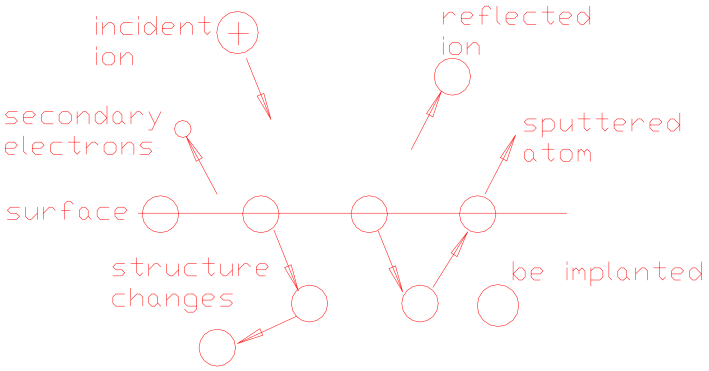

Fig.2-2 Sputter process

Microstructure is a critical consideration when polycrystalline or amorphous thin films are sputtered. Because in sputtering deposition, substrate temperature is low relative to the coating material melting point. An essential feature of the thin film is that they are formed from a flux that approaches the substrate from a limited set of directions, consequently, the metallurgical grains tend to be columnar. The grain or growth boundaries presents preferred diffusion path that often extend through the entire coatings. Early in 1969, evaporated coatings structure zone model was published, in 1973, the zone model was extended to magnetron sputtered metal films by adding an axis to account for the effect of argon pressure[44,45].

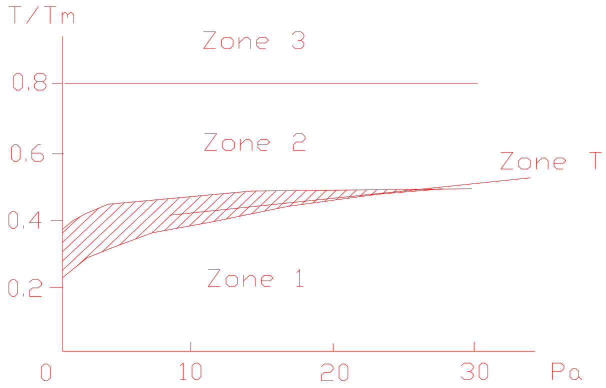

Fig.2-3 Structure zone model of magnetron sputtered metal films

From the zone model, zone 1 is columnar structure, its tends to extend to high temperature region while substrate surface irregular. Intense energetic ion bombardment during deposition of refractory metal can largely suppress the development of zone 1 structure at low T/Tm. Zone 2 is columnar with increased grain size, and zone 3 closes to the crystalline structure of bulk material. Zone T structure is dense with a mirror-like surface topography. The zone model gives a general guideline of a certain kind of materials, while depositing of other materials or using different sputtering techniques, other zone models need to develop[46].

Comparing with evaporation coatings, sputter has low deposition rate, but the film adherence is much better, since the evaporated atoms in an energy of only 0.1eV order, while sputtered atoms from a few eV to several tens eV. Many kinds of sputtering techniques are widely used in industry as well as in research, such as, DC sputtering, RF sputtering, magnetron sputtering, reactive sputtering, ion beam sputtering etc. I will give a brief introduction to bias DC diode sputtering, magnetron sputtering and reactive sputtering since they are involved in the following experimental works.

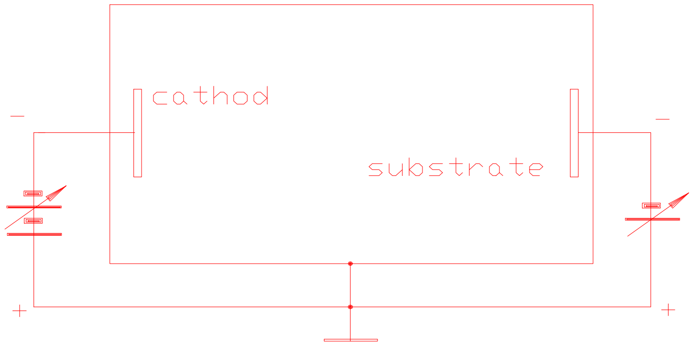

Fig.2-4 Bias DC diode sputtering.

Bias DC diode sputtering is an improvement of the most simple DC glow discharge by introducing bias voltage to the substrate. When the substrate applied negative bias, a fraction of positive ions in the plasma will bombard the surface of deposited film as well, and some trapped impurities will be knocked out from the film. As a result, film purity will increase.

The fraction f of impurity trapped in a film is given by

$$f = \frac{\alpha N}{\alpha N + R}$$

Where, N is the number of atoms of impurity bombarding unit area of film in unit time, a is the effective sticking coefficient, R is the deposition rate of the film.

While introduce negative bias, the fraction becomes

$$f = \frac{\alpha N - B}{\alpha N - B + R}$$

Where, B is the rate of trapped impurity being sputtered out from the film.

In the above equation, it comes the general methods applied to reduce impurity in sputtering deposited films. Decrease N by increasing background vacuum and using high purity target, or one can decrease a. Apply bias with a suitable B term, or increase deposition rate R will work too. But all of them are limited either by technique difficulties or material properties, and generally it need to combine them to get high quality films.

The effect of energetic ion bombardment is very complex as many surface processes involved. Some important properties of the deposited thin films such as crystalline, residual stress and adherence, some physical parameters and chemical compositions will be modified too, and there is not a general model that could be applied to all kinds of material[47-49]. For instance, negative bias is appreciated to deposit high quality refractory metal films like niobium, the energetic ion bombardment reduce impurities of the film and increase the grain size, but for other kinds of films, the grain size might decrease while being bombarded. There are reports showed that the A15 compounds are not benefited from ion bombardments[101,103].

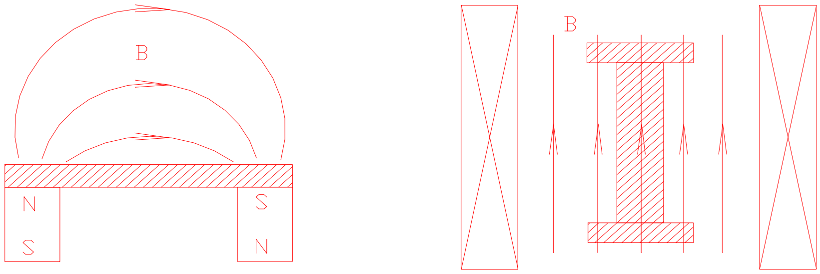

Fig.2-5 A planar magnetron and a cylinder post-magnetron equipped with electric mirrors.

In magnetron sputtering technique, a few hundred Gauss magnetic field is applied on surface of the target, electrons will rotate along the magnetic flux with diameters around a millimeter while massive ions are nearly unaffected. The result is equal to increasing of argon pressure as electron travel longer path and causes more ionization collisions with ambient argon atoms. Unlike diode sputtering, in a magnetron, most of electrons are confined near surface of the target instead of bombarding the substrate, consequently, substrate temperature will not rise too high, and 'cold' sputtering deposition can be performed.

Magnetron technique markedly increase practical deposition rate of the sputtering, reduce sputtering pressure and benefit with implications where free atomic paths become macroscopic. It opens a new range of possibilities for easy manipulation and control of thin film growth and properties. Over the past 3 decades, magnetron sputtering has been established as one of the most important tool in thin film deposition technology[50,51].

Reactive sputtering operated by introducing reactive gases beside the inert ones during the glow discharge process. The reactive gases will chemically react with the target material in an ambient plasma conditions and deposit reaction compound films on the substrate. The reaction could occur on the surface of the target, in the plasma or on the surface of the substrate depends on involved materials and the sputtering situations.

2.2 Sputter niobium films

RF currents flow only on a very thin surface on superconductors too, but the penetration depth of RF current cannot be determined by the equation of normal conductor as the DC resistance of a superconductor is negligibly small or really zero. The RF current penetration depth of a superconductor is determined by the effective penetration depth, which is related to the London penetration depth, and has a range between 30 and 200nm for various superconductors. The rest major part of the wall of a superconducting RF cavity (usually has a thickness of a few millimeters) served only as substrate.

While niobium substrates have very poor thermal conductivity and poor mechanical properties, moreover the price is much more expensive than that of OFHC copper. Therefore, OFHC copper cavities sputtering coated with niobium films come as a very good solution to SC cavities fabrication. It is not only cost saving particularly for a large RF superconducting project, but also being expected to achieve a better cryogenic performance since the thermal stability and thermal break-down threshold of the cavity is improved.

Niobium sputtered films have been widely investigated in the last 20 years in the context of different applications of superconductivity[52]. Although Residual Resistivity Ratio (RRR) of the sputtered thin niobium film is not so important as that of bulk niobium due to the good thermal conductivity of OFHC copper substrate, RRR is still an universal parameter determining the critical temperature of the superconductor. In niobium film, RRR also determine the magnetic field penetration depth, while it is mainly determined by grain-boundary scattering.

Sputtered niobium films generally have submicron size grains, which is at least three orders of magnitude tiny as that of bulk niobium. They have some properties superior to the bulk material. E.g. its Tc and upper critical magnetic field is higher, some films have Tc around 9.5K instead of the bulk value 9.2K, and it was demonstrated the highest Hc2 of niobium film is by a factor of 30 larger than the bulk sheet[53]. Niobium sputtering coated RF cavities are insensitive to ambient magnetic field, and usually get a lower BCS surface resistance that yield higher Q_0 than that of bulk niobium cavities.

It is well known that the RF losses in bulk niobium cavities (or lead-plate cavities) depend on the magnetic flux trapped during cooling down from the nc to the sc state. In a niobium cavity, the magnetic field induced local residual surface resistance R_M is proportional to the ambient

$$R_M = R_N \cdot \frac{H_{Ext}}{H_{C2}}$$

field's component normal to the surface Hext,

Where R_N is the normal surface resistance at low temperature,

Due to the much higher Hc2, sputter niobium cavities are quite insensitive to the ambient magnetic field. And in the frequency no more

$$R_N = 25 \cdot \sqrt{\frac{f(GHz)}{RRR}}$$

than several hundred MHz, let's say 500MHz, shielding of the earth's magnetic field that required by bulk niobium (and lead-plate) SRF cavities become unnecessary, and can be saved.

From BCS theory, higher Tc often yields lower surface resistance, moreover, between clean and dirty limit, superconductor yields a minimum BCS surface resistance when the coherent length become comparable with the electron mean free path. In sputtered niobium films, due to the reduced electron mean free path, BCS surface resistance below one half as that of heat treated bulk niobium cavities was achieved[54].

Besides Tc and RRR, other features as adherence, stress and thickness of sputtered niobium films are of great care too during the deposition process. Good adherence of sputtered films often get on clean, finely polished substrates, and a smooth surface also yields low surface resistance close to the theoretical value which derived from ideal surface. It is very important to have a very clean, smooth copper substrates surface like bulk niobium cavities. Similar surface treatments such as mechanical polishing, electric polishing, chemical polishing, high pressure pure water rinsing are needed.

Some features are related to the film thickness, e.g. RRR depends monotonically on the film thickness which mainly due to the grain size growing, but topography of thick films commonly become more rough with the grain size increasing that result in larger RF surface resistance[55]. Meanwhile, thick film usually posses high stress that should be avoided in SRF cavities, because the temperature variation of the cavities is several hundreds centigrade from sputter depositions to cryogenic applications, thermal stress, if big enough, could cause the niobium films strip off from the wall of copper cavities.

But the thickness of sputtered niobium films cannot be too thin as well. One reason is that certain penetration depth existed e.g. 30 to 40nm for niobium, the cryogenic SC state might be damaged if the RF current penetrates the super-conducting film and flows on the nc copper. Another reason is that thin niobium films often has not a integrity crystalline structure, with many impurities such as oxygen and carbon in the films, film quality will be far from being appreciated. Generally, niobium films sputtering coated on SRF cavities are no less than 1 micron in thickness, and the maximum thickness is around 4 microns.

It was noted that RRR depends on film thickness mainly due to the grain growing with the niobium film thickness. There is another factor although of minor importance, the gettering effect of the sputtering deposited niobium films. Like titanium, sputtered fresh niobium films will getter ambient gas atoms, as more impurity gas atoms buried in sputtered films, surroundings become more clean and following sputter will get more pure films. But if too much impurity buried in the interface of the copper substrate and the deposited niobium film, cryogenic properties of the cavity will be poor. Generally, background vacuum better than 10^{-7}Pa is necessary.

2.3 Sputter niobium QWRs

Sputtering coated niobium films on OFHC copper QWRs have been successfully fabricated at LNL, bias DC diode sputter technique is used in the deposition of niobium films. Australian National University developed a DC magnetron sputtering configuration independently[56-59]. Since the arrangement of magnets in a QWR is somewhat complicate and difficult to control the magnetron discharge, bias DC diode sputtering seems to be a simple and flexible choice. Based on cooperation of Peking University and CIAE, the study on sputtering coated niobium films on a copper QWR is in progress[60].

In the sputtering deposition, copper substrate surface situations greatly determine the niobium film quality. Welding or brazing locations always get different film topography compared with other areas that caused by the different interface between the deposited niobium film and the substrate. These locations are trouble making areas some times, that deteriorate the cryogenic performance of cavities. With brazing, the cavities cannot be sputtered at temperature above 500℃ for a long time, as thermal diffusion problem of the brazing material; without it, the sputter temperature can as high as 700 to 800℃ that benefit to get high quality films. At LNL, bulk copper cavities without any brazing or welding are developed. Constrained by the limited mechanical resource, Peking University chose a resonator with brazing.

Homogenous films coated on all the interior cavity surface is the preliminary requirement, the copper cavities have to be modified from the 'standard' SC QWR, e.g. its electrodes are coaxial straight cylinders without additional central beam tube, and the end plate is curved. From electric field analysis by MAFIA, beam hole 20mm in diameter directly excavated on the 60mm diameter central electrode comes as a good compromise; beam quality will not degrade much. While the curved end plate resulted from LNL's sputtering experiments. They found that the sputtered niobium films often get thickness problems in the corner areas with the general plain end plate, by increasing the curve and avoid a sharp corner the problem was sloved.

Sputter system include vacuum chamber, vacuum monitor, turbo-molecular pump set, baking system, argon inlet, DC power supplies, niobium target and electric feed-through. The niobium target is 2 to 3 mm thick and diameter 120mm that is in the middle point between the inner and outer conductor of the cavity. Since an uniformly distributed electric field is of critical importance in the DC sputtering, the cavity wall need to be prolonged by a metal collar which gives the lower cavity part homogenous film deposition. LNL used it first, while CIAE independently developed it[61] and applicated in the sputtering configuration at Peking University.

In the beginning, a dummy QWR with holes in different regions on the cavity wall was used in investigation of the sputtering. The sample carrier system cannot employ exposed screws and nuts that usually used in magnetron sputtering, so as not to disturb the electric field[62]. Quartz samples were mounted in these holes, after sputtering, film thickness measured by a step, other features like RRR, Tc by the standard four-probe DC resistance measurement, and film surface analyzed by a Scanning Electron Microscope (SEM). Fig.2-6 shows profile of the sputtering arrangement, and table 2-1 is typical sputter parameters.

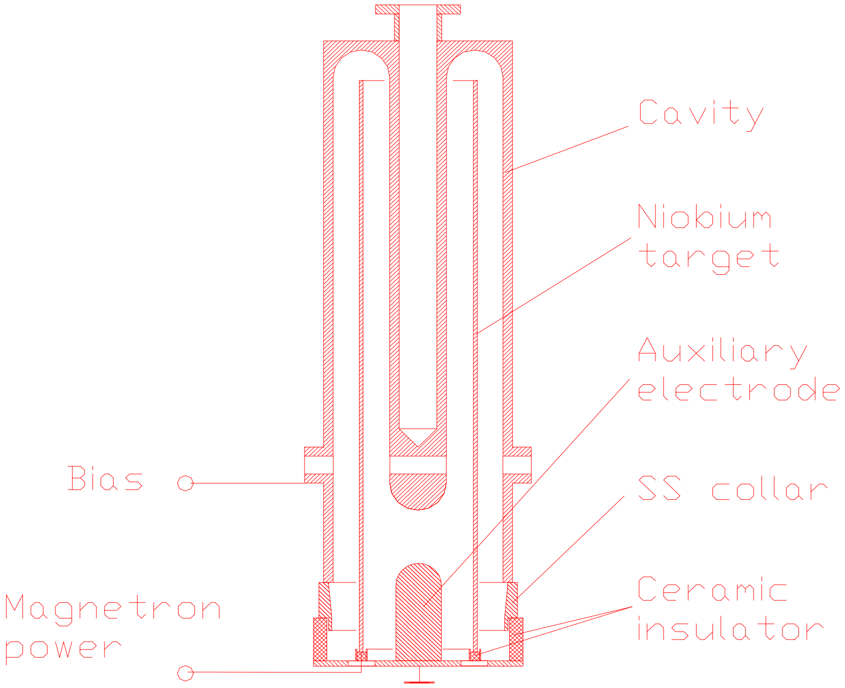

Fig.2-6 QWR sputter profile. (vacuum system emitted)

Table 2-1 QWR sputtering parameters

Argon	20Pa
Voltage	-600V
Current	6A

Bias	-100V
I_{Bias}	5A
Temperature	400-700°C

In sample measurements, niobium films with thickness 1 to 3 microns RRR should be 10 to 20. Because the surface area is different between the inner conductor and the outer conductor of the cavity, different deposition rate on them is existed. The inner conductor generally get a deposition rate 2 to 4 time as that of the outer one that could be controlled by varying argon pressure and related discharge conditions.

The QWRs were made from OFHC copper with purity 99.99%, lower grade OFHC copper (99.95%) also been used at LNL. The standard process after machining is tumbling, bright dipping, electropolishing, chemistry with SUBU, passivation, high pressure ultra pure water rinsing and electronic grade ethylic alcohol rinsing[63].

Tumbling is an important mechanical finishing in the cavity fabrication process. After machining, the cavity filled with water, finishing media and detergent totally 50-60% of the resonator volume. The finishing media is preformed resin-bonded media which is abrasives like aluminum-oxide powders from a few microns to about 25 microns in diameters bounded into polyester or urea-formaldehyde resins in different shape and size. Amount of the media is 1/5 to 1/3 in volume of water. Put the cavity on a rotating machine with a rate about 2 to 3 seconds per turn. The tumbling speed should be very slow, it takes for several days to get rid off all tracks of the machining and get a bright shining surface.

Bright dipping is used to remove copper oxide scale or tarnish, the solution is 50% hydrochloric acid or 20% nitric acid plus 80% phosphoric acid. The process is simply to immerse the cavity in the solution around 2 minutes.

Electropolishing is employed to remove about 50 microns of the copper surface, solution is phosphoric acid and normal butanol. By measuring V-I curve of the solution, electropolishing curried at the lowest resistance point. Since the V-I characteristic varies with the process time, it is needed to repeat the measurement and change the voltage and current in a few minutes all the process[64].

Chemical polishing or SUBU, which transferred from CERN, is the final polishing process. The solution contains sulphuric acid 5g/l, ammonium citrate 2g/l, hydrogen peroxide 50ml/l and normal butanol 50ml/l. Temperature and time is the two major controlled parameters in SUBU, constant temperature of 70℃ with variation less than 5℃ is highly suggested, and generally the process takes 30 minutes.

Passivation refers to the process of forming a protective film on the copper cavity. The solution is citric acid and sulphuric acid. Spray uniformly the solution on the cavity surface, wait it dry and repeat several times the process, the cavity surface will be covered by a compact oxide layer that prevent further oxidize of interior copper cavity body.

High pressure, 80 to 100Bar ultra pure water (18MΩ cm) rinsing (HPWR) is of critical importance for removing dust and contamination from the cavity surface. After the HPWR, the drying process, cavity transport and assembly should be curried at every possibility to avoid any dust and contamination. The cavities usually need to perform HPWR several times before and after the niobium sputtering.

At LNL, the niobium target is made from bulk niobium sheet with RRR 200 to 300. Electric wires, screws and nuts that connected to the target are all niobium made, significantly reduce contamination of alien materials. Bake the vacuum chamber including the cavity at 400℃ for 50 hours before sputtering, and background vacuum reaches 10^{-7}Pa. The cavity temperature is 400℃ in the beginning of sputtering, after sputtered for 20 to 30 minutes, it increases to 700 - 800℃. It takes several hours to cool down the cavity temperature and start the next sputtering run, totally 4 to 8 such runs are needed to reach the 2 to 3 microns film thickness. The tuning plate is sputtered independently in another chamber.

The best niobium sputtered QWRs get Ea 7.7 MV/m at input RF power approximately 7W, and the maximum accelerating gradient reached 10MV/m, comparable with bulk niobium QWRs. In the ALPI operations, the niobium sputtered cavities showed a better frequency stability than that of the bulk niobium cavities. Due to the thick copper wall (around 1cm) the sputtered cavities are much more rigid and insensitive to the pressure vibrations of liquid helium.

2.4 Sputtered 1.5GHz monocell spherical cavities

In 1992, niobium sputtered four cell 350MHz spherical cavities reached a maximum acceleration gradient of 8MV/m, and 1.5GHz monocell cavities got 14MV/m at CERN[65,66]. They developed a magnetron sputter configuration of the SRF cavities. Different magnetron configurations have been developed at Saclay[67], and LNL. Today, the maximum acceleration gradient of the best sputtering coated niobium 1.5GHz spherical cavities is above 20MV/m.

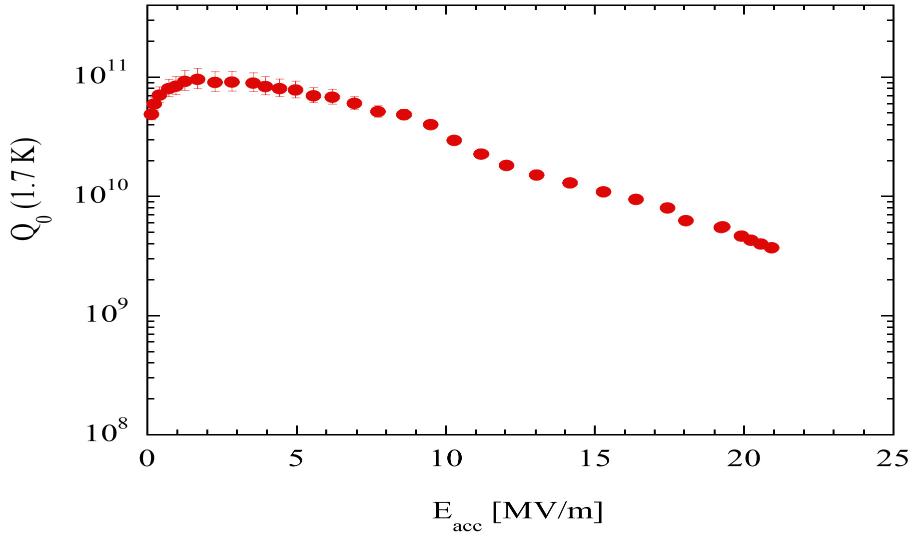

Fig.2-7 Performance of one CERN’s sputter 1.5GHz cavity

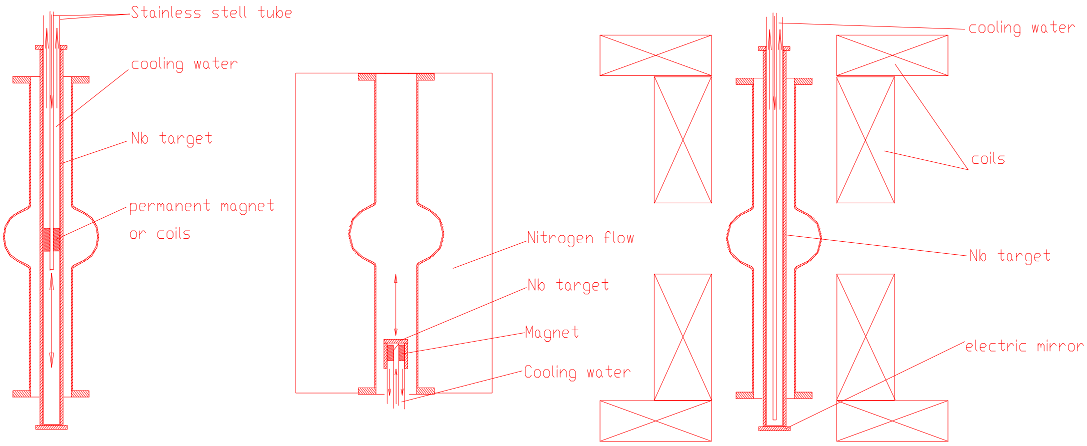

(a) (b) (c)

Fig.2-8 Different magnetron configurations
(a) CERN (b) Saclay (c) LNL

Sputter 1.5GHz cavities usually use seamless cavity. There are three different kinds of methods to fabricate seamless copper resonators that used in niobium sputtering, spinning, hydroforming or electroforming. CERN studied the surface resistance properties of niobium films on all the three kinds of copper cavity substrates and found that the spinning cavities yields best cryogenic rf performance[68]. They also investigated sputtering medium like Xe, Kr, Ar, Ne or Ar-Ne mixtures at CERN, while at LNL and Saclay only studied argon. All the standard niobium films is approximately 1.5 microns in thickness, RRR in the range of 20 to 30 and Tc 9.4 to 9.5K.

The spun OFHC copper resonators are usually 1 to 2mm thick with very shining interior surface, since the aluminum mandrels used in spinning are finely polished. There is no absolutely necessary of time consuming tumbling process. The cavities undergone electropolishing, chemical polishing, HPWR, drying and ready to sputter. Due to larger stress generated in the spinning process, the cavity wall becomes quite rigid which is benefit to mechanical stability in an ambient liquid helium surrounding. Any annealing that might soft the copper cavity should be avoided.

At LNL, only spun cavities had been sputtered. The system consists of a turbo-molecular pump set, argon line and dosing valve, niobium target with water cooling, DC magnetron power supply etc., and the resonator served as a part of the vacuum chamber. The background vacuum is around 5×10^{-8}Pa after baking 24 to 48 hours at 150℃. Outside solenoids generate a magnetic field about 200Gs in the cavity center. In the sputtering, the cavity temperature was kept constant at 150℃. Other parameters are listed in table 2-2.

Table 2-2 Sputter parameters with outside solenoids

Ar	0.3Pa
U	400V
I	4A
Time	20min

Sputtered cavities only reached Q_0 $1\text{-}2\times10^{8}$ at 4.2K, and the maximum acceleration gradient was a few MV/m limited by cryogenic power due to the low Q value[69]. From sample measurements, niobium films on the two iris of the cavity are much thicker than other areas; while the average thickness of niobium films on other areas is 1.5 microns, the two iris were 3 to 4 microns or even more in some sputtering runs. After many sputtering experiments failed to solve the problem, it was decided to abandon the outside solenoids and adopt CERN's configuration.

A permanent magnet and a small solenoid was used in side the niobium cathode to replace of the outside solenoids in the following sputtering. It could move up and down freely to sputter at various locations of the target, magnetic field on the target surface is around 200Gs too. In a few runs, film thickness variation less than 15% over all the cavity's sputtering surface was achieved. The sputter parameters are listed in table 2-3.

Table 2-3 Sputter parameters with center magnet.

Temperature	150°C
Argon pressure	0.2Pa
U_{cell}	400V
I_{cell}	3A
T_{cell}	20min
U_{tube}	400V
I_{tube}	2A
T_{tube}	6*×3min

** 3 different locations on each beam tube.*

Unfortunately, the cryogenic RF performance of the sputtered cavity has very little improvement although the film homogeneity improved a lot. Sample measurement with niobium films deposited on quartz substrate for RRR and Tc cannot give us more information. One sputtered cavity was cut into 1×2 cm^2 pieces, and we measured the several hundreds Nb/Cu samples by the AC susceptibility technique[70,71].

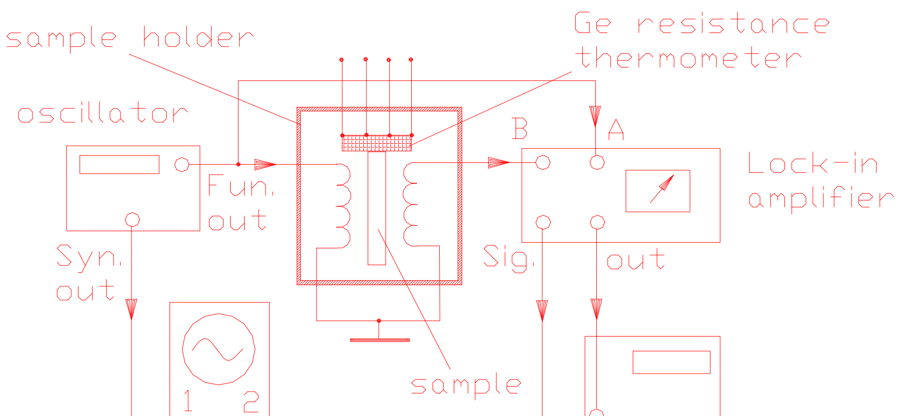

Fig.2-9 Block diagram of the AC measurement

Since AC lock-in detection is sensitive to all sc states of the samples no mater metal or ceramic substrates, while the DC resistance measurement works only on insulator substrates and could only detect the sc state with the highest Tc, all rest sc information of the sample will be shielded. We wished to find out some thing by the AC measurement that could give an explanation to the poor RF performance. But we were disappointed to see that the result nearly told us nothing.

The sputter chamber was moved into a new room - a hundred thousand class clean room, and cavity assembly in a ten thousand room. Diameter of the niobium cathode increased from 30mm to 40mm, and three major improvements in the pre-sputtering procedure had been done[72],

1) Installed a new hydraulic circuit for the chemical treatment, the previous bath system was replaced. The new system avoid etching the outer surface of the cavity and reduce the risk of bath pollution.

2) A new ultra pure water system was mounted, it has higher flow capacity than the old one. The prolonged rinsing effectively improved cavity surface cleaning.

3) Instead of alcohol rising and drying by filtered nitrogen flow, drying the cavity in a rough vacuum (200mbar) nitrogen flux, dust contamination reduced significantly by this way.

HPWR of the sputtered cavities makes an obvious improvemeny of the

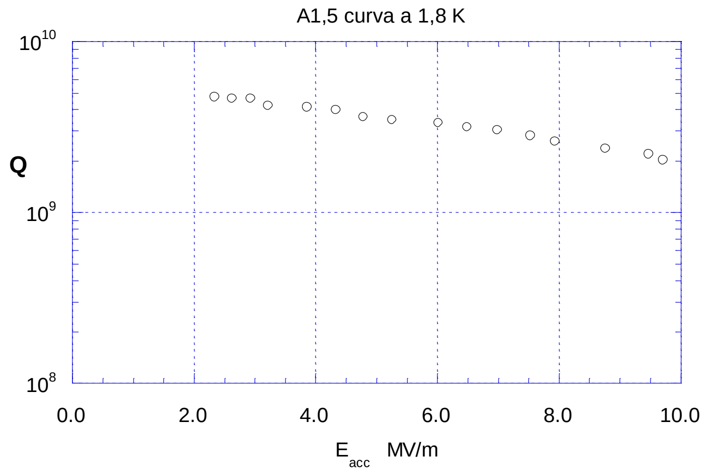

rf performances, and all the above efforts has a contribution to recent improvement of the cavity features. One cavity got Q_0 10^9 at 4.2K, and the maximum acceleration gradient reached 10MV/m at 1.8K.

Fig.2-10 Q vs. Ea curve of one 1.5GHz cavity at 1.8K

2.5 Discussion

Sample analysis of sputtered niobium films is the primary step in investigation of niobium sputter-coated SRF cavities; film crystalline structure, thickness, Tc and RRR are important diagnosis of the sputter deposition. Good niobium film is required to get good SRF cavity, but good niobium film does not grant of good cavity. Other situations like surface polishing and cleaning, substrate cavity fabrication and interface of niobium film and substrate are important factors too. Investigation is continued.

One advantage of sputter coated niobium cavities is that the copper cavities could be sputtered and stripped off niobium films several times until good cavity got or the substrate etched too poor to sputter again. 5.5M hydrofluoric and 0.9M copper nitrate mixture can be used in stripping off the niobium films from the copper cavities.

In the early days of sputter niobium cavities, the None-Quardic Losses which made Nb/Cu cavities get very poor Q value at high acceleration gradient was proved to be the result of magnetic flux penetrate of the niobium films. But resent studies showed that the NQL is not an intrinsic feature of sputter Nb/Cu cavities, the problem seems to be how can we get and reproduce the best cavities.

Sputter niobium coated low beta QWRs and high beta spherical cavities are still under investigation and development, medium beta SRF cavities began to join in the sputtering coated resonators family recently[73]. Many efforts on the development of sputter-coated niobium SRF cavities have been done, and there are more left to further studies, the sputtering technique will be applicated better as we understand it more well.

Chapter 3

Sputter niobium films on a model RFQ

3.1 Design of superconducting RFQ

Radio-Frequency-Quadruple (RFQ) is a successful linear accelerator structure for low velocity ions with beta from about 0.01 to 0.05, it is essentially an alternating-gradient-focussing channel with acceleration added as a perturbation to the fundamental structure, focuses and accelerates ion beam with the help of electrical RF quadruple fields. It proposed by Kapchinskii[74] first in 1970. As the RFQ can simultaneously focus, bunch and accelerate ion beam directly from ion source, and appropriate to get strong focusing and high capture efficiency, it has been applied in many laboratories as an injector for Alvarez accelerators, and began to dominate the area of low energy linac from 1980s[75,76].

Supercouducting RFQ (SRFQ) modeled in 1988 by I. Ben-Zvi[77]. It was demonstrated that RFQ is very suited to fabricate it a superconducting resonator since the RFQ posses many structures with good properties, e.g. the four-vane RFQ has a high mechanical stability, low stored energy and high degree of field symmetry that make them easy to stabilize against acoustical vibrations.

The first lead-plate prototype SRFQ was fabricated and tested at Stony Brook[78]. Although its accelerating gradient only reached 1.1MV/m, some distance below the designed value 2.0MV/m, the investigation proved that SRFQ is feasible to fabricate, improve and operate.

Design of RFQ is something different comparing with the design of general rf cavities. Because it is impossible to separately consider the resonator and the beam dynamics with RFQ. It is necessary to understand well dynamics of the ion beam as well as the resonator and cryogenic, and blend them all into a practical design. With many studies on it, the design procedure of the RFQ has matured and it was no long considered to be an exotic and mysterious device again. But the design of a superconducting RFQ is still in progress, and many special considerations should be given, since there is not a SRFQ in the world under operation.

Fig.3-1 is the diagram of the four electrodes of a four-vane RFQ (a) and a four-rode RFQ (b). Fig.3-2 is a longitudinal profile of one RFQ electrode and Fig.3-3 shows the RFQ cross section with its rf electric field. They give a simplified imagine of the RFQ structure.

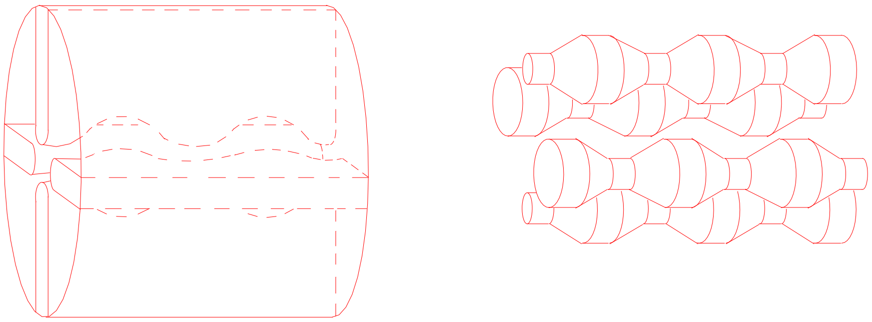

(a) (b)

Fig.3-1 Four-vane RFQ (a), and four-rod RFQ (b)

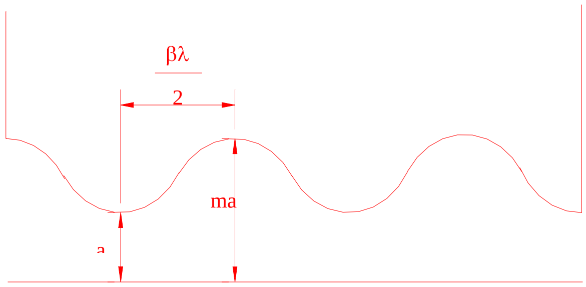

Fig.3-2 Longitudinal profile of one electrode

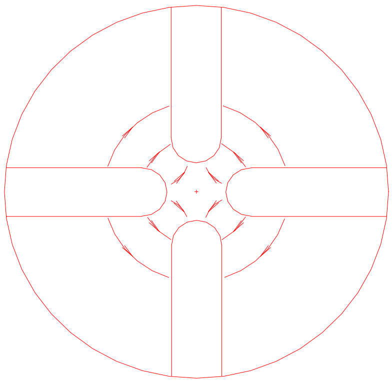

Fig.3-3 RFQ cross section and rf electric field.

To simplify the resonator fabrication and reduce the stored energy, short SRFQs called superconducting RFQlets were suggested[79]. It combines the advantages of rf focussing with wide transit time factor curve, low stored energy, small size and flexibility of the individual resonator approach. LNL's earlier SRFQ concept design adopted the idea of superconducting RFQlets too[80].

But shorter SRFQ need more inter tank drift space, and complicate the cryogenic system. Especially the first result in a drifting of the transverse beam envelope and cause mismatching in the following RFQs. At LNL, the later SRFQ design changed to two SRFQs with moderate length, within the limit of stored energy of approximately 4 Joule[81].

The beam accelerated in a linac must be formed into bunches at the resonant frequency or subharmonic first. The general bunching process with other kind of beam buncher discard 40% to 50% of the beam. While the RFQ could use adiabatic bunching to gently gather and accelerate nearly 100% of the beam form the ion source, this makes it very attractive for rare ions, such as exotic ions, polarized ions or high charge state ions. But adiabatic bunching need very long space which limit the applications in SRF structure. In SRFQ design, external buncher often become the first choice, although the capture efficiency is only 50% to 60%.

The acceleration efficiency (longitudinal shunt impedance) of a RFQ decrease with beam velocity, along with a field distribution error sensitivity goes as the square of the cell length, sets a upper limit to the RFQ output energy of approximately 2q/A (MeV/u). Where q is charge state of the ion, A is the mass in amu. Fortunately, this energy is compatible with the injection energy requirement of higher-energy linac accelerator that uses other rf acceleration structures.

The design of normal conducting RFQs or SRFQs has been discussed in many literatures, and some authors gave a lot of numerical results. It is no need to repeat all the procedures at here, only list those factors that frequently used in the RFQ design.

Acceleration parameter

$$A = \frac{m^2 - 1}{m^2 I_0(ka) + I_0(mka)}$$

Where, m is the modulation parameter, a is the minimum radius of the aperture, k=2π/βλ - wave number, and I_0 is the first kind of Bessel function.

Focussing efficiency

$$x = 1 - A \cdot I_0(ka)$$

Focussing factor,

$$B = \frac{qV}{M \cdot c^2} \cdot \frac{A}{a^2} \cdot x$$

Where, q is the charge state, M is the mass and V is the inter-vane voltage.

RF defocusing factor,

$$\Delta = \frac{\pi^2}{2} \cdot \frac{qV}{M \cdot c^2} \cdot \frac{A}{\beta^2} \cdot \sin \phi_s$$

Where, φ_S is the reference rf phase

Average radius of the aperture

$$R_0 = \frac{a}{\sqrt{x}}$$

Accelerating gradient

$$Ea = \frac{\pi A V}{4\beta\lambda}$$

Accelerating gradient to peak surface electric field ratio,

$$\frac{Ea}{Ep} = \frac{kR_0 A}{4F}$$

Where F is the field enhancement factor which weakly depends on the modulation parameter m and the vanes transverse radius of curvature ρ. F equals to 1.2 to 1.5 in most case, and approximately given by,

$$F = \sqrt{\frac{P^2}{2} + \left[I_0\left(\frac{k\beta R_0}{\sqrt{2}}\right) \cdot \frac{AkR_0}{2} \right]^2}$$

Where , $P = \frac{\rho}{R_0}$

A lot of numerical equations are used in the initial design of a RFQ, while in detail design procedure, computer codes are employed. Among the codes, SUPERFISH as a 2D code could be used in four-vane RFQ resonator design and analysis. Four-rod structures need to be solved by a 3D code such as MAFIA. But there is no code today that precise enough to generate a complete RFQ design, models or prototype resonators and application of the traditional rf cavity cut-and-try technique still takes an important role in the RFQ design.

The design of RFQ is different and more difficult compared with design of other kind of rf cavities because the beam dynamics cannot be separated individually from the resonator design. Special computer codes have been developed to give an aid in the RFQ design. In the RFQ codes, PARMTEQ is the most widely used. It was developed at LANL early 1980s and applicated in many other laboratories later, the code calculate the beam dynamics and generate a table of the accelerating cells[82].

Four-vane RFQs are generally applicated in high frequency linacs (several hundred MHz), at frequency lower than 100MHz, diameter of the four-vane resonators will become prohibited, and longitudinal shunt impedance of the four-rode RFQs will be superior to them. At the low frequency region where low energy heavy ion beam is accelerated, four-rode RFQ could be chosen.

As mentioned above, adiabatic bunching can capture and accelerate nearly 100% of the inject DC beam, it can be realized by 'tapering' the accelerating structure in a RFQ, that is nearly impossible in other individual rf cavities. But real adiabatic bunching need accelerating structure infinitely long, and in normal conducting RFQ, the bunching structure is only an approximation to a real adiabatic one. Neither Stony Brook nor LNL adopted adiabatic bunching in their SRFQ design. The choice of an additional beam buncher will simplify the SRFQ design and fabrication, although 30% to 40% of ion beam is discarded.

Because the peak surface magnetic field is quite low in a SRFQ, and heat generated by the dissipated rf power on the resonator surface could be removed easily, the parameter Hp/Ea is considered of minor importance. To get a high accelerating gradient, the peak surface electric field to accelerating gradient ratio had been intensively analyzed and optimized in LNL's SRFQ design.

Since Stony Brook used lead-plate SC structure to realize the prototype SRFQ, there would be less problem of thermal stability of the cavity as high thermal conductivity of the OFHC copper substrate and each SRFQ electrode dissipate RF power no more than 1W. LNL’s bulk niobium SRFQ has something disadvantage, because the four electrodes are hollow to be cold by liquid helium directly, the rest three electrodes would be no problem except the fourth one – the bottom electrode which use a tyflon siphon to pipe out helium gas. Although calculation showed that a siphon with 1cm inner diameter could be enough to such a task, in the SC cavity operation situation would not be so simple, e.g. any bubble or liquid helium trapped in the siphon will cause trouble.

There are two tuning plates of SRFQ at both sides of the cavity, instead of only one in a QWR. Tuning plate deform of 1mm will cause the SRFQ resonate frequency shifts approximately 100kHz, while the same deform of tuning plate will shift frequency about 10kHz in a QWR.

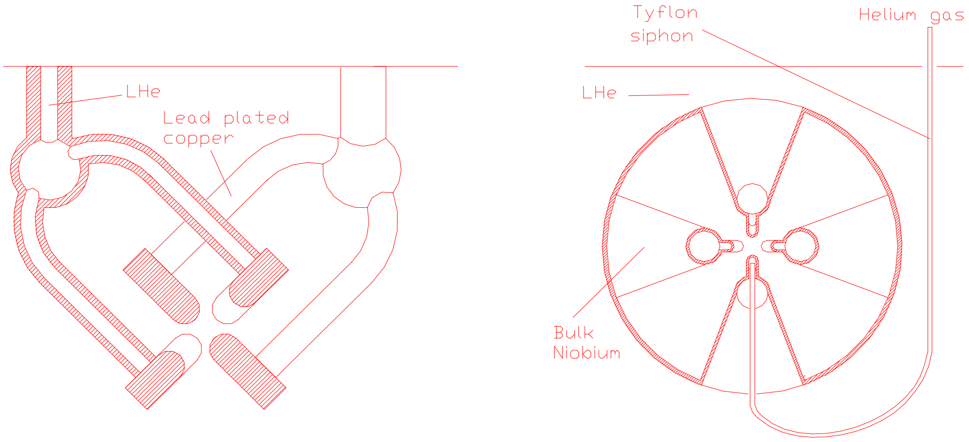

(a) Stony Brook (b) LNL

Fig.3-4 Schematic diagram of two kinds of SRFQs

Table 3-1 Design Parameters of LNL's SRFQs[83,84]

	SRFQ1	SRFQ2	
Vane length	137.8	74.6	cm
Frequency	80	80	MHz
Intervane voltage	148	280	kV
Tank diameter	65	65	cm
Hp	280	295	Gs
R_{Sh}	3.2	3.2	MΩ /m
Q_0*	7×10^8	7×10^8	
P_S	<7	<7	W

* Calculated with BCS surface resistance times 20

3.2 Post-magnetron configuration

In the LNL new positive injector project, two SRFQ resonators had been designed, and a bulk niobium one - SRFQ1 is under construction. Fabrication of the bulk niobium SRFQ is a complicate and very costly procedure since the structure is complex and many components need to be EBW welded. Early in the year of 1996, a side project of sputtering niobium on the SRFQ resonator was proposed, and a sputter system based on post-magnetron configuration has been built from 1997. The system include a half-size dummy RFQ model, vacuum chamber and pump set, target and magnetron power supply, and an outside chamber solenoid[85].

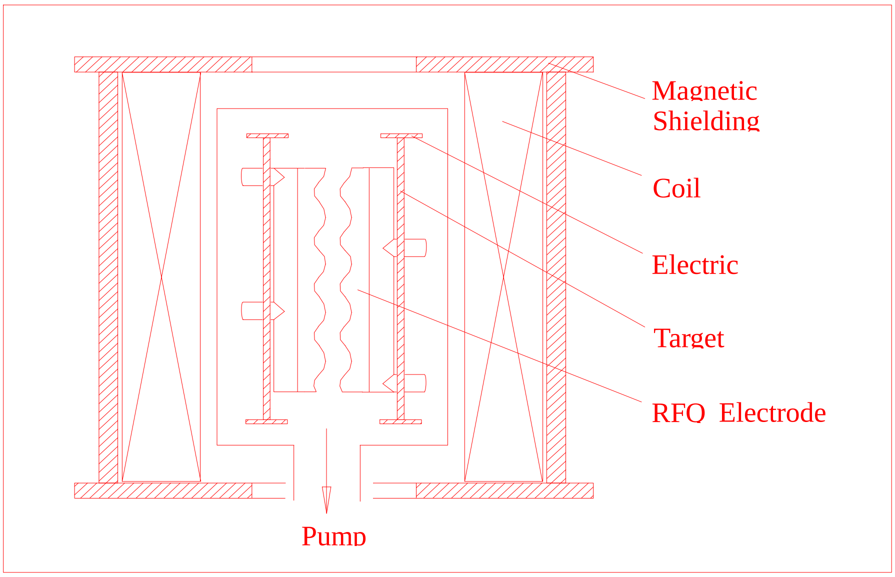

Fig.3-5 Configuration of the sputter system

The solenoid is a massive magnet with coils, it generates a uniform magnetic field about 250Gs in the vacuum chamber, and a 1.6 ton crane used in moving it for mounting and dismounting targets or samples. A 160A DC power supply with cooling water connected to it, and because the solenoid wound up by thick copper tubes, the ohmic heating is not quite intensive, there is no need of cooling water for the solenoid itself in operation.

Without baking, the background vacuum is approximately 1×10^{-5}Pa with viton seals of the top flange after 24 hours pumping. Bake the chamber at 150℃ for 4 hours, vacuum could increase to $3\text{-}5\times10^{-6}$Pa. It could reach 10^{-7}Pa with all copper gasket seals and after baking more than 24 hours. High initial vacuum is necessary in niobium sputtering.

Geometry of the RFQ's four electrodes is very complex compared with QWRs or spherical cavities, it is not easy to design the target that could uniformly sputtering deposit thin films on all the electrode surface. A FORTRAN 2D code was developed to simulate the thickness distribution of sputtered films on RFQ surface. Although it could not solve the problem quantitatively since geometry of the RFQ is really 3D and the scattering of sputtered atoms by collisions with ambient argon gas takes an important role in the film deposition which is difficult to quantitatively solve, it yields some helpful information.

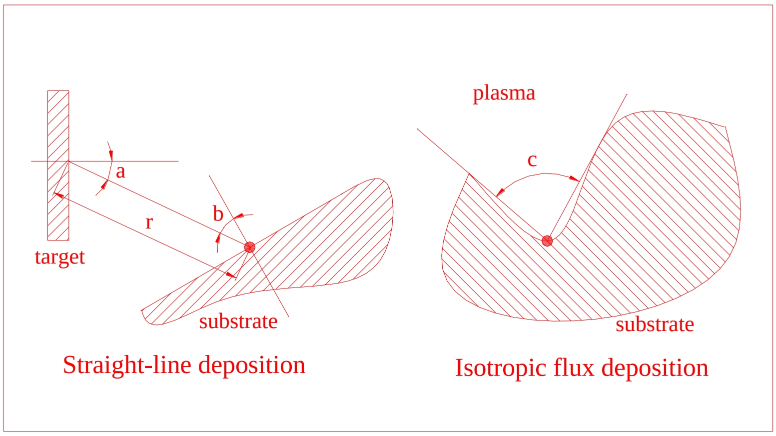

Fig.3-6 Two kinds of contributions of the film deposition

In the simulation, two factors were considered, one is 'ray of light' that sputtered atom deposit on the substrate in a straight line regime, and another is isotropic atom flux which caused by collision scattering. After several collisions with ambient gas atoms, the sputtered atoms lost their original history and become isotropic flux that the thickness of deposited films depends on the angle open to the vacuum.

As cylindrical symmetry, in the 'ray of light' regime, film thickness is

$$t = \frac{C \cdot \cos\alpha \cdot \cos\beta}{r}$$

Where C is a constant factor, r is the distance between the target and the substrate, α and β is the respected angle.

In the isotropic flux regime, thickness becomes

$$t = D \cdot \phi$$

Where D is another constant, φ is the open angle of the interested substrate location.

At pressure lower than 10^{-2}Pa while mean free path of the sputtered atom larger than the dimension of the vacuum chamber, and there is nearly no collision with ambient gas atoms, the first regime would be a good solution. If pressure high enough (larger than10Pa) that the mean free path reduced to less than one mm, many collisions would occur before the sputtered atoms arrive at the substrate, the second one would be a good approximation. Unfortunately, argon pressure is 0.1 to 1Pa in the sputtering, the mean free path of sputtered atoms is of cm order, neither of the two regimes could solve the problem individually.

In the simulation code, film thickness was calculated by a combination of the two factors. Since it is difficult to give the weight of each factor quantitatively, only some qualitative results can be seen. At higher argon pressure, isotropic flux will be a major contribution, and at lower pressure, straight-line sputter will dominate the film deposition. The thickness uniformity could be controlled by different target shape and location, while adjust sputter pressure will modify the film uniformity.

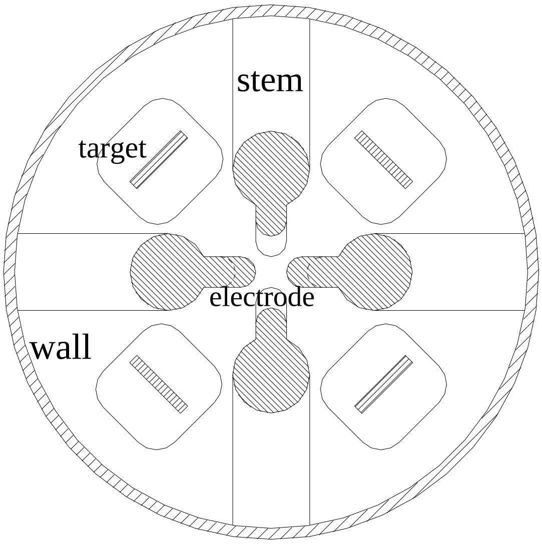

Fig.3-7 Cross section of the model RFQ and target.

It was demonstrated that sputter deposition of thin films simultaneously from every direction tends to get columnar structure that is not appreciated in rf applications[86]. Movable small magnetron like that of the 1.5GHz monocell cavities were discussed, it would deposit niobium films on the

RFQ at limited areas and by moving up and down, all the electrode surface could be uniformly coated. But we need at least four of them to sputter a RFQ, water cooling and electric feed-through is not easy to realize in our present chamber. Moreover, movable magnetrons cannot access the center part of the RFQ, and film quality on the tips of the electrodes will be very poor. The strap targets with outside solenoid were employed, since no need of cooling water and the target can be easily mounted on the location to sputter the center part.

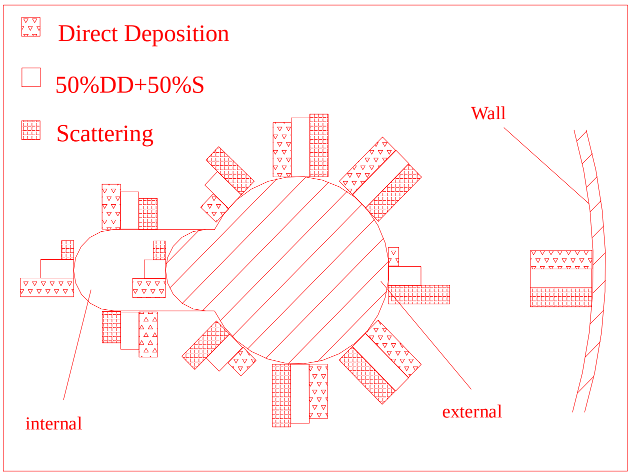

Fig.3-8 Film thickness in different sputtering regimes.

3.3 Experiments with stainless-steel and copper

The system was tested by sputter of stainless steel targets at first. SS targets with various shapes had been sputtered, from 20mm diameter column to 30×3, 20×3, 20×4mm^2 straps, all of them were approximately 700mm in length, and finally fixed on 20×3 and 30×3 mm^2 bars. We tried single SS target with single electrode installed, and two SS targets with four (all) electrodes. The characteristic sputtering V-I curve is shown in fig.3-9. Quartz substrates (0.5×1cm^2 with thickness 1mm) were mounted on different locations of the electrode in the experiments, by measuring the film thickness, more information about the sputter deposition was got. Table 3-2 and 3-3 listed the parameters of two different runs.

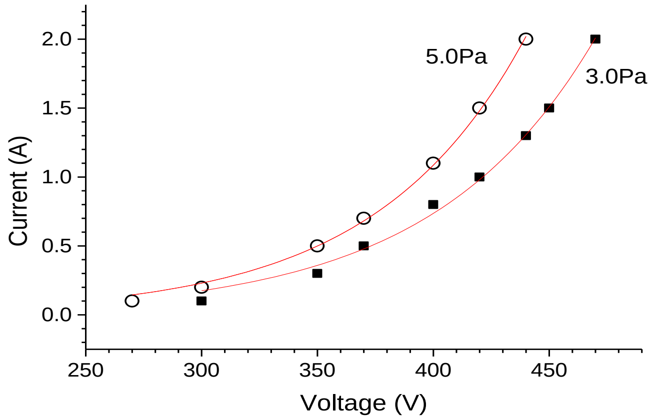

Fig.3-9 Characteristic curves of the single SS target sputtering

Table 3-2 Sputter parameters of the single SS target

Argon	5.0	Pa
Voltage	450	V
Current	2.0	A
B	180	Gs
Time	40	min

Table 3-3 Sputter parameters of the double SS targets

Argon	3.0	Pa
Voltage	500	V

Current	2.0	A
B	210	Gs
Time	30	min

From the film thickness distribution, it is obvious that the scattering of sputtered atoms takes an important role in film deposition at high argon pressure, and the better thickness uniformity achieved in the single target sputtering came as the result of no shielding by other electrodes. While in the double targets sputtering there were four electrodes, and the vanes' tip points nearly sealed from the plasma, so that films were very thin in these areas. Lower argon pressure should be applied in the sputtering to improve film thickness uniformity.

Because there were always dark zone problems with the stainless steel targets that some local zones particularly near the electric mirrors randomly got weak plasma or no plasma at all, and after sputter, targets surface at these zones showed gray or black color. We guess it was a material problem of the stainless steel since it is an alloy, not a problem of the magnetron configuration, because in some other runs, especially the target surface was clean and finely polished, there was no problem of dark zone. To solve the problem, copper targets were tested.

The copper targets are 700×20×3mm^3 copper bars with SS electric mirrors (60×60mm^2) on the two ends. The targets were polished and then ultrasonic cleaned. During the sputtering, no dark zone was found in the plasma, and all targets surface was finely etched. Parameters of the four copper targets sputtering are listed in table 3-4. Like sputter of SS targets, sputter of copper could only operate in high argon pressure (larger than 1Pa).

Table 3-4 Sputter parameters of the four copper targets

Argon	5.0	Pa
Magnetic field	200	Gs
Voltage	500	V
Current	3.0	A
Time	20	min

In the sputtering, temperature of the four targets rise very quickly as they were not cold by cooling water, after only 20 minutes of continue run, three of the four copper targets were broken due to high temperature. Because niobium has a very high melting point, near 2500℃, the problem of high target temperature would not be so serious in niobium sputtering. As this reason, the present target configuration without cooling water was adopted in the design of niobium targets.

Sputtering of the RFQ in higher argon pressure tends to increase the isotropic atom flux factor in the film deposition, the external areas of the four RFQ electrodes and the chamber wall will be sputtered well. While internal electrode areas will receive little flux as they are shielded with each other. Film thickness was measured by an Alpha 200 step, measured result corresponds to the film thickness simulation, see fig.3-10.

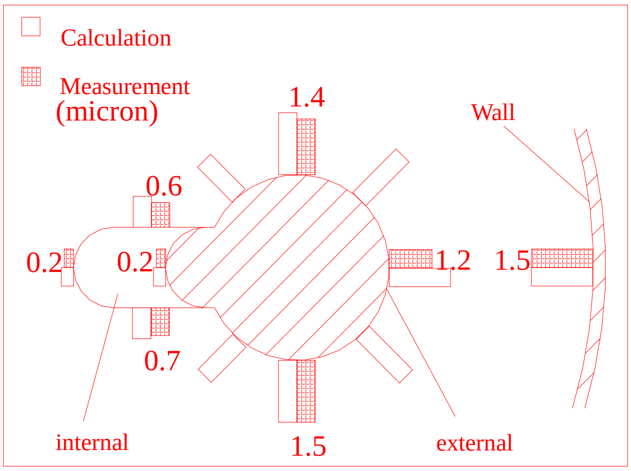

Fig.3-10 Copper film thickness distribution on the RFQ

After successful running of the copper sputtering, niobium targets were designed and manufactured. The vacuum chamber and the RFQ model was dismounted, strip off the surface copper and stainless steel films, polished, ultrasonic cleaning and then remounted.

3.4 Sputter of niobium

Four niobium targets (each one 670×30×3mm^3) and corresponding eight electric mirrors (60×60×3mm^3) made up from a high purity niobium sheet (RRR about 200). All screws and nets that used to fix the targets are made up by niobium, niobium electric wires with diameter 1mm connected to the targets, as there is no commercial niobium electric feed-through, a bulk niobium tube covered the feed-through to avoid film contamination of alien material during niobium sputtering.

All the niobium components had been etched in 1:1:1 acid solution (sulphuric acid, hydrochloric acid and phosphoric acid) for about 30minutes to strip off approximately 50microns surface layer. Following ultrasonic cleaning, drying and then mount. Since inner diameter of the RFQ chamber is 285mm, the targets were placed in a distance around 80mm to the RFQ axis where is the optimum target position from film deposition simulation.

In the sputtering, niobium targets could be sputtered stable at very low argon pressure, 0.1 to 0.2Pa. The first sputtering experiment with niobium targets was curried out at 0.5Pa, after a few seconds vibration, the plasma became very uniform with beautiful blue color, there was no dark zone and all the target surface was finely sputtering etched. Film thickness was measured, it confirms that at such a low pressure, the internal RFQ electrode areas sputtered well. The only poor film thickness points takes place at the external electrode areas where is nearly at 90° to the target and receives very weak “ray”.

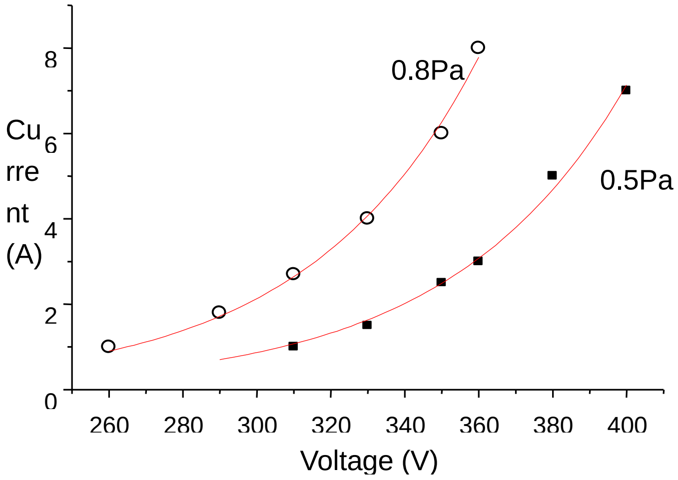

Fig.3-11 V-I curve of four niobium targets sputtering

Table 3-5 Parameters of the first niobium sputtering

Argon pressure	0.5	Pa
Magnetic field	250	G
Voltage	400	V
Current	7.0	A
Time	50	min

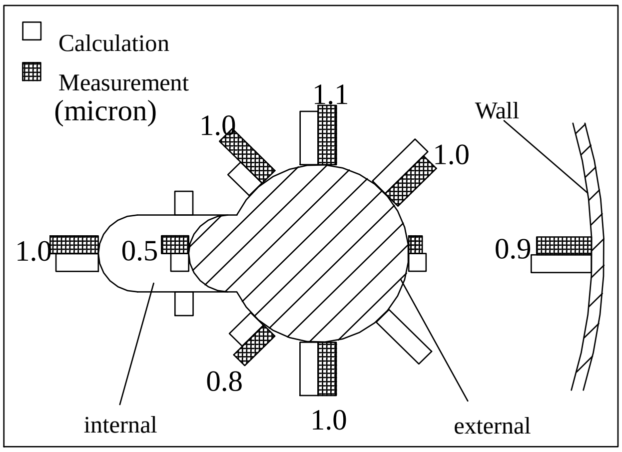

Fig.3-12 Niobium film thickness distribution

The problem of thin film on the external RFQ electrode area could be solved by increasing argon pressure in the sputtering, both experiment and film simulation already showed this. Because the external area widely opens to the plasma, it will receive more isotropic atom flux. While the internal RFQ electrode area shielded with each other, receiving little flux, it will be sputtered well by an appropriate target position and decreasing argon pressure to increase the straight-line deposition factor.

In the film thickness simulation, it was found that sputter at a moderate argon pressure - 3Pa, all the RFQ surface will be sputtering deposited uniform enough: when the most thin film on RFQ surface reaches 1 micron, the thickest area would be less than 2.5 microns. In the SRF applications, this film uniformity is all right considering the complex geometry of a SRFQ.

As been mentioned in chapter 2, in niobium sputtering, lower pressure will enhance energetic atom bombardment effect to the sputtered film that improve the film crystalline structure, meanwhile less argon atoms will be trapped in the forming film, film quality will increase. Since increase sputtering pressure will not only affect the RFQ surface film thickness uniformity, film quality will be modified too, related problem should be studied carefully.

In the first sputtering run, niobium films with RRR only 2 to 7 were got, the quality was quite poor. Because the targets were new, although been etched, the surface remained a lot of oxides, deposited film too thin, 0.1to 1.1 microns, and the background vacuum only reached 10^{-6}Pa. In the following runs, background vacuum increased to 10^{-7}Pa, film quality getting better and better. Especially sputtered at 3Pa, niobium film samples with thickness quite uniform, 0.6 to 1.7 microns and RRR from 6.5 to 15, close to the requirement of SRFQ sputtering if only the film's DC SC figure considered[87].

Table 3-6 Sputtering parameters of uniformly distributed film

Argon pressure	3.0	Pa
Magnetic field	250	Gs
Voltage	380	V
Current	8.5	A
Time	70	min

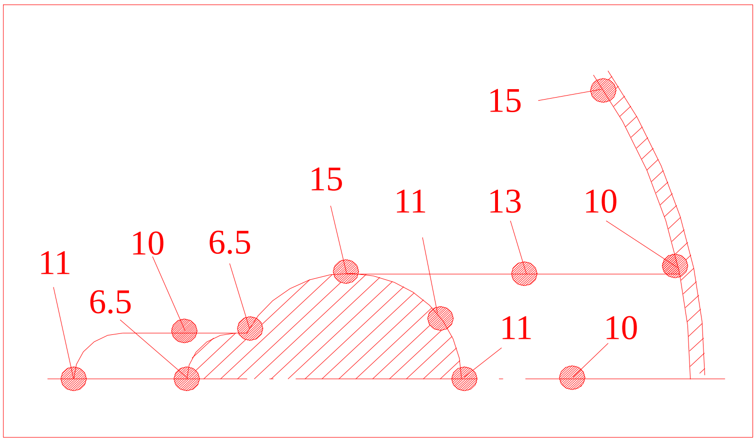

Fig.3-13 RRR distribution on the RFQ surface

But surface color of all the niobium films sputtered at higher argon pressure is black or dark gray, which only occurred at the external RFQ electrode areas while sputtered at lower pressure. The black color comes as the film surface filled with voids that absorb light, which is prohibited in SRF applications since this structure significantly increases the surface resistance. By this reason, the sputtering pressure should be kept lower and other measures instead of increasing argon pressure that could solve the problem of poor film quality on the external RFQ electrode need to be found out.

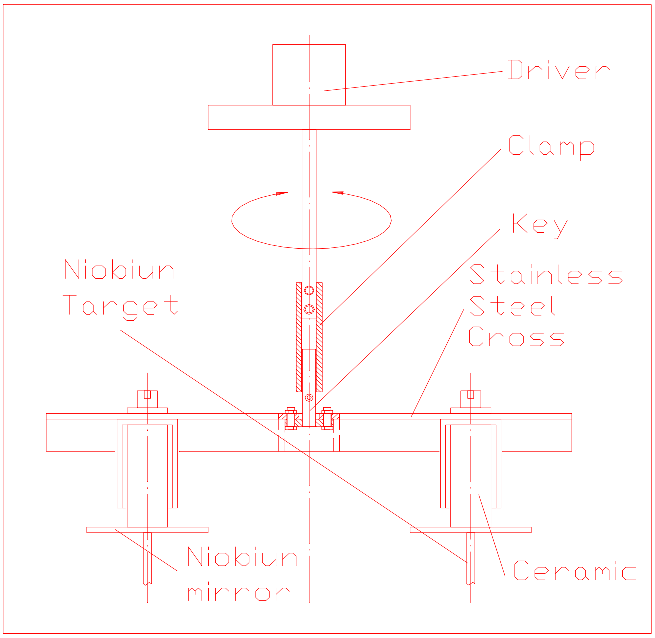

Fig.3-14 Target suspension and rotation system

According to the RFQ deposition condition, external electrode areas generally get thin film when sputtered at lower argon pressure since they are nearly at 90°to the targets and poorly sputtered. A target suspension and rotation system was designed, by rotating the target, RFQ electrode external areas would receive more direct sputtering at lower argon pressure, and the corresponding film quality could be improved.

In order to increase the film quality, in the rotating target sputtering experiments, higher discharge current and larger deposition rate was used. Since current limit of the electric feed-through is only 12A, while sputtered at high current, temperature of the target, model RFQ and the feed-through rises quite rapidly that often cause the most brittle part – the electric feed-through with ceramic-metal brazing, broken. As it broken several times that the experiment was delayed. But only a few sputtering runs already shown hopeful result.

Table 3-7 Parameters of rotating target sputtering

Argon pressure	0.3	Pa

Magnetic field	250	Gs
Voltage	440	V
Current	12	A
Time	40	min

Table 3-7 is the parameters with rotating niobium targets, fig.3-15 is film thickness and RRR distribution on the RFQ section of a rotating targets sputtering experiment. It showed that niobium film thickness uniformity and DC SC features on the model RFQ surface is close to the requirements of SRFQ sputtering.

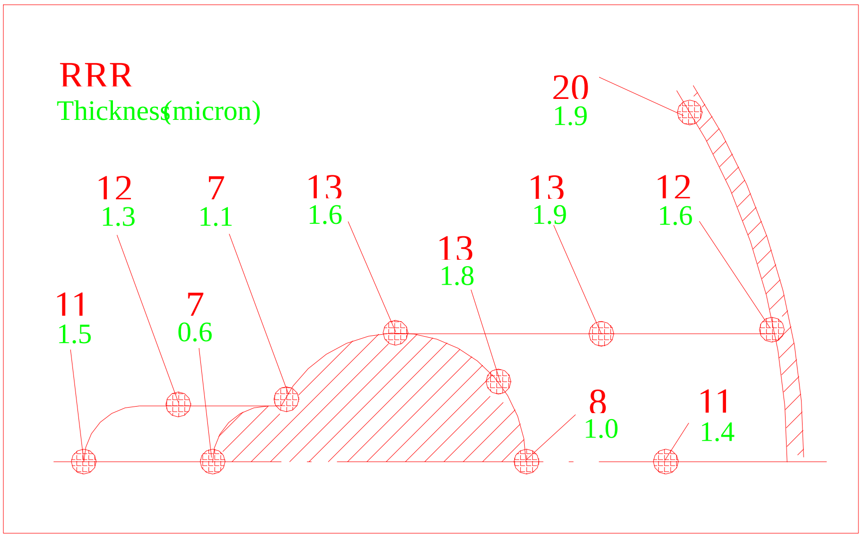

Fig.3-15 Model RFQ film thickness and RRR distribution

Although the film color on the RFQ electrode external areas has greatly improved a lot, it is still a distance to the required mirror like one as that of other areas, and further experimental studies are needed in the future.

3.5 Discussion

The experimental study of sputtering niobium films on the model RFQ indicates that, although the complex geometry of a SC RFQ increased the difficulty of coating uniformly distributed SC films on the RFQ surface compared with that of spherical cavities or QWRs. It is possible to sputter niobium films uniform enough with higher quality on the entire RFQ surface, after many efforts and experimental research quality of the sputtered sample is close to SRFQ requirement. Next step is sputtering niobium film on an OFHC RFQ substrate. Since sample study is the preliminary step, while cavity as substrate is the most important method and the final goal – a sputtering coated SC RFQ.

An OFHC copper model RFQ is under construction while the thesis being written, it would be sputtered better at the present magnetron configuration. Because the SS dummy RFQ filled with exposed screws, nuts and samples during sputtering, the rotation angle of the targets was limited to less than 40°to avoid arcs in the process. But for copper RFQ, there will be no such a problem, the rotation angle of the targets could increase to 45°that greatly benefit to the film deposition of RFQ electrode external areas.

In the sample study, sputter current limited by the electric feed-through that 12A is the maximum discharge current, while in the copper RFQ cavity sputtering, a stronger feed-through with current limit 20A that permit for higher current and deposition rate so as to improve film quality. Another factor limit film quality in the sample sputtering is possible film contamination by the ceramic standoff that suspend the target, as its safe use temperature is no more than 400℃, but in sputtering, the target got a temperature higher than 1000℃,the problem was found out in the experiment of thermal diffusion of V_3Si films and will be discussed in chapter 6.

The final solution is to use more complicate target with cross sections that sputter the external RFQ electrode directly, but it will increase the difficulty to mount and dismount the targets, unless the above mentioned methods cannot solve the problem, it should not be employed. In a short word, the sputtering coated SC RFQ is very hopeful.

Chapter 4

Cosputter V_3Si superconducting films

4.1 Introduction

From more than ten years ago, some laboratories have begun investigation of superconducting materials other than niobium as surface coatings for SRF cavities. Among the materials investigated there were B1 compounds NbN, A15 compounds Nb_3Sn and V_3Si, ternary compounds (NbTi)N. High Tc materials such as YBCO had been studied also[88-93]. From the BCS theory, higher Tc yields lower BCS resistance, as a result, the cavity would have a better Q factor than that of niobium one, or to achieve the same performance at higher cryogenic temperature, e.g. 4.2K instead of below 2K. Another advantage is the higher Tc the higher upper critical magnetic field, which makes it possible to have a high acceleration gradient more than niobium cavities had achieved.

Material with higher Tc generally has a shorter coherence length, and poor normal conductivity. The existed structure defects or peculiar impurities will severely degrade the RF performance. Usually the material has a large residual surface resistance, and the Q value of a cavity decreases much more rapidly while increasing the accelerating gradient, together with the difficulties to get real defect-free cavity inner surface, their applications are limited. Up to now, only a few coated Nb_3Sn cavities reach a comparable performance with that of bulk niobium cavities[94]. But they need very good bulk niobium cavities as the substrate, and thermal diffusion of tin on surface of the cavities at elevated temperature 1100℃. The fabrication procedure is complex and very costly, and remained in study.

V_3Si has a Tc of 17K and its upper critical magnetic field is near two times as that of niobium. It is the first found A15 superconducting material and the only one A15 superconductors that larger scale single crystal had been formed[95]. It has many properties similar to that of Nb_3Sn, and will be a potential coating material for SRF cavities.

There are many methods to deposit V_3Si thin films, such as co-evaporation of vanadium and silicon[96], magnetron sputtering[97], gettering sputtering[98], alternate evaporation of vanadium and silicon then annealing[99], reactive sputtring[100]. All of them are needed to perform at high temperature, and the optimum temperature is between 800 and 900℃. At this temperature range, annealed V_3Si films with Tc around 17K were got, near the bulk value, while magnetron sputtered V_3Si films with Tc only reached 16K.

Since V_3Si films deposited at low temperature usually cannot form good crystalline, and oxygen, nitrogen or carbon contamination in the film will be high[101]; while at higher temperature, better crystalline could be formed and contamination will decrease. But high temperature commonly is not convenient to be achieved in high vacuum requirement. If the temperature is too high, there are problems of thermal diffusions between the films and the substrate materials, and some contents needed e.g. oxygen or nitrogen that served as stabilization material of the A15 phase[102] might eliminate too. Consequently, film quality will not increase any more.

To a copper cavity, the coating process should be operated under a lower temperature because the melting point of copper is only 1080℃ and at temperature above 400 to 500℃, the cavity wall will be annealed very soft, moreover, at high temperature the thermal diffusion between copper substrate and V_3Si films becomes another problem. It is the major difficulty to sputter perfect V_3Si films on a copper cavity.

Another noted point is, unlike that of niobium films, when sputtering A15 compounds, large product of the argon pressure and target-substrate distance is required to thermalize the energetic sputtered atoms with the ambient argon gas atoms and reduce ion bombardments[103].

4.2 Facing-target magnetron

In our sputtering experiment, a home made facing-target magnetron is used, the target thickness is about 3mm and diameter 50mm, with cooling water inlet and outlet ballows, the distance of the two targets is adjustable. Facing-target magnetron is a special type of magnetron, it consists of two separated targets facing to each other[104-106]. The magnetic flux is enclosed on the two targets that are at negative potentials, the magnetron becomes a structure of electron trap. The magnetron is very good at confinement of plasma as well as electron.

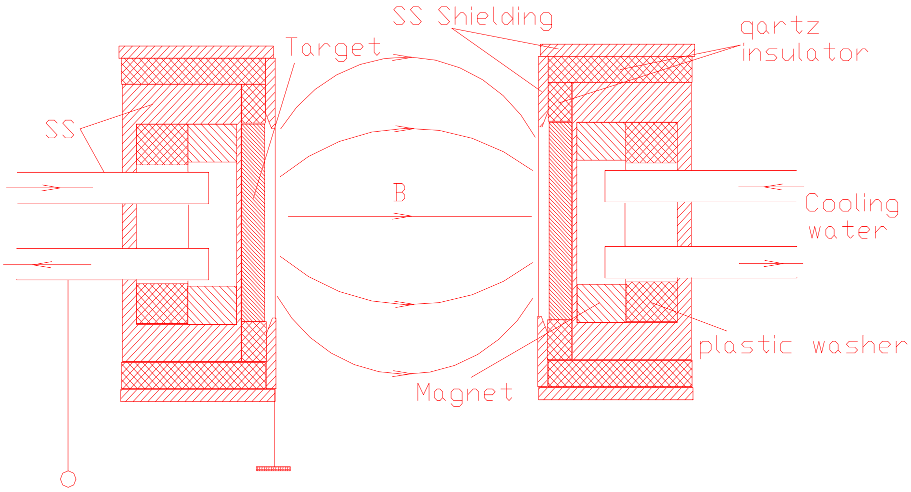

Fig.4-1 Magnetic field of the facing-target magnetron

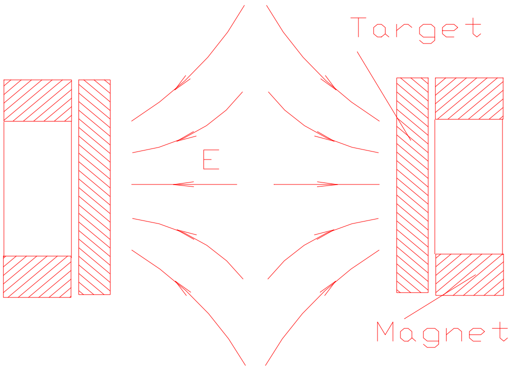

Fig.4-2 Electric field distribution of the magnetron

Usually assumes a relationship in the form of $I=CU^N$ to the V-I characteristic curve of a magnetron, where C is a constant depends on the magnetron type, geometry, sputtering medium pressure and other related conditions. In facing-target magnetrons, the exponents N from 30 to 40 are found. To the magnetron we used, n is 26 to 34 corresponding to argon pressure of 0.5 to 1Pa. While that of general magnetrons[107,108], the value is commonly between 5 and 15.

Facing-target magnetron is characterized by its steep sputtering V-I curve, and its capability of sputtering at very low argon pressure (10^{-2}Pa). The magnetron can reach high sputter current at comparatively low voltage. It is widely used in industry because of its high deposition rate and for its peculiarity of a narrow plasma confinement. This aspect makes the technique suitable to sputter multicomposition materials onto low melting point substrate due to the reduced plasma substrate interaction.

The two targets of a facing-target magnetron are generally connected to a same magnetron power supply and sputtered at the same voltage. In our experiment instead, the magnetron are driven by two independent DC magnetron power heads. One was connected to the silicon target, another to the vanadium target, and sputtered at different voltage and current in order to get stoichiometric V_3Si films.

4.3 Vacuum system

Diameter of the main vacuum chamber is approximately 320mm, and its height about 360mm. The bottom connects to a three-port tube, which linked to a 300l turbo-molecular pump by an all-metal pneumatic gate-valve. The molecular pump is a special type that can operate under corrosive gases such as HCl, SO_2 (since we will use the same system for reactive sputtering of V_3Si films by introducing silane gas). And its preliminary pump is a rotary pump connected to the turbo pump by a ballows so as to avoid vibrations of the rotary. A load-lock is installed in the vacuum system, so that the samples can be mount and dismount without opening the main chamber.

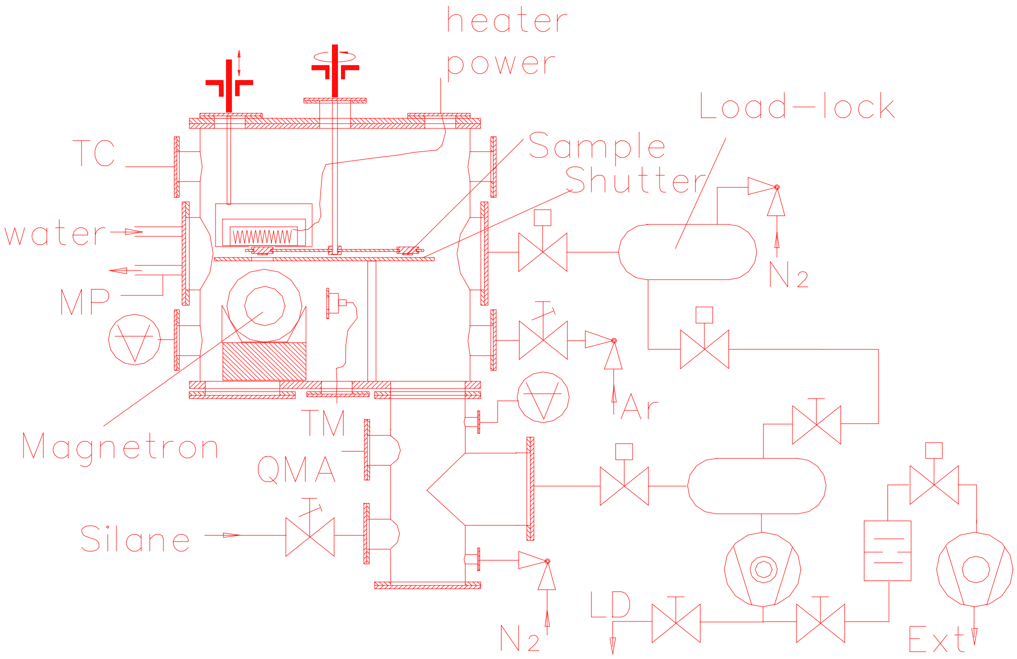

Fig.4-3 Block diagram of the vacuum system.

Although the stainless steel vacuum chamber is a smaller one, it consists of more than 50 connection flanges, and the system is quite irregular in shape. In order to bake the whole system uniformly, we have to cover every flange with a heater jacket, the total power of all heaters sums up about 15kW. A control system had been designed, it includes eight thermal-controllers, eight thermal-couples and eight solid-state relays. All the heaters are divided into eight groups according to their different locations in the vacuum system, and controlled by corresponding control units. The system works very stable. After 24hours pumping, the background vacuum usually reaches $5\text{-}6\times10^{-5}$Pa without any backing, while baking at 110℃ for as short as 8 hours, it could improve up to 5× 10^{-6}Pa, to the limit of the pump. In the sputtering of A15 material, 10^{-5}Pa is enough.

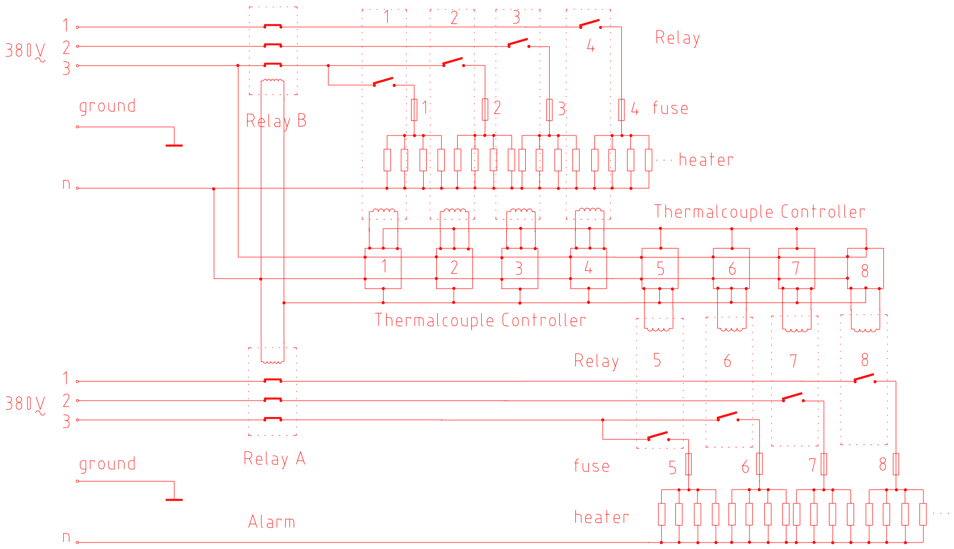

Fig.4-4 Block diagram of the baking system

A stainless steel carousel carrying eight copper samples holders were fabricated so that eight sputtering runs could be performed within one pumping cycle. Chose copper as the sample holders comes from two considerations, one is that we wish sputtering V_3Si film on a copper cavity in the future, another is that copper has a good thermal conductivity. Most of substrates used in the sputtering are 1cm^2 square sapphires with thickness 0.5mm, some samples are deposited on quartz substrates and copper foils. A quartz thickness monitor is installed in the chamber; film thickness and deposit rate could be measured in situ.

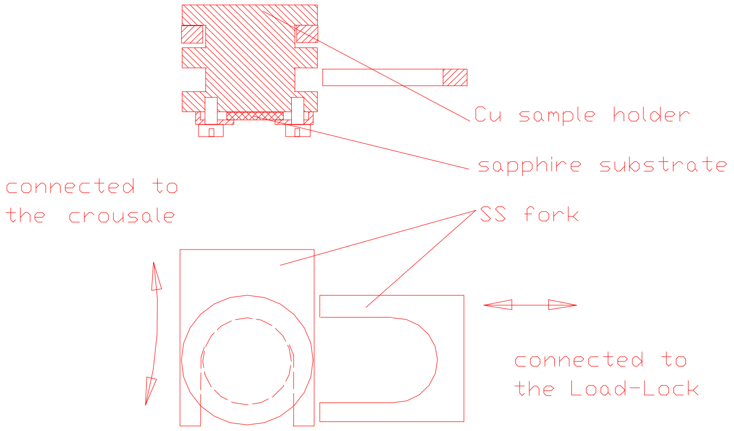

Fig.4-5 Schematic diagram of the sample carrying system

A collaborated K-type thermocouple is used to relatively monitor the sample temperature. Since the samples are on the carousel, fix the thermocouple on it would cause many troubles when rotating, taking and putting samples, while measuring a similar holder that fixed on the shutter is much more convenient. The samples was heated by thermal irradiation with a commercial boron nitride coated prolytic graphite heater, it was replaced by a home made tungsten lamp after it failed to get high temperature - higher than 700℃.

In the first operation of the heater, there were severe periodic arcs on the heater surface and on its electric feed-through during sputter because they are exposed to the plasma. We covered all the exposed electric wires with ceramic bushes, and the situation became better but there were still random arcs on the hot ceramic surface, might caused by charge accumulation. After completely shielding the heater with niobium sheet, the electric feedthroughs with stainless steel flakes and, ground all metal shielding, the heater works very well, it could be turned on during sputter.

In order to get temperature above 700℃, a massive tungsten lamp heater was made. 0.25mm diameter tungsten wire is wound on an alumina cylinder and put inside a bulk molybdenum oven, it is shielded by one niobium shielding and then two stainless steel shielding. And all shielding include the bulk molybdenum are grounded, while electric feed-through are covered by ceramic bushes. It takes about 2 hours to heat the samples from room temperature to higher than 600℃; it could keep the temperature for several minutes after electric power turned off. Although it cannot be left on during sputtering since the heater center has a temperature of approximately 2000℃, and electron emissions from the hot tungsten filament will cause discharges in the surrounding of plasma. It works in the way to turn off the heater and then begin sputter.

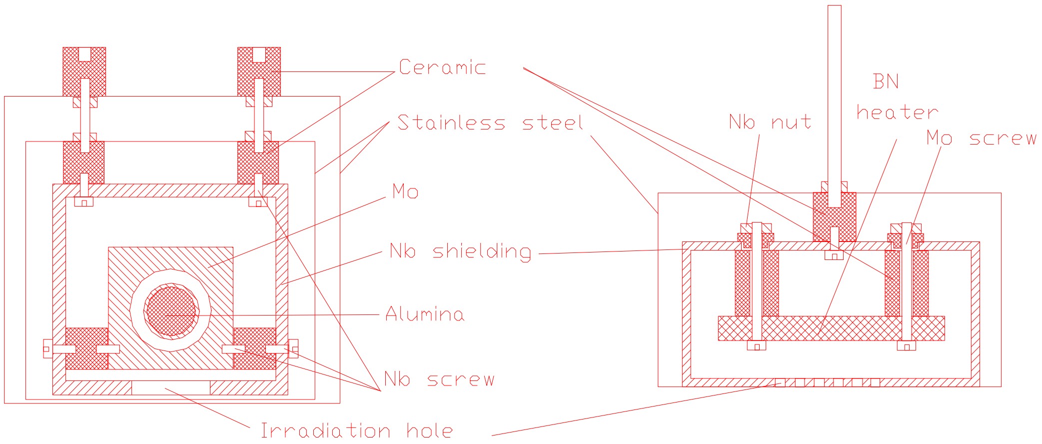

Fig.4-6 Two heaters used in the experiments

4.4 Sputter with niobium

The system was tested by sputter of niobium films. Two high purity niobium targets (RRR about 250) are connected to a DC magnetron power head, and sputtered at various argon pressure while the distance between the two targets been adjusted. All the sputters were run at room temperature. The color of the plasma is blue, it is caused by ionization of argon atoms. Because color of the niobium plasma in self-sputtering should be gray, it is covered by the more bright blue color in argon atmosphere ionization[109].

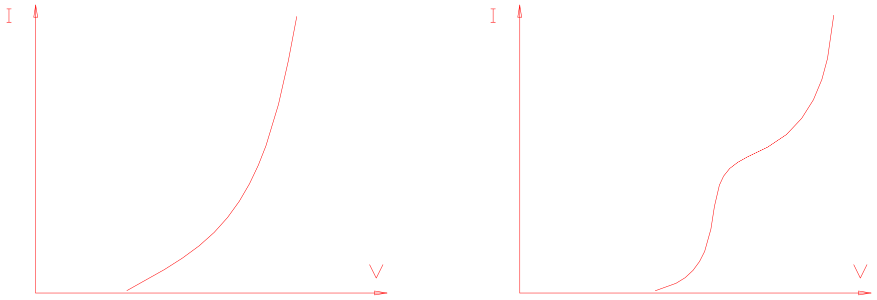

(a) (b)

Fig. 4-7 Sputtering V-I curves with two types of magnets
(a) ring shaped magnets, (b) columnar magnets

By monitoring deposition rate with the quartz thickness monitor, the optimum distance between the two targets was found, it is a range instead of a fixed value, from 40 to 50mm - from diameters of the targets to a little less. At which distance, the shape of the plasma is like a sphere between the two targets, and the maximum deposition rate of niobium film is about 120nm/min.

In the test sputtering, discharge can be sustained stable at 5 to 6×10^{-2}Pa. The characteristic V-I curve of secondary ionization of a facing-target magnetron has not been observed when using two ring shaped magnets, since it would occur above the limit of the magnetron power, which is only 1.5kW. After the ring magnets being replaced by two columnar magnets, it was observed. See fig.4-7 (b).

The first two niobium samples have poor qualities, RRR is 2 and 3, while the third only reaches 5. It might because the surfaces of the two targets had been severely contaminated or oxidized, and position of the magnetron was wrongly placed in center of the chamber where argon pressure is not uniformly distributed being near the pumping port. The magnetron was put aside then - as far away as could be placed from the port later, and following sputters got good niobium films with RRR from 10 to 20. Typical sputter parameters are listed in table 4-1.

Table 4-1 Parameters of niobium sputtering

Argon	0.5	Pa
Voltage	360	V
Current	1.2	A
Deposition rate	100	nm/min
Film thickness	1.5	μ m

4.5 Cosputter of V_3Si

In the sputtering experiments, a high purity vanadium target (99.7%) and a silicon target with purity 99.999% was used, Ga-In alloy (liquid) was applicated to give good electric and thermal conduction to the magnetron. When the two targets were driven independently, the regime becomes unstable, particularly at lower argon pressure and higher voltage difference. At argon pressure lower than 1Pa, sputtering with target voltages ratio larger than 2:1 was always accompanied by plasma oscillations, and extinguish or arcs generated in a few seconds, there was no stable discharge sustained at low argon pressure.

In the facing-target magnetron, the two targets seriously react to each other during sputter: turn on the power of only one target, the other target will response immediately from electric induction, it will have a same current if it is grounded, or get a same potential while being suspended. It is quite difficult to adjust sputtering parameters since voltage or current of one target change, the other will shift too. As arcs on one target surface will result in the other one, the discharge is not safe to magnetron power head, one of them was broken in a few runs.

The high sputter current that had been easily reached when sputter niobium films with a single head now becomes nearly unachievable. Finally, argon pressure increased to 3-5Pa to perform proper discharge. Further increasing of pressure will cause serious glow discharges and arcs on the electric feed-through as well as on the targets, since sputter voltage of the vanadium target was as high as 950V during the process.

Copsuttering experiments were performed at various temperatures, from room temperature up to 700℃. In the attempts to get 700℃, two BN heaters were broken due to the high current needed. Although the heater itself can be heated up to 2000℃ according to the advertisement, the brittle ceramic structure prevents a very tight electric connection with the feed-through, which is often no problem at low current, and got troubles in high currents.

The BN heater was replaced by the tungsten heater then. We installed a liner driver to lift the new heater while rotating the carousel for changing new samples, and push it as close as possible to the sample holders during sputter, the required 700℃ was got. But it is noticed that the heater center is very hot too, since the first time we wand a 0.25 mm diameter tantalum filament - it was broken very soon. And a tiny piece of ceramic bush in the center location was melted when occasionally heating the samples above 700℃ after the tantalum wire replaced by tungsten one. It might give an explanation to the reason why it did not like the old BN heater, the new one must be turned off during sputter, otherwise, arcs generated on the hot heater surface in an ambient plasma surrounding would cause the heater power turn off automatically. Typical sputter parameters are listed in table 4-2.

Table 4-2 Sputtering parameters of copsutter of V_3Si films

Argon	4.0	Pa
V voltage	950	V
V current	0.3	A
Si Voltage	400	V
Si current	0.2	A
Temperature	500	℃
Time	20	min
Film thickness	0.5	μ m

Some samples sputtered at lower temperature were annealed at 700℃ with the carousel and the sample holders in, and finally at about 800℃ after all copper and stainless steel components of sample holders and the carousel being moved out from the vacuum chamber in order to improve film qualities. To anneal at 800℃, the samples were carried by a niobium oven on which the thermocouple fixed, and put the oven directly inside the heater.

4.6 Film analysis

A commercial Scanning Electron Microscope (SEM) with an attachment of Energy Dispersive X-ray Spectrometry (EDS) is a powerful instrument in analyzing of thin film surface and material compositions. But is our case, the EDS technique showed some uncertainties in the V_3Si thin films composition measurements. Moreover measured composition of the films was found to depend on the energy of injected electron beam.

Actually, the electron beam energy should be no less than 10keV to ensure good accuracy in the EDS measurement, because the characteristic X-ray energy of vanadium is about 5keV, while that of silicon is only 1.8keV. Even at an energy less than 7keV, some electrons begin to penetrate the thin V_3Si film and knock into the sapphire substrate, since film thickness is only 0.5um. Consequently, the analysis program would calculate the film composition including adsorption corrections without accounting for the difference between the film and the substrate, so it cannot accurately detect compositions of the thin V_3Si films.

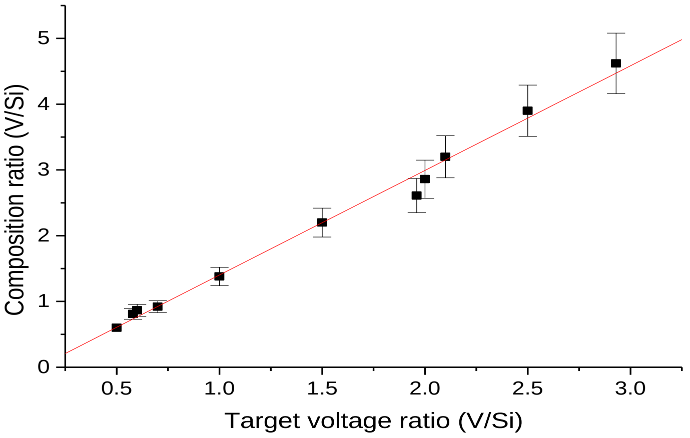

Fig.4-8 Sputter voltage and EDS measured compositions

Although EDS cannot measure composition of the V_3Si films at high accuracy, it is a very convenient diagnostic and gives us helpful information about which direction to take for the futures runs. We found that the EDS measurements showed that the film composition ratio of vanadium and silicon has a liner relationship with that of the sputter voltages. See fig.4-8, electron energy is 10 to 12 keV in the EDS measurements.

In order to analyze composition of the thin film accurately, Rutherford

Backscattering Spectrometry (RBS) technique is used. It has an accuracy better than 5% and has been proved to be a very valuable technique for this purpose. Beside distinguish of the chemical composition, it could measure the film thickness as well. In the RBS measurement, 1.8MeV He^+ ion beam from the 2MeV LNL accelerator is used.

The quality of V_3Si superconducting films is measured by the standard four-probe DC resistance measurement. There is no transition above 4.2K found in all the samples sputtered at room temperature, and all of them has a RRR less than 1.0, under the SEM, no crystalline or grain growth trice was found on the sample surface. It means that the V_3Si films are highly disordered or amorphous when sputter at such a temperature.

When temperature increased to 300-400℃, a few sputtered samples showed very weak transition between 8 and 9K, and only after sputtering temperature increased to 500℃, Tc above 10K has been detected, but the samples always get an RRR less than 2. Further increasing of temperature to 600℃, RRR greater than 2 and Tc higher than 12K have been measured, while only at 700℃, we got V_3Si samples with Tc above 13K. It confirms the already known conclusion again that high temperature is necessary to get high quality A15 superconducting compounds.

From the RBS data, the V_3Si samples sputtered at 500℃ showed that the A15 phase been formed with silicon contents from 21% to 32%, while the best sample has a silicon content about 28%, unlike that of the bulk material which should be approximately 25%. Tiny amount of contamination of copper was found in samples sputtered at temperature higher than 500℃, while vapor pressure of copper is not so high at a temperature range from 600℃ to 700℃, it might resulted from ion bombardments on copper sample holders by negative ions and reflected neutral atoms or plasma aid sublimation of the hot copper surface.

When annealing the sputtered V_3Si samples at 600℃ and 700℃ for three hours, it is found that the film qualities (RRR and Tc) are weekly depend on the composition (in the above mentioned composition range), but strongly on the process temperature. After removing all copper components, some samples were annealed at 800℃ for two hours, only those samples sputtered at lower temperature showed improvements, while the rest sputtered at 600℃ or 700℃ showed no improvement due to the result of copper contamination.

In order to get high quality V_3Si film, we sputtered some samples at room temperature, and anneal them at 800℃ for 2hours. But the thermal stress in the film was so high that all samples were broken in the first run. The sputtered film thickness had to be reduced to only 0.3μ m in the following run, and after annealing, the best sample get an RRR 4.5 and Tc 14.4K.

We tried to anneal the sputtered samples finally at 800℃ for 3 hours in a different configuration, the surface of the films faced to the heater this time unlike the previous annealing that the films faced to the niobium shielding, to our surprise, film quality increased a lot. The highest Tc is 15.9K and RRR 12.3, all samples with silicon content ranges from 20% to 30% got Tc beyond 15.5K.

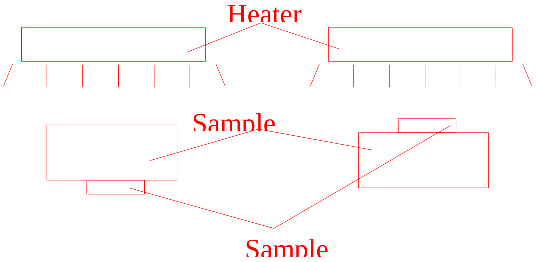

Fig.4-9 Annealing samples in two different ways

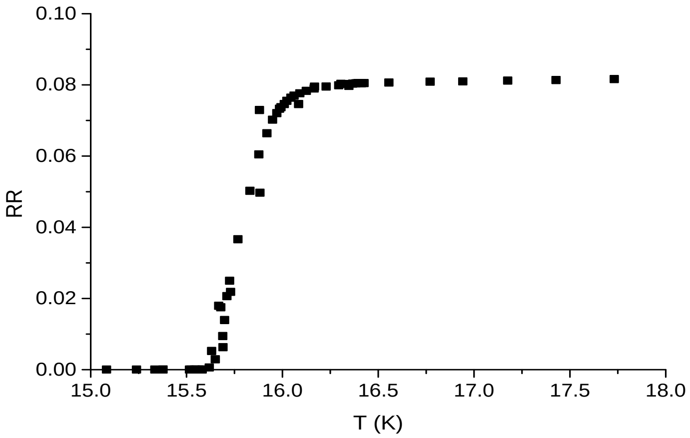

Fig.4-10 SC transition of an annealed sample

The reason that we had not got good V_3Si films before is clear then, the process temperature of the film was lower than the measured value as it was only the temperature of the sample holders. Since the interface of the sapphire substrate and the copper sample holder acts as a thermal barrier, real temperature of the film surface is much lower than that of the holder. And the temperature difference could be as high as several tens to more than a hundred centigrade, especially in the high temperature region where thermal irradiation dominate the thermal transfer.

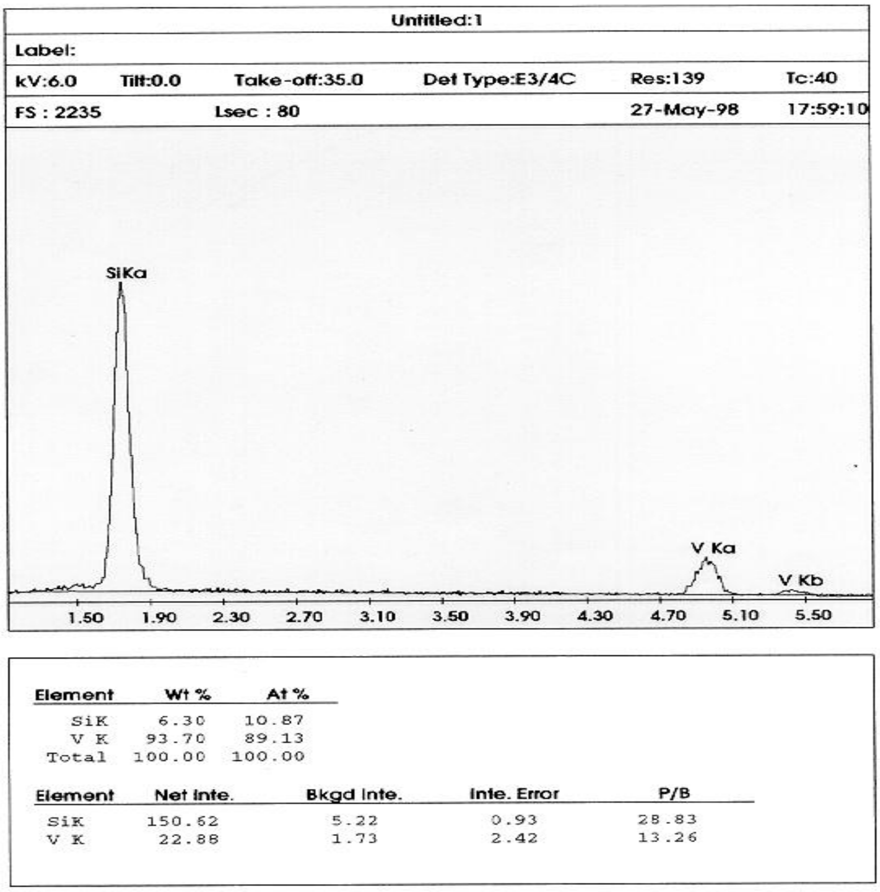

Untitled:1

Label:

kV:6.0 Tilt:0.0 Take-off:35.0 Det Type:E3/4C Res:139 Tc:40

FS : 2235 Lsec : 80 27-May-98 17:59:10

Element	Wt %	At %
SiK	6.30	10.87
V K	93.70	89.13
Total	100.00	100.00

Element	Net Inte.	Bkgd Inte.	Inte. Error	P/B
SiK	150.62	5.22	0.93	28.83
V K	22.88	1.73	2.42	13.26

Fig.4-11 EDS figure or a sputtered sample

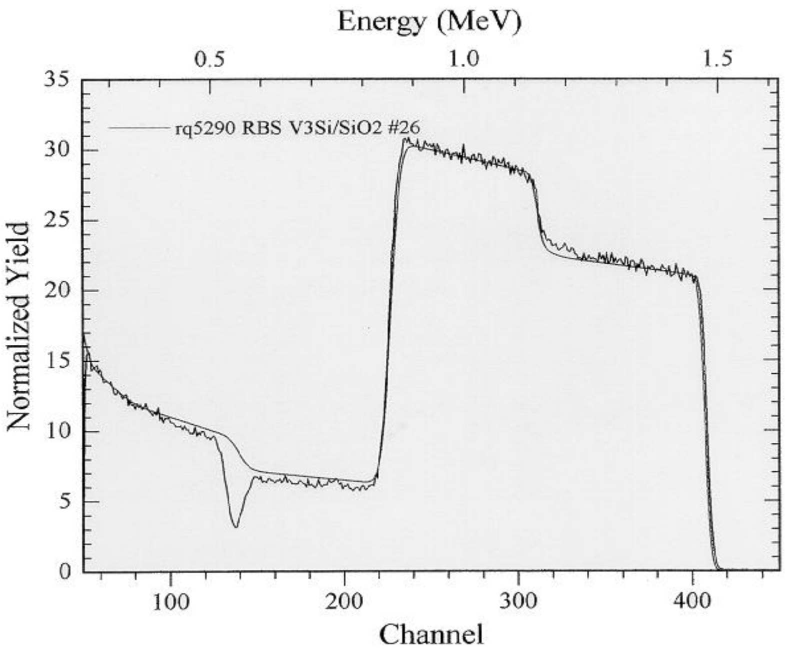

Fig.4-12 RBS figure of a sputtered sample

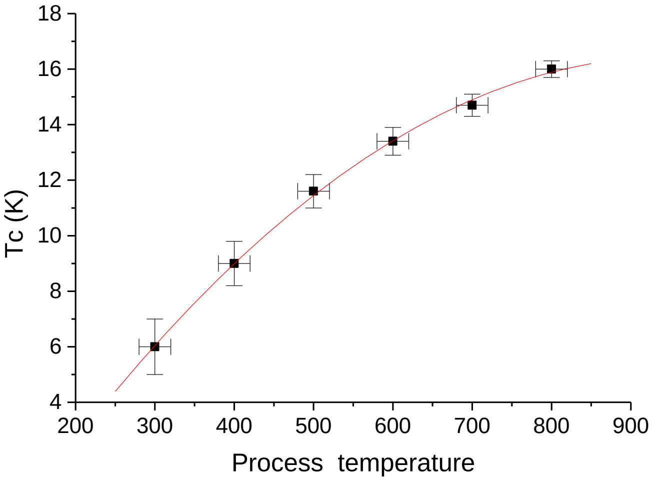

Fig.4-13 Tc of the V_3Si film vs. Process temperature

4.7 Discussion

It is interesting to note that the film composition mainly depends on the sputter voltage instead of sputter current or power - which is a general case in magnetron sputtering, when sputter V_3Si films with the facing-target magnetron. A simple explanation lays in the fact that the plasma is common in a facing-target magnetron, positive ions bombard the targets that cause consequent sputtering of target atoms and secondary electrons, while current represents compensation of lost electrons during the process.

Electric field distribution is determined by voltages of the two targets, cathode sheaths, plasma potential and distribution in the facing-target magnetron, and decide which part of positive ions in the plasma will bombard corresponding targets. Higher target voltage is appreciated to attract more ions to bombard the target and cause more rapid sputtering. Consequently, composition in the film will increase.

To find out the real relationship of target voltage and film composition will be somewhat difficult, because the potential drops in cathode sheath and in plasma are quite different. And there is no accurate method to predict them for procedures involved in magnetron sputtering are very complex and some of them are not clearly known up to now. In addition, sputtering yield of vanadium and silicon is different and changes with ion energy in distinct form. To see the problem somehow, we have to simplify it greatly.

Let us assume the plasma is uniformly distributed in a sphere shape between the two target, and there is a balance plane in the plasma, while plasma will not have an effect to the balance plane, and electric field only depends on target voltage and distance to the balance plane. Ions will bombard which target is decided just by their positions to the assumed balance plane.

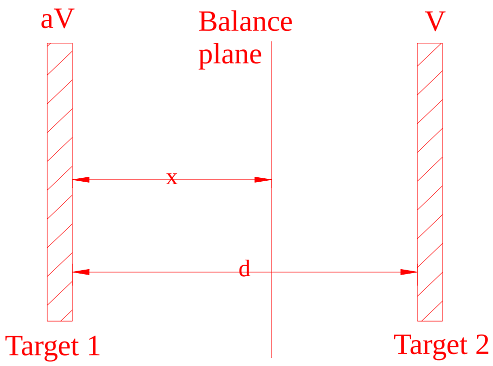

Fig.4-14 Target voltage and assumed balance plane.

See fig.4-14, position of the balance plane is assumed only depends on voltages of the two targets. It can be solved by any static electric field calculation code, such as POISSON, MAFIA and so on. The approximate relationship of voltage and distance to the targets is,

$$x = \frac{\sqrt{a} + \sqrt[3]{a}}{4} \cdot d$$

Volume of the part with a height x in a sphere is

$$V = \pi \cdot \left(R \cdot x^2 - \frac{x^3}{3} \right)$$

Where, R is the sphere radius

Introduce the above two equations, and assume the radius equals to a half of the distance between the two targets, then the volume ratio of the two parts is

$$\frac{V_1}{V_2} = \frac{5a + 6a^{\frac{2}{3}} + 12a^{\frac{5}{6}} - a^{\frac{3}{2}} - 3a^{\frac{4}{3}} - 3a^{\frac{7}{6}}}{32 - 5a - 6a^{\frac{2}{3}} - 12a^{\frac{5}{6}} + a^{\frac{3}{2}} + 3a^{\frac{4}{3}} + 3a^{\frac{7}{6}}}$$

The equation denotes that the relationship between target voltage and ion bombardment is nearly linear in our experiment range, while the exact relationship might be more complex. Fig.4-15 shows the calculated and RBS measured film compositions versus target voltage ratio. Since data of sputtering yields of vanadium and silicon at argon ion energy below 500eV are not enough, we assume that the sputtering yield of vanadium and silicon is equal and does not change with the voltage. From all these simplified assumptions, the composition can be calculated very roughly.

Facing-target magnetron is a structure of electron trap, while applied different voltages to the two targets, confinement of electron and plasma will be eliminated, especially at higher voltage difference as potential wall of the trap decreased much. A lot of electrons will be lost without ionization during the sputter process, consequently there is not enough secondary electrons to sustain the discharge. That is the reason why it is nearly impossible to sputter at low argon pressure, and difficult to get a larger sputter rate even at higher pressure.

The optimum deposition temperature of high quality superconducting V_3Si film is above 800℃, since high temperature is benefit to form better crystalline. But high temperature will cause more copper trapped in the films in our sputtering system. From this point of view, it is quite difficult to sputter V_3Si superconducting films good enough to coat a copper cavity by the cosputtering technique[110].

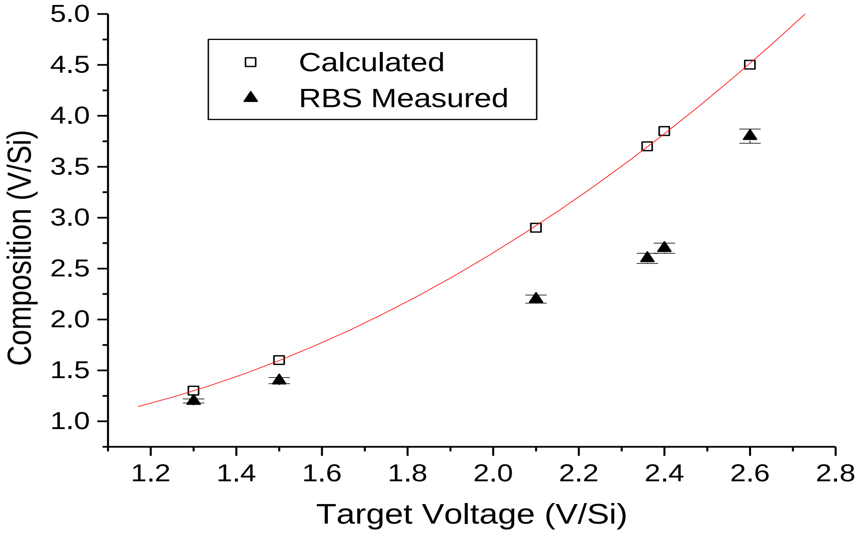

Fig.4-15 V_3Si film composition and target voltage

The experiment indicates that facing-target magnetron could work in the regime to sputter films of two kinds of materials with various compositions simply controlled by applying different voltages to the corresponding targets. Although the facing-target magnetron is very useful to sputter high quality films of compounds as well as single elements, it does not work very well at higher voltage difference between the two targets, in which situation will loss the merit of the magnetron.

Not only stoichiometric composition is required when sputtering of superconducting V_3Si films, higher sputtering or annealing temperature is also important. It is difficult to coat very good superconducting V_3Si films on a copper cavity and make a high performance SRF cavity by the magnetron cosputtering technique.

Because the high process temperature and the difficulty of target configuration in cosputter of V_3Si on a cavity. There are two solutions, one is use a refractory metal instead of copper, e.g. niobium, as the substrate cavity, another one is to study of other deposition technique as for reactive sputtering.

Chapter 5

Reactive sputtered V_3Si films

5.1 Introduction

Reactive sputtering technique with silane gas in an argon atmosphere is widely used in semiconductor industry, while in V_3Si superconducting films it also found a role. The process temperature and the film quality is of great concern when the technique used in sputtering V_3Si films since the optimum process temperature of the A15 super-conducting film is 800 to 900℃. Which is too high for some substrates such as copper or quartz, due to the high vapor pressure of copper at 800℃ or higher temperature, and there is a serious thermal diffusion between quartz substrate and V_3Si films at elevated temperature[111].

It is well known that reactive sputtering technique by introducing the reaction gases in an ambient of plasma drastically decreases the sputtering deposition rate, and compositions of the deposited films is very sensitive to the process conditions. Models of the reactive sputtering can be found in literatures[112-114], from analysis of the sputtering deposition and consumption of the reaction gases, the model predict that there exists a simple linear relationship among the film composition, deposition rate and partial pressure of the reactive gas. It is possible to keep a constant film composition at different partial pressure of the reactive gas with appropriate deposition rate.

Comparing with the cosputtering of V_3Si, reactive sputtering technique will be much feasible to coat superconducting V_3Si films on a substrate cavity, because the target material - pure vanadium is commercially available and it can be shaped to suit the sputtering of SC cavities like the sputtering of niobium films. Sputtering with a bulk V_3Si cathode is difficult to get the needed target shape as the material is quite brittle and the special material cannot be found in categories of almost all companies. Cosputter with vanadium sheets plus silicon pieces will encounter the same problem of target fabrication, and further more, the sputter parameters should be controlled strictly since the sputtering yields of vanadium and silicon change differently with sputter voltage.

But reactive sputtering will have another problem, that is variation of the film composition. Because the composition is sensitive to the film deposition rate, different locations on the cavity surface often receive different deposition rate, although by a correct discharge time solution will lead to a uniform total film thickness. In reactive sputtering, film composition will be varied in different cavity surface areas. If there is only one kind of reaction product, the problem can be avoided by introducing a sufficient partial pressure of reaction gas, but in argon/silane discharge, many kinds of vanadium compounds can be formed.

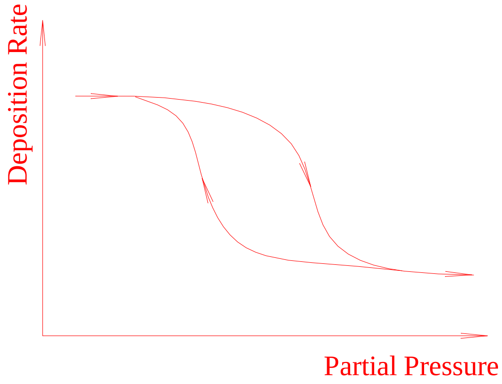

Fig.5-1 General reactive sputtering curve

Generally, it is very important to trace the characteristic curve of the reactive sputtering. Since reactive sputtered films with a stoichiometric composition need to be deposited at higher rate in most commercial applications. While in most case, high quality films are got under higher sputtering deposition rate, in the special one of V_3Si superconducting films, high quality films (higher RRR and Tc) were got under lower deposition rate and deposited on hot substrates. Since the constant stoichiometric compositions could be easily repeated by choosing appropriate deposition rate versus partial pressure of silane gas, and the reactive sputtering curve is quite difficult to measure in our vacuum configuration, the reactive curve had not been studied systematically.

The home made facing-target magnetron and the vacuum system had been introduced in chapter 4 of co-sputtering, a QMA (Quadruple Mass Analyzer) was installed before reactive sputtering, and old targets were replaced by two vanadium disks. Since silane is one kind of dangerous, toxic and explosive gas, its transportation, restore and operation must be carried out very careful in case of any careless harzard[115]. The silane line and restore system was installed and tested by warranted staffs of a service company.

5.2 Sputtering experiment

The vanadium targets were sputtered without silane first at room temperature to remove the surface oxide. The plasma color is blue like that of niobium sputtering. Then introduced silane gas and increase the partial pressure step by step tried to measure the reactive curve. But the efforts failed, because the reactive curve is too steep to figure out. At lower voltage with silane partial pressure 5×10^{-2}Pa, the deposition rate is only a little less than that of without silane; at 6×10^{-2}Pa the plasma was distinguished, it is only around 1 percent variation of the total pressure and close to the precise limit of the vacuum readout. If the sputter voltage increased to have a stable reactive sputtering, without silane the discharge power will increase beyond limit of the DC magnetron head, 1.5kW.

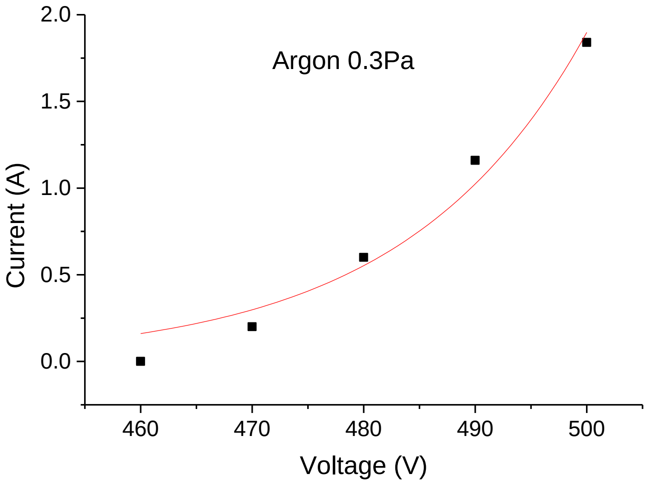

Fig.5-2 V-I curve of vanadium sputtering

Two ion gauges had broken in a very short time in reactive sputtering operations, as the pyrolysis of silane on the hot tungsten filament will generate hydrogen gas and made the filament quite brittle. We have to turn off the ion gauge during sputtering to keep it a reasonable life time, and turn on the ion gauge again to change a new pressure while the sputtering stopped. This made the measurement of reactive curve nearly impossible since the characteristic hysteresis effect of reactive sputtering, the measured deposition rate, sputter voltage and current at the reaction region seemed randomly scattered. It was also found that the total pressure readout was less than the sum of individual silane pressure and argon pressure, which might due to different ionization efficiency of silane and argon.

The maximum sputtering temperature was limited to 500℃ to avoid copper contamination from the copper made substrate holders which had been mentioned in the previous chapter, and to protect the tungsten lamp heater as the hot tungsten filament broken easily in the reactive sputtering process. All the substrates were 1cm^2 square sapphire ones with thickness 0.5mm.

The reactive sputtering was curried out from room temperature up to 500℃, and silane partial pressure from 0.8Pa (approximately one half of total pressure 1.5Pa) to 0.1Pa or one tenth of total pressure (1Pa). Deposition rate was measured on situ by the commercial quartz thickness monitor, by choosing appropriate sputter current or power, recorded deposition rates were from 0.2nm/s to 1.3nm/s. All samples were sputtered in thickness 0.5 to 0.6μm.

Table 5-1 Parameters of the reactive sputtering

Argon	0.9	Pa
Silane	0.15	Pa
Current	0.39	A
Voltage	480	V
Sputter temperature	500	℃
Deposition rate	0.6	nm/s
Annealing temperature	800	℃
Annealing time	3	hour

After all copper components were removed out of the chamber, some samples were put inside a niobium oven and annealed at 800℃ for 3 hours to increase the film quality. Because two tungsten filaments in the heater were broken during the reactive sputtering, the heater was replaced by a new BN one then. The background vacuum was 1×10^{-5}Pa at room temperature and $2\text{-}3\times10^{-4}$Pa at the elevated temperature. It takes about one hour to increase the sample temperature to 800℃ from the ambient room temperature, and 3 to 4 hours to cool down below 100℃ after the heater turned off.

It could be deduced by observing the reactive sputtering conditions that chemical reaction takes place on the vanadium target surface, as sputtering always need several seconds to stable after a new silane pressure adjusted, which means the target surface chemically changed in the process.

5.3 Measured results.

Scanning Electron Microscope (SEM) and Energy Dispersive X-ray Spectrometry (EDS) techniques were applicated to analyze the surface and composition of the sputtered V-Si films. The sample was measured by the standard four-probe DC resistance measurement, which gives Residual Resistance Ratio (RRR) and Tc of the films.

The measured compositions showed that silicon content in the films has an approximately linear relationship versus the deposition rate while silane partial pressure and sputtering temperature is fixed. When deposition rate and the temperature keeps constant, silicon content in the films has a linear relationship with silane partial pressure. See fig.5-3 and fig.5-4.

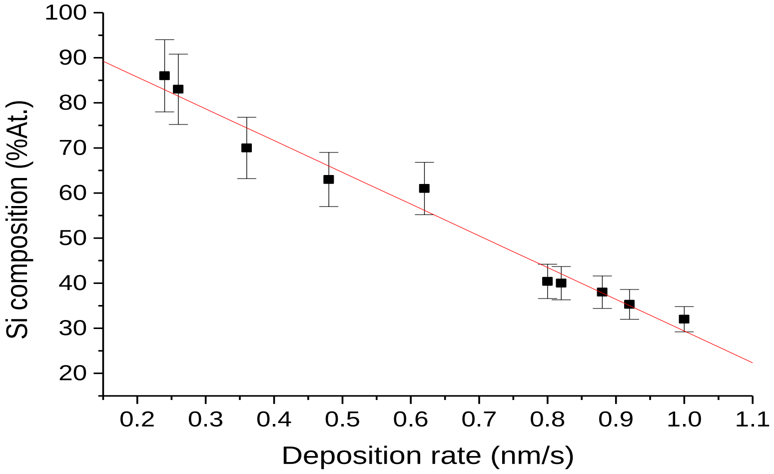

Fig.5-3 Silicon content versus deposition rate
Fixed Silane partial pressure 0.6Pa,
Argon 0.7Pa, temperature 500℃

Another factor that influences the composition of deposited V_3Si films is the sputtering temperature. From fig.5-5, high sputtering temperature will benefit for increasing silicon content in the deposited films. It can be explained in the variations of reactive sticking coefficient of the silane gas at different temparatures[116] or the silane pyrolysis rate increases with the process temperature[117] that the sputtering deposited film composition has a relationship with the process temperature. As the targets are cold by cooling water, their temperature will change the same way in different sputtering runs, in this case, film composition affected by the sample temperature indicates that at least there are some reactions occurred on the deposited film surface in the reactive sputtering of V_3Si films.

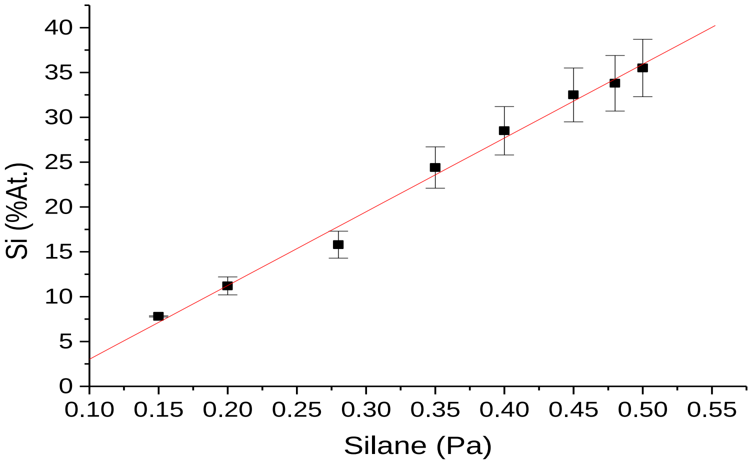

Fig.5-4 Silicon content versus silane partial pressure
Fixed deposition rate 1.2nm/s, Argon 0.8Pa
Temperature 500℃

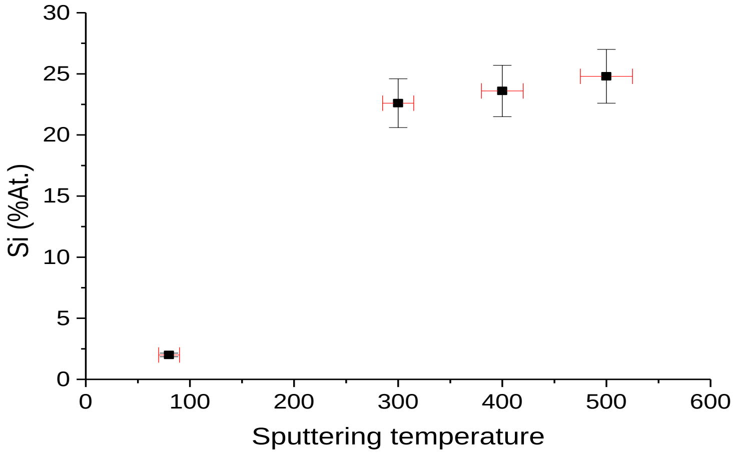

Fig.5-5 Silicon content versus sputter temperature.
Fixed Silane partial pressure 0.15Pa,
Argon 0.9Pa, deposition rate 0.6nm/s

Because sputtering deposition rate, silane partial pressure and process temperature has a contribution to the V_3Si film composition in the reactive sputtering, to get stoichiometric V_3Si films at different temperature need to adjust silane partial pressure or/and the deposition rate. But in the reactive sputtering of SC V_3Si films, stoichiometric film composition is of minor importance comparing with the process temperature when quality of the film was concerned.

If there is only one kind of product compound in reactive sputtering, the regime can be simplified to give and maintain a sufficient partial pressure of reactive gas. But in the reactive sputtering of V_3Si films, there are several kinds of compounds could be formed. See fig.5-6, there are several RRR peaks versus different silicon contents in which metal vanadium, V_3Si superconductor and VSi_2 compound can be pointed out, the rest two peaks corresponding to V_3-Si_2 and V_2-Si composition respectively. For this reason, it is important to use a reasonable deposition rate and maintaining a appropriate silane partial pressure to get the required stoichiometric composition in the reactive sputtering of V_3Si superconducting films.

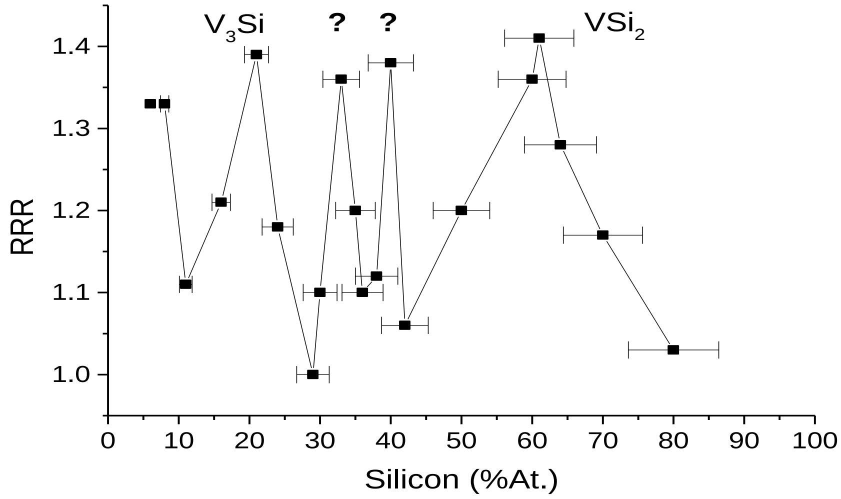

Fig.5-6 RRR and different silicon composition

Temperature 500℃, silane 0.3 to 0.6Pa,

Deposition rate 0.3 to 1.3 nm/s

Superconducting transitions above 4.2K were found in samples sputtered at 300℃ or higher temperature. While those sputtered at 500℃, V_3Si samples with silicon content 10% to 30% at. got Tc higher than 6K. The best samples which was sputtered with the parameters given by table 5-1 got a RRR 1.7 and Tc 11.8K, and after annealed at 800℃ for 3 hours, its RRR increased to 16.7 and Tc 16.1K. The highest Tc of 16.2K was achieved by another sample sputtered and annealed at the same conditions. All the annealed samples with silicon content 10% to 30% at. got Tc beyond 15K and RRR 8 to 17.

Under SEM, it was found out that some V_3Si samples were randomly covered by submicron silicon rich particles on the surface. Although we cannot explain why there was not on other samples, it comes as a natural phenomenon in low pressure argon/silane glow discharges to generate negative charged silicon rich clusters[118,119], and some of the clusters will stick on the films. Before annealing at high temperature, crystalline structure of the sputtered V_3Si films was highly disordered or amorphous, no trace of grain growth was found.

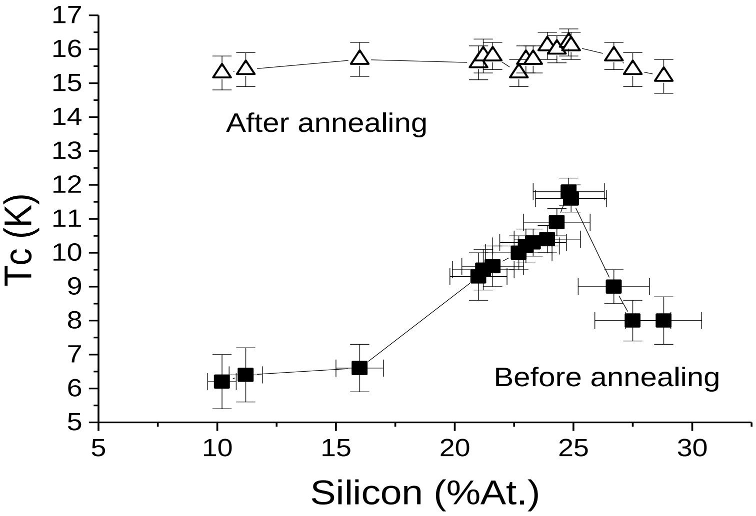

Fig.5-7 Tc vs. silicon content before and after annealing

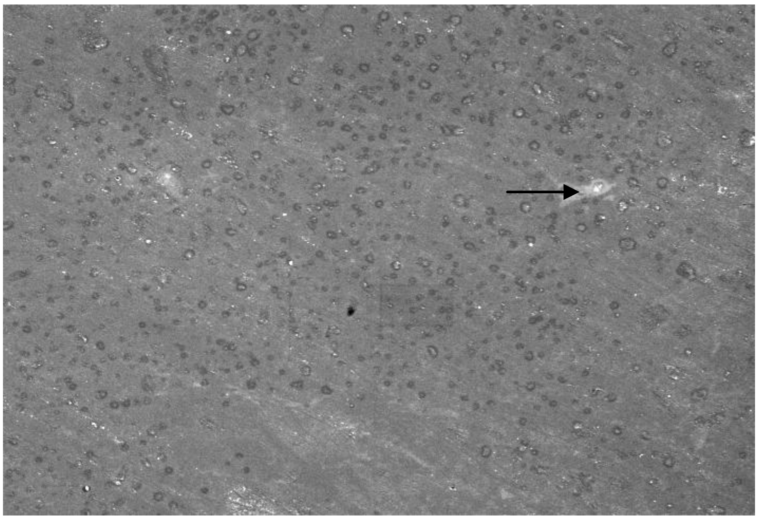

Fig.5-8 One sample covered by silicon rich particles.

Surface grain structure of sputtered V_3Si films had been found only after annealing at high temperature. Some of the samples showed grain structures like a combination effort of sputtering and annealing. The average grain size of the annealed samples is quite different, from 0.1 to 0.5 micron, and the film composition, RRR or Tc value did not show any obvious relationship with the grain size. Only the samples' RRR or Tc becomes higher when the film composition close to the stoichiometric value of V_3Si.

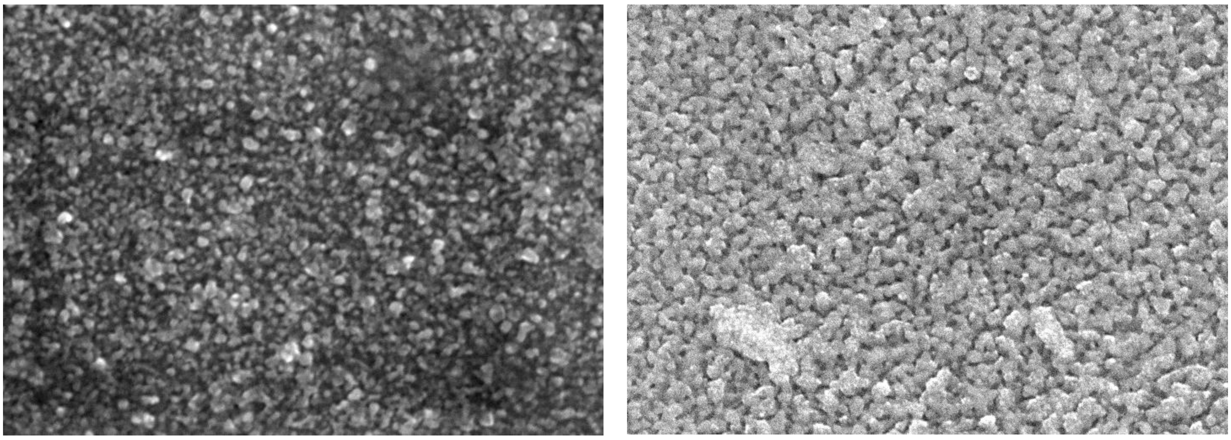

(a) Grain size 0.2 microns (b) Grain size 0.5 microns

Fig.5-9 Surface topography of two annealed samples

Stoichiometric V_3Si films have been sputtered at silane partial pressure from 0.1Pa or one tenth of total pressure (1Pa) to 0.33Pa or approximately one third of the total pressure. To get stoichiometry V_3Si films, a linear relationship of deposition rate and silane partial pressure was found. The RRR and Tc measurement also demonstrated that lower deposition rate tends to get better V_3Si films, even if the EDS measured result showed that their compositions have a little difference.

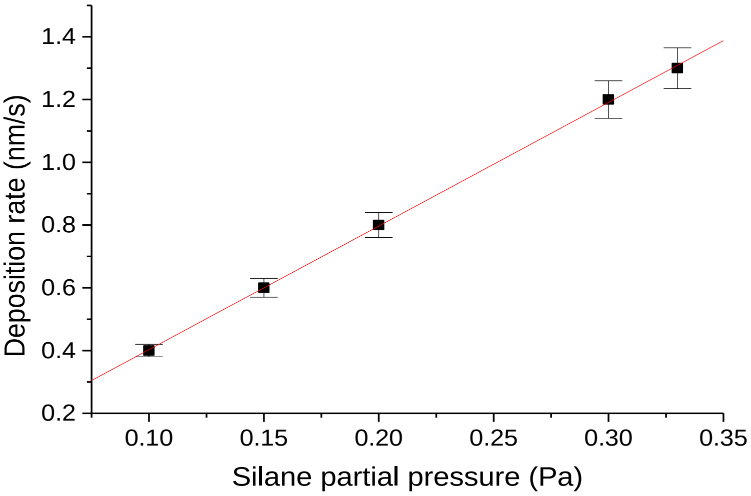

Fig.5-10 Deposition rate vs. silane for stoichiometric V_3Si films

Sputtering temperature 500℃, argon 0.8Pa

Sample get lower Tc and RRR at higher deposition rate and higher silane partial pressure might be the result of more hydrogen absorbed in the sputtered V_3Si films. Because most of produced hydrogen in the reactive sputtering would be pumped out at lower silane pressure, and absorption of hydrogen by the film would be less. After annealed at 800℃ for 3 hours, most of the absorbed hydrogen were released, and all the V_3Si films sputtered at stoichiometric composition get Tc beyond 16K. After annealing there is nearly no difference between the samples sputtered at low deposition rate or at deposited at high rate.

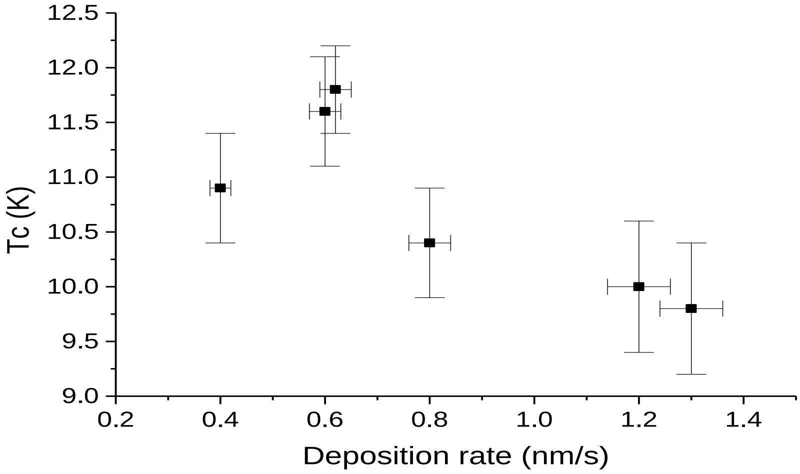

Fig.5-11 Tc of the V_3Si samples at different deposition rates
Sputtering temperature 500℃ (Before annealing)

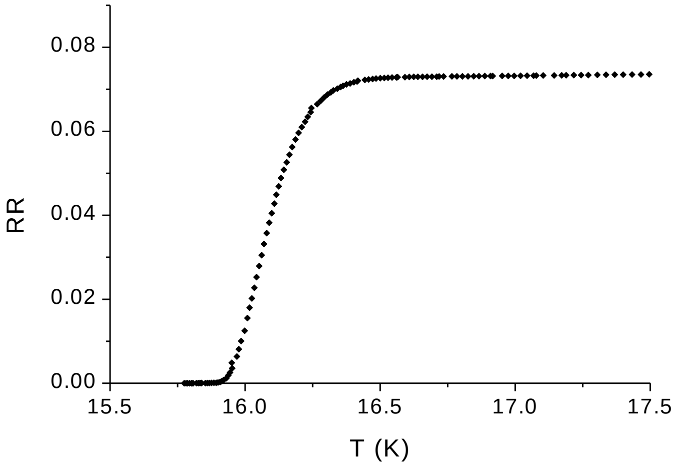

Fig.5-12 DC transition of an annealed V_3Si sample

5.4 Discussion

In the reactive sputtering of V_3Si superconducting films, stoichiometric composition had been got under different deposition rate and different silane partial pressure. Sputtering temperature has a influence on the film composition too. High quality film was got at lower silane partial pressure with lower deposition rate and higher process temperature. When annealing temperature reached 800℃, V_3Si films with silicon contents from 10% to 30%at. has got Tc greater than 15K.

To sputter a V_3Si SRF cavity, reactive sputtering could be better solution than cosputtering. There are two reasons, one is the difficulty to make an appropriate target for coating the cavity in the cosputtering, another is that quality of the cosputtered film is not so good as that of the reactive sputtering. Because the best sample in the cosputtering is only RRR 12.3 with Tc 15.9K, while in the reactive sputtering, it is RRR 16.7 and Tc 16.2K. Whatsoever their difference is not very significant.

Another choice is to study reactive diffusion: sputter vanadium films on a niobium substrate cavity and then, annealing in silane atmosphere to generate V_3Si films. Because bulk vanadium cavity is more expensive than a niobium one, and thermal conductivity of vanadium is very poor, moreover, the thermal diffusion rate is much low in bulk material and the diffusion time might be too long to any practice or the process temperature needed too high. Copper cavities are cheaper and good at thermal conductivity, but the high process temperature limited their applications on this field, and could be considered in the future with thermal diffusion barriers.

But reactive diffusion of V_3Si film in silane atmosphere will be a quite complex procedure, because the outer surface of the niobium cavity will be reactively diffused too in silane. If the produced niobium-silicon compound is thick enough, the cavity wall will have a quite poor thermal property since the compound has a very low thermal conductivity[120]. The details of thermal diffusion of niobium in vanadium films or in V_3Si, and vanadium, silicon or V_3Si diffusion in niobium is far away from been cleared. Intensive studies need to curry out first.

As had been noted, the different deposition rate existed in different areas of the cavity will result in composition variation during reactive sputtering of V_3Si superconducting films that might degrade the cryogenic

RF performance of the cavity. If the discharge deposition is carefully controlled, the difference of deposition rate will not be significant and the film composition can be kept in a tolerable region. But even if the film composition on the surface of a cavity will not give any trouble, the film itself could not be good enough.

Some samples were measured by AC measurement, the AC current frequency fixed at 193Hz to avoid any multiple of the commercial electricity. The results showed that the sputtered films are in multiphase even after 3 hours annealing at 800℃. Fig.5-13 gives an AC transition curve of an annealed sample with Tc 16.1K in the DC measurement[121]. Reactive sputtered V_3Si films' Tc measured by AC method was approximately 14K to 15K, while the onset is corresponding to the DC transition data. The film is obviously in multiphase, as the highest Tc phase shielded all other phase in DC measurement. The poor AC features of the sputtered V_3Si films will not yield good RF performance. In this case, reactive diffusion remains the only choice of a V_3Si coated cavity.

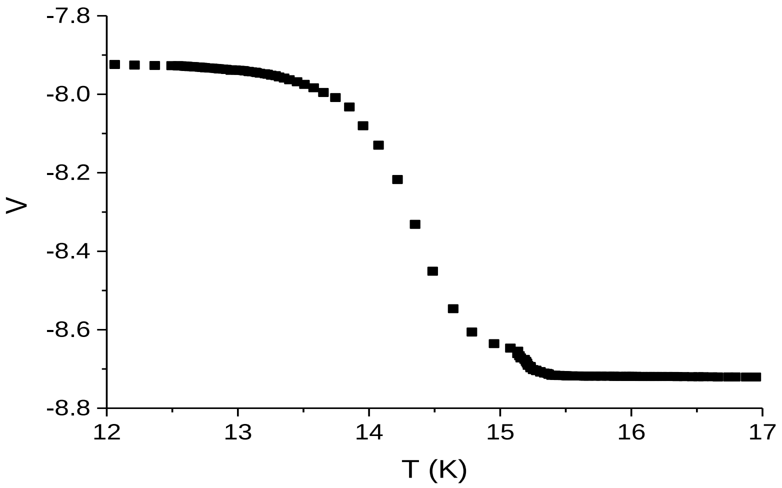

Fig.5-13 AC superconducting transition of an annealed sample

In AC measurement, Tc of the film is below 15K, at least 1K lower than the DC result, and Δ Tc around 1.5K, four times larger than that of DC measurement.

Chapter 6

Thermal diffusion of V_3Si films

6.1 Introduction

Prior to the thermal diffusion of V_3Si SC films, magnetron sputtering of V_3Si films was investigated. Chapter 4 and chapter 5 introduced the experimental study of Co-sputtered of V_3Si films and reactive sputtering respectively. Although the magnetron sputtered V_3Si films got highest RRR of 17, their Tc were only around 16K, a bit lower than that of bulk material, 17K. Meanwhile, RF residual resistance of the sputtered V_3Si films measured by dielectric resonator technique is quite high[122]. The same problem of high residual surface resistance of magnetron sputtered V_3Si films discovered at Napoli University measured by microstrip resonator technique[97]. As a general case, sputtered V_3Si film has high residual surface resistance. It should be avoided in SRF applications, since a SC cavity cannot achieve superior quality with high residual resistance.

Thermal diffusion technique of Nb_3Sn films on bulk niobium cavities has been showing a promising way to upgrade SC cavities. And thermal diffusion of Nb_3Sn films by two steps: sputtering coated niobium films on sapphire substrates followed by thermal diffusion in Tin vapor got Nb_3Sn films as good as those on bulk niobium. But techniques usually employed like co-evaporation and magnetron sputtering formed Nb_3Sn films commonly characterized by high residual surface resistance like magnetron sputtered V_3Si films, since they suffered from non-stoichiometric and weak super-conducting phase as well as weak coupling across grain boundires[123].

Thermal diffusion of V_3Si film comes as an alternative coating technique since V_3Si has very similar property as that of Nb_3Sn. But diffusion of silicon on the surface of a bulk vanadium cavity is not the best solution, because of poor thermal conductivity of the material (50% lower than bulk niobium) and higher temperature or longer process time needed in bulk diffusion process. The former would lead to an interior thermal breakdown threshold of the SC cavity, and the second would increase difficulty and cost to the fabrication procedure. Sputter vanadium films followed by thermal diffusion expected to be an ideal answer to the problem. Since sputtered film generally has smaller grain size (at least three orders less) compared with that of bulk material, and the column nature of the film gives a thorough diffusion path up to the entire depth of the film. So that a substrate cavity with better thermal conductivity could be chosen, and the diffusion temperature as well as the process time could be drastically reduced.

In the diffusion experiments, sapphire substrate was used for coating vanadium films as it has a high stability in elevated temperature. Film composition was measured by EDS technique, and quality of the film was detected by the standard four-probe DC resistance measurement. Since a SC cavity with V_3Si film coating is pursued, some samples were coated on niobium substrates and measured by AC inductive measurement. SC features of the diffused V_3Si films on sapphire are quite good, Tc higher than 16.8K, close to its bulk value. Because of the large diffusion rate of vanadium in niobium substrate[124], no reliable SC V_3Si film was formed on niobium substrate. A stable material coatings that could serve as diffusion buffer layer between niobium substrate and vanadium film have to be coated on the niobium substrate before coating vanadium film, but the process is very difficult.

Bulk vanadium annealed in silane atmosphere also got good V_3Si samples, there is no principle difficulty to fabricate a V_3Si film coated SC cavity by this technique. The only problem is the poor thermal conductivity of vanadium that performance of the cavity at high accelerating gradient will be seriously limited.

Because temperature in the thermal diffusion of V_3Si film could be reduced to 800˚C that is not too high to a copper cavity, diffusion of V_3Si films on copper substrates was studied too. Before annealing in silane, the copper samples were sputtering coated with vanadium films on both sides to prevent sublimating of copper in the diffusion process. As the experiment time was very limited, only a few runs has not got good SC V_3Si film yet.

Since the study of V_3Si SC films as surface coating material for SRF cavities has been on the right track, it is expected that the first V_3Si film coated SC cavity would be in a not so long future.

6.2 Sputtered V_3Si SC films

In the former experiments of co-sputtering and reactive sputtering, V_3Si films were sputtered by the homemade facing-target magnetron at 500℃ and then annealed at 800℃ for several hours. Film thickness is about 0.5μm, and highest Tc of the film in DC measurement is around 16K while transition width 0.3K to 0.5K. In AC inductive measurement, the film generally shows a Tc of less than 15K and transition width approximately 1.5K. Although the best sample has a RRR as high as 17 while perfect bulk V_3Si only get 80, its AC measured figure is not satisfactory. The film suffered from multiphase and the DC measurement could only reveal the super-conducting phase with highest Tc while all information of other SC phases with lower Tc are shielded, but in the AC measurement, information of all other SC phases in the film could be detected.

RF surface resistance of two V_3Si samples, one co-sputtered and the other one reactive sputtered with RRR 12 and 13 respectively were measured by dielectric resonator technique. The resonator has a frequency of about 14GHz, measured results are shown in fig.6-1, and a magnetron sputtered niobium film sample was measured as a comparison. Although the niobium sample only has a RRR about 13 which is far from the best ones, it showed much lower residual resistance comparing with the two V_3Si samples. The high residual surface resistance of sputtered V_3Si films hampers RF performance of SC cavities, other coating technique that yields lower residual resistance should be investigated.

Table 6-1 Sputtering parameters of the three samples

V_3Si film co-sputtering parameters

Argon pressure	Vanadium voltage	Vanadium current	Silicon voltage	Silicon current	Time
0.8Pa	950V	0.3A	400V	0.2A	15min.

V_3Si reactive sputtering parameters

Argon pressure	Silane Pressure	Voltage	Current	Time
0.9Pa	0.15Pa	500V	0.4A	20min.

Magnetron sputtering of Niobium film

Argon pressure	Voltage	Current	Film thickness	Time
0.3Pa	400V	2.0A	1.2μm	20min.

Sputtering parameters of the three samples are listed in table 6-1, and results of the RF measurement see fig.6-1.

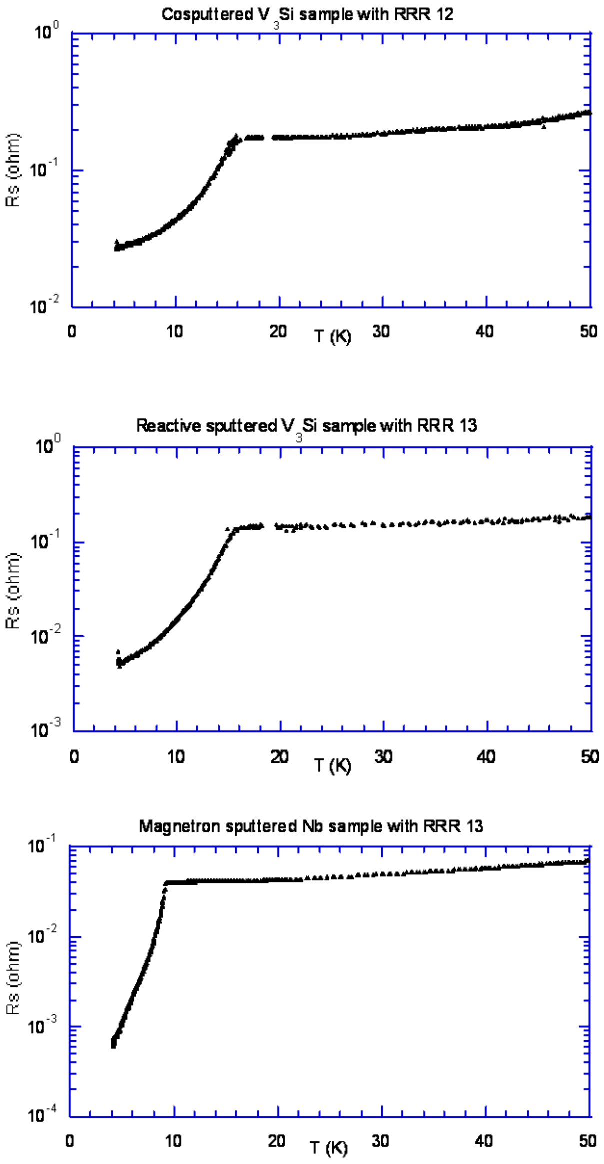

Fig.6-1 Surface resistance of samples measured at 14GHz.

6.3 Thermal diffusion of V_3Si films on sapphire substrates

Since it is a common case of sputtered SC films of A15 compounds with high residual surface resistance which should be prohibited in SRF applications, other film coating technique instead of magnetron sputtering should be chosen. Because of the successful progress on thermal diffusion of Nb_3Sn SC cavities, V_3Si cavity could be fabricated following the same direction.

Thermal diffusion of V_3Si SC films by two steps: sputter vanadium films on substrates and then anneal them in silane atmosphere, is a better solution to deposit thin V_3Si films in SRF applications. Magnetron sputtering by either the co-sputtering or the reactive sputtering experiment of V_3Si film only got sample with highest Tc around 16K, while they show very high residual surface resistance. V_3Si films with Tc higher than 16.8K were easily formed by thermal diffusion. From this technique, lower residual surface resistance and superior performance of V_3Si SC cavities could be expected.

In order to solve the problem of short lifetime of the ion gauge in silane atmosphere, a capacitance manometer was installed. It works stable at pressure no less than 1Pa, but does not measure very precise at lower pressure. Because it has not any hot filament, the corrosive silane gas would not affect its operation.

Vanadium films were sputtered on sapphire substrates at room temperature, then the samples were annealed in silane atmosphere and in vacuum at 800 to 900℃ for about ten hours. The best V_3Si sample got Tc a little higher than 16.8K, very near its bulk value, but only has a RRR about 9. The sputtering parameters are listed in table 6-2, and the thermal diffusion parameters in table 6-3. The transition curve of a V_3Si sample measured in the stand four-probe DC measurement is shown in fig.6-2.

Table 6-2 Sputtering parameters of vanadium film

Argon Pressure	Voltage	Current	Film Thickness	Time
0.5Pa	450V	1.0A	1.4μm	12min.

Table 6-3 Thermal diffusion parameters

Silane Pressure	Heater power	Temperature	Diffuse in silane	Anneal in vacuum
1.0Pa	300W	850℃	2h	12h

Although the diffused V_3Si sample shows a satisfactory transition curve, its RRR is less than 10, much lower than that of the sputtering coated V_3Si film. From EDS measurement, the film surface was covered by a silicon-rich layer and contaminated by aluminum. After strip off the contaminated surface layer, the beneath film found to be a very good superconductor. It reveals that silane decompose rate is higher than the rate of silicon diffusion in vanadium film so that a silicon-rich layer accumulated on the film surface.

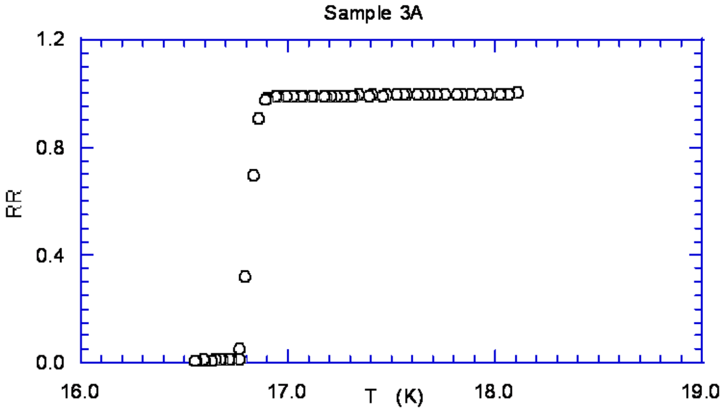

Fig.6-2 DC transition curve of a thermal diffused V_3Si sample

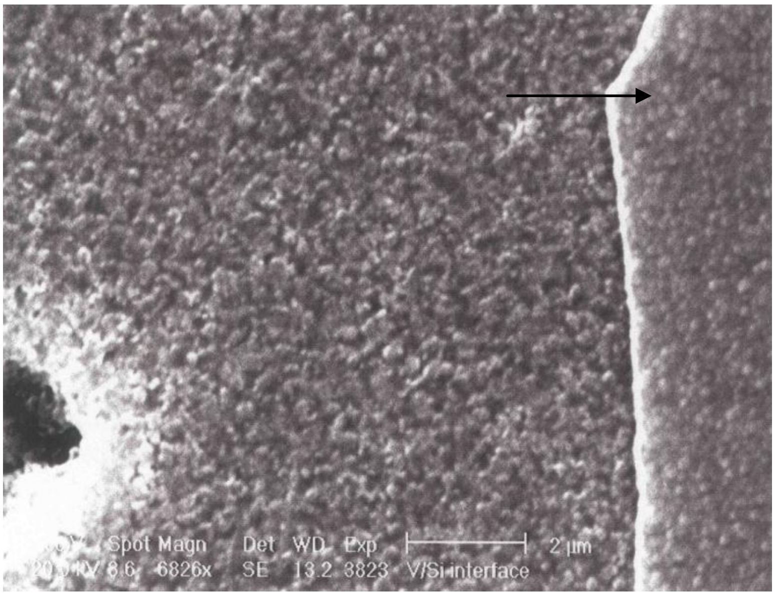

Fig.6-3 Image of one V_3Si sample surface under SEM

The right corner shows a different crystalline structure as it is a layer of silicon-rich and contaminated by aluminum. It was stripped off at the rest area, where good superconductor found.

Composition of silicon on the film surface decreases when reducing the annealing temperature to 600℃ and 700℃, no good superconductor formed even by properly increasing the process time to reach the same film composition as that of samples annealed at high temperature. Since temperature is of crucial importance in thermal diffusion of the V_3Si SC film, the annealing temperature was kept at 800 to 900℃ in all the following runs. After silane pressure reduced to $1.2 \cdot 10^{-2}$Pa, V_3Si sample with very sharp transition ($\Delta Tc < 0.1K$) was got again, the film surface was no longer covered by a silicon rich layer, but the problem of aluminum contamination remained to solve.

Table 6-4 Optimized diffusion parameters

Silane Pressure	Heater power	Temperature	Diffuse in silane	Anneal in vacuum
$1.2 \cdot 10^{-2}$Pa	300W	850℃	10h	2h

When thickness of vanadium films increased to 3.5 microns, the diffusion time in silane atmosphere prolonged to 20 hours. DES measured film composition with silicon content around 25%, but cracks in the sample were detected under SEM. See fig.6-4, the cracks might be caused by higher thermal stress in thicker sputtering deposited film, or structure expansion of the reaction product compound during the thermal diffusion process.

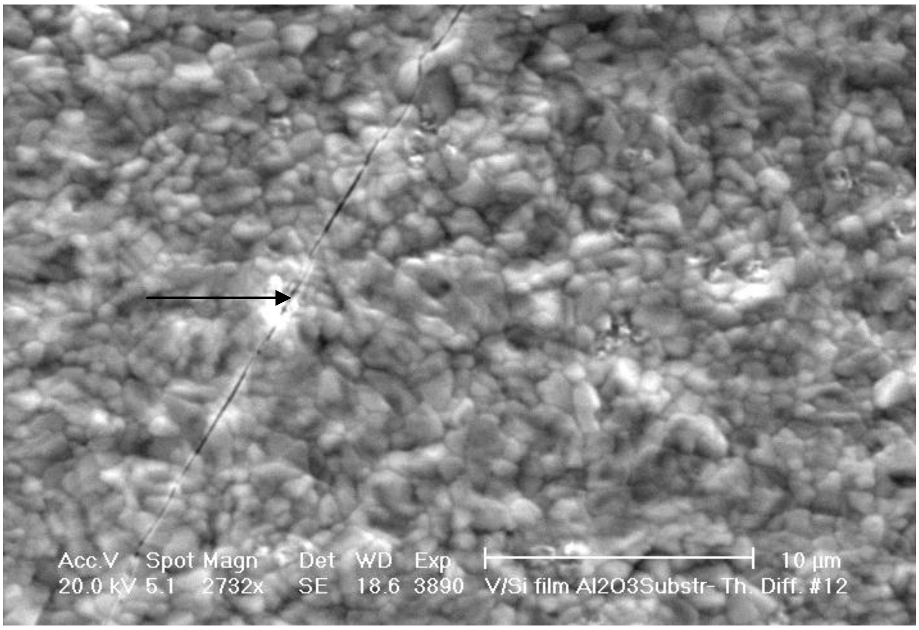

Fig.6-4 A diffused V_3Si sample with cracks

6.4 Diffusion on Niobium and Copper substrate

High purity niobium sheet (RRR 200 to 300) was chemically etched about 50µm to strip off the oxidized surface layer. The samples was sputtering coated with 3.5µm thick vanadium film, and then annealed in silane atmosphere at 800 to 900℃ for 10 to 20 hours in silane, another 10 to 20 hours in vacuum. No SC transition except that of niobium itself was detected in the AC inductive measurement. The reason of failing to form V_3Si SC films on niobium substrate was granted to aluminum contamination at first.

As aluminum was found on surface of all the annealed samples, in some samples the aluminum contamination is more than 20% of the total film composition. The contamination source was located to ceramic standoffs used in the heater. After the home made tungsten-filament molybdenum-oven heater replaced by a commercial BN heater again and remove all the above mentioned ceramic standoffs, the problem of aluminum contamination was solved, but there was still no higher SC transition detected in all the samples.

Table 6-5 Sputtering parameters of vanadium film

Argon Pressure	Voltage	Current	Film Thickness	Sputtering time
0.5Pa	450V	1.0A	3.5µm	30min.

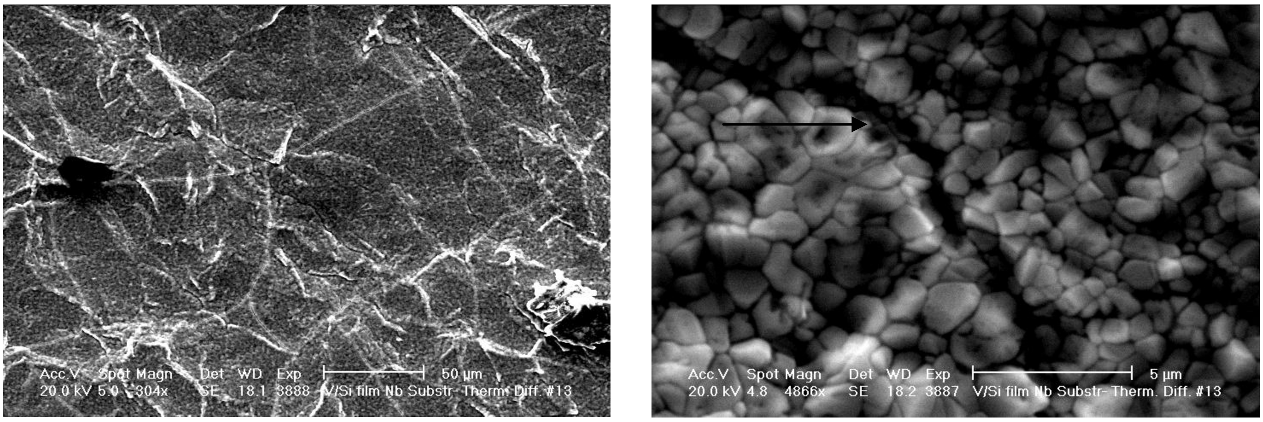

Fig.6-5 SEM image of a V/Si sample on niobium substrate

Sample surface filled with submicron size cracks, while EDS measured composition of silicon and vanadium is usually 2:1 which corresponds to VSi_2 – one kind of semiconductor.

Under SEM, the film surface filled with cracks, as a result of structure expansion during the chemical reaction of vanadium film with silicon decomposed from silane that the production material has a less density than that of vanadium. The film surface composition is always corresponding to VSi_2. Fig.6-5 is one sample surface imagine under SEM.

Because the sample had been annealed at 800 to 900℃ for approximately 30 hours, it is reasonable to imagine that the rest vanadium diffused to the niobium substrate, so that no stable V_3Si SC film formed. Niobium cannot serve as the substrate for thermal diffusion of V_3Si SC films, unless a diffusion buffer layer coated on it before the sputtering and diffusion process. One kind of material, CeO_2 could undertake such a task[125], but coat it on niobium is more difficult than coating V_3Si film.

OFHC copper foil in thickness 20μm was studied as substrate too. Vanadium films were sputtering coated on both sides of the copper substrates to prevent it from evaporation during the thermal diffusion process. Thickness of the vanadium film is approximately 3.2μm, the sputtering parameters is almost the same as those listed in table 6-5 except the film thickness and the deposition time, 27mininutes.

The first annealing experiment at about 850℃ damaged the copper sample. Then the temperature reduced to 800℃, but copper foil samples always been damaged in thermal diffusion runs. To avoid larger thermal stress of the laminated copper foils, niobium explosive bonded copper sheet (Copper approximately 3 mm with niobium 0.5 mm) from JAERI was used, its copper surface was sputtering coated on 3.2 microns vanadium film. OFHC copper sheet will be the same as substrate, but it needed an additional film sputtering that would require more time.

In the sputtering of vanadium film, the sample was heated to approximately 500℃ to reduce thermal stress of the deposited film. Then annealed in silane atmosphere at 800℃ for about 20 hours, there was not the problem of sample damage again. But time of the study was limited, only a few experiments with copper substrate has not detected SC transition of V_3Si film yet.

6.5 Diffusion in bulk Vanadium

Choosing bulk vanadium as the substrate has some merit, at least there is no need of sputtering. The spinning of 6Ghz monocell vanadium cavities will cost less and, most important, V_3Si film coated SC cavities could be easily fabricated and investigated in a shorter period. The diffusion rate in bulk material is much less than in sputtered thin film, since the dominant diffusion of bulk material is generally atom immigration through the lattice. However, in thin film diffusion, surface and boundary diffusion process becomes important, they are orders more rapid than the bulk diffusion. As chemical diffusion takes another important role in the process, the real image of silicon diffuse in vanadium is complicate. Only it is sure that higher process temperature and longer time is needed in bulk vanadium diffusion.

Substrates were made from the same vanadium sheet from where targets had been cut. After etched about 40μm in 1:1:1 acid solution, the samples was annealed at 900 ℃ in silane atmosphere for 20 hours and then in vacuum for another 80 hours. It is needed to note that the new heater was a little more efficient. Heating power of approximately 300W could heat the sample to 900℃, while that of the old one was only 850℃. The film property of thermal diffused V_3Si samples measured in AC inductive measurement was encouraging, Tc close to 16.0K and ΔTc less than 0.4K – still a distance to its bulk material, but much better than the sputtered V_3Si films.

Table 6-6 Diffusion parameters

Silane Pressure	Heat Power	Temperature	Diffuse in silane	Anneal in vacuum
$1.2\cdot10^{-2}$Pa	300W	900℃	20h	80h

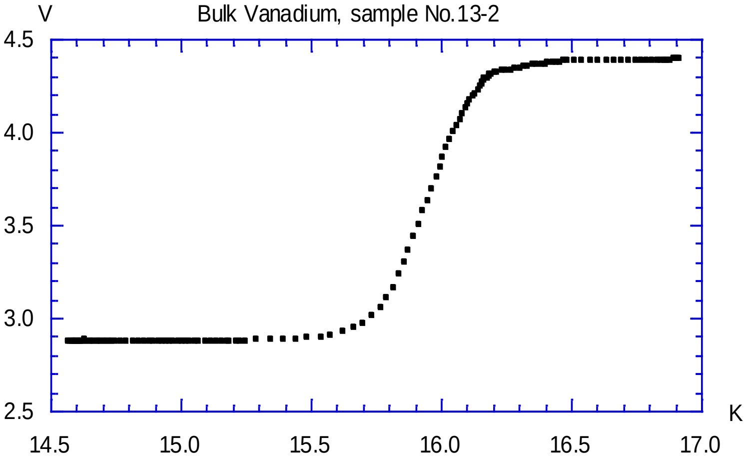

Fig.6-6 Transition curve of a sample in AC measurement

Usually the sample achieves higher Tc and more narrow transition width by increasing the vacuum annealing time in thermal diffusion of V_3Si films on bulk vanadium substrate. Unlike the diffusion in sputtered thick vanadium films (>3µm) on other kind of substrates, higher annealing temperature or longer process time often cause silicon content in the film increased too much and the sample became non-superconductor. And in the sputtering deposited film diffusions, thermal stress of the films always make trouble, cracks were commonly found out on sample surface, some times even damaged the film. In thermal diffusion on bulk vanadium substrate, there is a room to improve the film quality by higher annealing temperature or longer annealing time in vacuum.

6.6 Remained questions

In the V_3Si thermal diffusion process, substrate temperature is an important parameter. But silane decompose rate is quite large that surfaces of all components at high temperature were covered by silicon in a short time. Thermal couple did not work properly after the first run in silane, temperature read-out often reducing with time. It might be caused by current loses via deposited silicon layer that provides a bypass to the thermal couple, or by chemical reactions between silicon and materials the thermal couple made up of that reduce sensitivity of the device. In the meantime, V-I characteristic of the heater changes always with run by run or even in a single diffusion operation as a result of silicon deposition on surface. Precise temperature control becomes difficult.

Another problem is silane pressure decrease versus the operation time. Silane pressure often reduces 10% to 20% automatically after 10 to 20 hours running. There are two possible reasons, one is the filament of ion gauge covered by silicon that its electron emission efficiency reduces in the process, in this case, only pressure read-out decreases. Another is cooling down shrinking of the dose valve pout that reduces silane flow rate caused by volume expansion effect during silane inject from pressure line into the vacuum chamber, in this case, silane pressure really decreases. There exist other possibilities such as silane gas supply itself reduced, but seemed most unlikely since pressure of the silane storage bottle has not any obvious change. The newly installed capacitance manometer works well in pressure 10 to 1Pa, but does not work in vacuum range 10^{-2} to 10^{-3}Pa, otherwise reason of the problem would have been located.

Temperature of the heater is another important factor in the diffusion, but at present there is not a device in the laboratory that could monitor it. In an operation, a sample was put aside occasionally that one corner of it was shadowed by the niobium shielding. The shadowed area only got silicon content about 2% after annealing while non-shadowed area got 25%. Because the tiny temperature gradient of the small sapphire substrate could not cause so large a difference, the only clue is that silicon is mainly blown onto the film from the heater surface where silane decomposition major occurred. Because surface of the heater been covered by a silicon layer during the annealing, the diffusion situations not only decided by the heater temperature and its surface material, but also by history of the operation. It might give an explanation to why we have not reproduced results got from the old home made tungsten heater by changing to the new commercial BN heater.

It is easier to form V_3Si films on bulk vanadium as longer annealing time and higher process temperature always gives better SC properties unless after the entire vanadium sheet became V_3Si. However, diffusion in vanadium films showed some differences. Higher temperature or longer time often generates more cracks in the film, and silicon content increased too much that the film changed to non superconductor. Using two separate heaters, one for annealing in silane and one for vacuum, might provide a better solution to the problem of silicon increasing. But get perfect stoichiometric V_3Si films on a substrate cavity with very good thermal conductivity would be a difficult and long run.

Film measurement techniques presently available in the laboratory are not enough for analyzing the diffused V_3Si films. RBS and EDS cannot precisely measure composition of layered films thicker than 2μm. These techniques could only reveal composition of the film in surface section of a limited thickness, while film beneath and information of different phases is not known. Without a complete understanding of the film composition and crystalline structure, reliably to repeat perfect thicker V_3Si films would be very difficult.

The final problem is the difficulty of stripping off deposited V_3Si films. Hydrogen peroxide plus alkali such as sodium solution, is useful in stripping of niobium films from quartz or sapphire substrates, but they are no use at all to V_3Si films. Fluor hydrogen acid could strip off V_3Si films, while at the same time, the etching rate of niobium, vanadium or copper substrates would be much faster. Better solutions need to be searched out before the model cavity study. The chemical inert feature of V_3Si films provide another advantage of V_3Si cavity over niobium cavity, there is no trouble of oxidization after the cavity exposed to atmosphere for a long time, so the cavity maintenance would be simple[126].

Thermal diffusion of V_3Si films is a hopeful technique to fabricate V_3Si films coated SC cavities, it is much better than magnetron sputtering technique when the film quality concerned. Although there are still many technical problems to solve, some of them might need a long time research, we could say that it is on the right track now, and V_3Si films coated SC cavities with good RF performance could be expected in a not very long future.

A system for thermal diffusion of V_3Si film coated SC cavity has been designed and manufactured, by enlarging the vacuum chamber with a collar the total height of the chamber became 68cm that is enough for an 1.3 and 1.5GHz monocell cavity or higher frequency SC cavity with smaller dimension. Four layers of irradiation shielding with inner two molybdenum and outer two stainless steel, and a central heater with maximum power 5kW, the cavity could be heated up to 1000℃. It would be enough to run thermal diffusion in sputtered vanadium film and in bulk vanadium cavity.

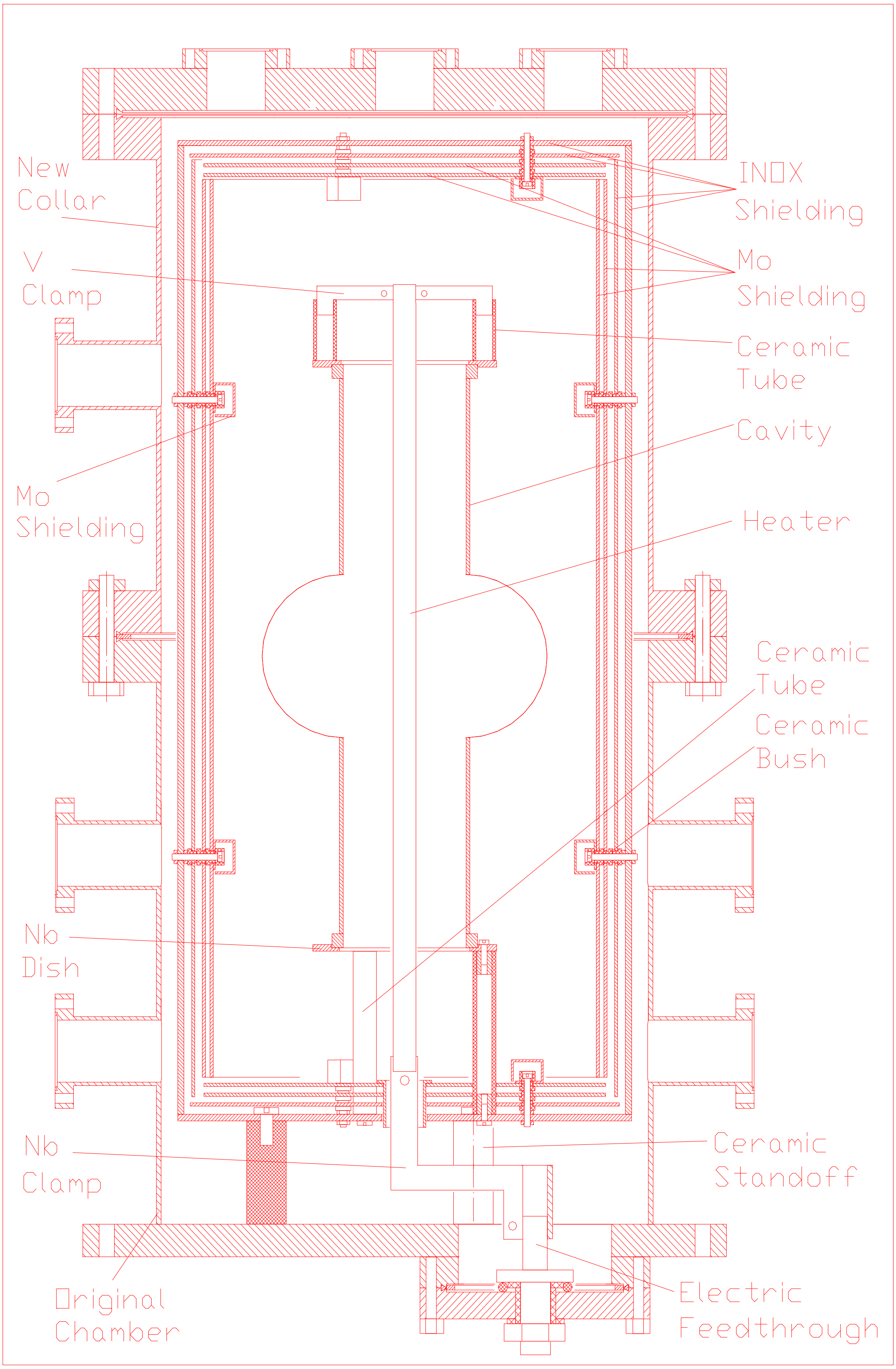

Fig.6-7 Diagram of the V_3Si cavity diffusion system

References

1. M. Puglist, S. Trieste, American Institute of Physics Conferences and Proceedings 184, Vol. 2, 1989, P1393.
2. G. Dome, Proceedings of CERN Accelerator School, CERN 92-03, 1992, P1.
3. D. A. Edwards, M. J. Syphers, American Institute of Physics Conf. Proc. 184, Vol. 1, 1989, P2.
4. M. Cante, W. W. Mackay, An introduction to the physics of particle accelerator, 1991, P152.
5. E. Raka, American Institute of Physics Conf. Proc. 184, Vol. 1, 1989, P288.
6. P. M. Lapostolle, Proc. CERN Accelerator School, CERN 96-02, 1996.
7. M. Pudlisi, Proc. CERN Accelerator School, CERN 92-03, 1992, P156.
8. J. L. Duff, Proc. CERN Accelerator School, CERN 94-01, 1994.
9. J. R. Delayen, Nucl. Inst. Moth. In Phys. Res., Vol. A258, 1987, P15.
10. M. Weiss, Proc. CERN Accelerator School, CERN 94-01, 1994, P913
11. J. W. Staples, American Institute of Physics Conf. Proc. 249, Vol. 2, 1991, P1485
12. J. Evetts, Concise Encyclopedia of magnetic and superconducting materials,1992
13. P. Schmuser, Proc. CERN Accelerator School, CERN 96-03, 1996, P1
14. B. Bonin, Superconducting material for cavities, Proc. CERN Accel. School, CERN 96-03, 1996
15. T. Yogi, G. J. Dick, J. E. Mercerean, Phys. Review lett. Vol.39, 1977, p826
16. H. Padamsee, Superconducting RF, AIP Conf. Proc. 249, Vol.2, 1992, p1403
17. C. Crawford, J. Graber, T. Hays, et. al., Particale Accelerators, Vol.49, 1995, p1
18. W. Weingarten, Superconducting cavities - basic, Proc. CERN accel. school, CERN96-03, 1996
19. A. Pisent, G. Bassato, A. Battistella, Proc. European Particle Accelerator Conference 96', EPAC96, 1996
20. I. Ben-Zvi, M. Birk, C. Broude, et. al., Nucl. Inst. & Meth., Vol. A245, 1986, p1
21. I. Ben-Zvi, J. M. Brennan, Nucl. Inst. & Meth., Vol. 212, 1983, p73
22. J. R. Delayen, Nucl. Inst. & Meth., Vol. A259, 1987, p341
23. T. Weiland, Particle Accelerator, Vol. 56, 1996, p61

24. P. Balleyguier, Nucl. Inst. & Meth., Vol. A413, 1998, p1
25. E. Haebel, Couplers for cavities, Proc. CERN Accel. school, CERN96-03, 1996
26. O. Henry, A. Mosnier, Proc. EPAC92', Vol.2, 1992, p877
27. G. Geshonke, Proc. 7th RF superconductivity workshop, 1995, p910
28. T. Furuya, K. Asano, Y. Ishi, et. al., Proc. 7th RF super. work.,1995, p729
29. C. Pasotti, P. Pittana, M. Svandrlik, Part. Accel. Conf. 97', IEEE, 1998, p3099
30. C. Benvenuti, D. Bonssard, S. Calatroni, et. al., Proc. 8th RF superconductivity, 1997
31. F. L. Krawczyk, PAC 97', IEEE, 1998, p3093
32. S. Takeuchi, JAERI, private conversation
33. S. W. Kitchen, A. D. Schelberg, J. Appl. Phys., Vol.26, 1955, p618
34. H. Klein, Proc. CERN accel. School, CERN96-03, 1996, p97
35. J. M. Brennan, B. Kurup, I. Ben-Zvi, J. S. Sokolowski, Nucl. Inst. & Meth., Vol. A242, 1985, p23
36. C. Arnaud, C. Benvenuti, Ph. Bernard, et. al., Proc. EPAC 92', 1992, p1275
37. E. Chiaveri, Proc. 7th RF superconductivity workshop, 1995, p181
38. S. Takeuchi, T. Ishii, H. Ikezoe, Nucl. Inst. & Meth., Vol A281, 1989, p426
39. P. Kneisel, R. W. Roth, H. G. Kurschner, Proc. 7th RF supercond. workshop, 1995, p449
40. W. D. Moller, Proc. 7th RF superconductivity workshop, 1995, p119
41. V. Palmieri, LNL, private conversation
42. W. R. Grove, Philos. Trans. Roy. Soc., Landon, 142, 1852, 87
43. B. Chapman, S. Mangano, Introduction to sputtering, Hand book of thin film deposition process and technology, 1988, p291
44. J. A. Thornton, The microstructure of sputter deposited coatings, J. Vac. Sci. Tec., Vol. A4, 1986, p3059
45. G. S. Bales and A. Zangwill, J. Vac. Sci. Tec., Vol. A9, 1991, p145
46. P. J. Kelly and R. D. Amell, J. Vac. Sci. Tec., Vol. A16, 1998, p2858
47. M. Andritshky, F. Guimarae, V. Teixerra, Vacuum, Vol. 49, 1998, p809
48. H. W. Zhang, S. Q. Yang, Vacuum, Vol. 46, 1995, p661
49. S. M. Rossnagel, J. J. Cuomo, Vacuum, Vol. 38, 1988, p73
50. T. P. Drusedau, M. Lohmann, G. Garke, J. Vac. Sci. Tech., Vol.A16, 1998, p2728
51. D. W. Hoffman, J. Vac. Sci. Tech., Vol.A12, 1994, p953
52. A. Andreone, A. Cassinese, M. Iavarone, et. al., Phys. Rev. B, Vol. 52, No. 6, 1995, p4473

53. W. Weingarten, Proc. 8th Workshop RF Superconductivity, 1995, p129
54. P. Darriulat, Proc. EPAC 98', 1998, p179
55. F.F. Mende, A.I. Spitsyn, N. A. Kochkonyan and A. V. Skugarevski, Cryogenics, Vol.25, No.1, 1985, p10
56. D.C. Weisser, M.D. Malev, Proc. 3rd workshop on RF superconductivity, 1987, p425
57. V. Palmieri, Proc. 7th workshop on RF superconductivity, 1995, p237
58. V. Palmieri, V.L. Ruzinov, S.Y. Stark et. al., Proc. EPAC 92', 1992, p1292
59. N.R. Lobanov, D.C. Weisser, Proc. 8th workshop RF Supercon.,1997, p1125
60. J.K. Hao, K. Zhao, B.C. Zhang, et. al., R&D of niobium-sputtered copper QWR for heavy ion linac in Peking University, Proc. 1st Asian Part. Acce. Conf., APAC 98', 1998
61. Jiang Weisheng，CIAE, private conversation
62. S.Y.Stark, LNL, private conversation
63. V. Palmieri, LNL, private conversation
64. F. Stivanelo, LNL, private conversation
65. P. Brown, E. Ciapala, G. Geschonke and E. Peschardt, Proc. EPAE 92', 1992, p54
66. Ph. Bernard, D. Bloess, T. Flynn, et. al., Proc. EPAC 92', 1992, p1269
67. P. Bosland, A. Aspart, E. Jacques and M. Ribeaudeau, Preparation and RF tests of L-band superconducting niobium coated copper cavities, Proc. ASC 98', 1998
68. C. Benvenuti, S. Calatroni, I.E. Campisi, et. al., Study of the surface resistance of niobium sputter-coated copper cavities, to be published on Physica C
69. W. Venturini, LNL, private conversation
70. M. Couach, A.F. Khoder and F. Monnier, Cryogenics, Vol.25, 1985, p695
71. O. Pena, Meas. Sci. Tech., Vol.2, 1991, p470
72. L. Badan, I.I. Kulik, V. palmieri, et. al., Recent improvement in Nb sputtering on copper 1.5GHz spun monocell resonators at LNL, LNL-INFN (Rep) 139/99, 1999
73. C. Benvenuti, D. Boussard, S. Calatroni, et. al., Production and test of 352MHz niobium-sputtered reduced-beta cavities, Proc. 8th Wrokshop RF Supercon., 1997
74. I.M. Kapchinskii and V.A.Teplyakov, Pribory I Tekhnika Eksperimenta, Vol.119, No.2, 1970, p19
75. A. Schempp, AIP Conf. Proc. 184, Vol.2, 1989, p1477
76. J.W. Staples, AIP Conf. Proc. 249, Vol.2, 1992, p1483

77. I. Ben-Zvi, Particle Accelerators, Vol.23, 1988, p265
78. A. Jain, H. Wang, I. Ben-Zvi, et. al., Nucl. Instr. Meth. in Phys. Res., Vol.A328, 1993, p251
79. I. Ben-Zvi, A. Lombardi, and P. Paul, Particle Accelerators, Vol.35, 1991, p177
80. X.L. Guan, A. Lombardi, A. Pisent, Beam dynamics design for a SRFQ linac at LNL, LNL internal report, 1995
81. A. Pisent, Beam dynamics of the new LNL injector, LNL internal report, REP.107, 1996
82. PARMTEQ, LANL
83. A. Pisent, G. Bisoffi, A. Lombardi, et. al., Proc. EPAC98', 1998, p758
84. A. Pisent, G. Bisoffi, A. Battistella, et. al., Status of the SRFQ project for the Legnaro new positive injector, Proc. EPAC96', 1996
85. G. Bisoffi, I. Kulik, A. Lombardi and V. Palmieri, LNL annual report, 1997, p226
86. V. Palmieri, I. Kulik, LNL, pravite conversation
87. I. Kulik, Y. Zhang, V. Palmieri, R. Preciso, F. Stivanello, W. Venturini, LNL-INFN (Rep) 149/99, 1999
88. M. Peiniger, M. Hein, N. Klein, G. Muller, et. al., Work on Nb3Sn cavities at Wuppertal, Proc. of 3rd Workshop RF Superconductivity, 1987
89. R. Dileo, G. Nobile, V. Palmieri, R. Vaglio, et. al., Weak superconductivity - progress in high Tc superconductivity, Vol. 4, 1987, p275
90. P. Fabbricatore, P. Fernandes, G. C. Gualco, F. Merlo, et. al., J. Appl. Phys., Vol.66, 1989, p5944
91. G. Gemme, P. Fabbricatore, R. Musenich, R. Parodi, et. al., J. Appl. Phys., Vol.77, 1995, p257
92. W. Weingarten, Progress in thin film techniques, Proc. 7th Workshop of RF Superconductivity, 1995
93. A. Andreone, A. Cassinese, A. DiChiara, et. al., Proc. 7th Workshop of RF Superconductivity, 1995, p535
94. Q. S. Shu, Large applications and challenges of state-of-art superconducting RF technology, CEC/ICMC-97, 1997, p1
95. D. Dew-Hughes, Physical Metallurgy of A15 Compounds, Treatise on Materials Science and Technology, Vol. 14, 1979, p137
96. T. P. Orlando, E. J. McNiff, S. Foner, and M. R. Beasley, Physical Review B, Vol. 91, No. 9, 1979, p4545
97. A. Andreone, A. Cassinese, A. DiChiara, et. al., J. Appl. Phys. Vol. 78, No. 3, 1995, p1862
98. L. R. Testardi, J. M. Poate, and H. J. Levinstein, Physical Review B, Vol. 15, No. 5, 1977, p2570

99. S. D. Stefano, A. D. Chiara, G. Peluso, et. al., Cryogenics, V0l. 25, 1985, p194
100. J. R. Gavaler and J. Greggi, IEEE Trans. on Magnet., Vol. MAG-21, No. 2, 1985, p517
101. L. R. Testardi, R. L. Meek, J. M. Poate, et. al., Physical Review B, Vol. 11, No. 11, 1975, p4304
102. J. R. Gavaler, High Tc superconducting films, J. Vac. Sci, Tech. Vol. 18, No. 2, 1981, p247
103. R. E. Somekh, J. Vac. Sci. Technol., Vol. A2, 1984, p1285
104. S. Kadokura, T. Tomie, M. Naoe, IEEE Trans. Magn., Vol.MAG-17, 1981, p3175
105. K. Tominaga, Vacuum, Vol.41, 1990, p1154
106. M. Matsuoka, Y. Hoshi, M. Naoe, J. Vac. Sci. Tech., Vol. A5, 1987, p52
107. L. Kostadinov and D. Dobrev, Vacuum, Vol. 41, 1991, p35
108. M. Rossnagel and H. R. Kaufman, J. Vac. Sci. Tech., Vol. A5, 1987, p2276
109. V. Palmieri, Private conversation
110. Y. Zhang, V. Palmieri, R. Presco, W. Venturini, INFN-LNL(Rep) 143/99, 1999
111. S. Q. Wang and J. W. Mayer, J. Appl. Phys., Vol. 65, No. 12, 1989, p4774
112. S. Berg, T. Larsson, C. Nender and H-O. Blom, J. Appl. Phys., Vol. 63, No. 3, 1988, p887
113. T. Larsson, Vacuum, Vol. 39, No. 10, 1989, p949
114. S. Berg. T. Nyberg, H-O. Blom and C. Nender, J. Vac. Sci. Tech. A, Vol. 16, No. 3, 1998, p1277
115. P.D. Moskowitz, V.M. Fthenakis, P. Kalb and L.L. Hamilton, Compendium of suggested safe practices for the storage, distribution, use and disposal of silan and related gases in silicon thin-film deposition, Brookhaven National Laboratory, 1988
116. R.J. Buss, P.H. William, G. Breiland, and M.E. Coltrin, J. Appl. Phys., Vol.63, No.8, 1988, p2808
117. B.S. Meyerson, and J.M. Jasinski, J. Appl. Phys., Vol.61, No.2, 1987, p785
118. E. Stoffels, W. W. Stoffels, G. M. W. Kroesen and F. J. de Hoog, J. Vac. Sci. Tech. A, Vol. 14, No. 2, 1996, p556
119. K. Satake, Y. Inoue, O. Ukai and Y. Takeuchi, Appl. Phys. Lett., Vol. 73, No. 13, 1998, p1799
120. A.F. Belov, V.S. Terentyeva, Russ. Metall., No.5, 1982, p78
121. Y. Zhang, V. Palmieri, W. Venturini, R. Preciso, LNL-INFN(Rep) 144/99, 1999
122. C. Antonio, Napoli University, private communication

123. M. Perpeet, A. Cassinese, M. A. Hein, T. Kaiser, G. Muller, H. Piel, J. Pouryamout, Applied Superconductivity Conference 1998, ASC98’
124. C. Benvenuti, CERN, private conversation
125. R. Vaglio, Napoli University, private conversation
126. Y. Zhang, V. Palmieri, W. Venturini, F. Stivanello, R. Preciso, Thermal diffusion of V_3Si films , to be published on LNL-INFN report